VILNIUS UNIVERSITY
CENTER FOR PHYSICAL SCIENCES AND TECHNOLOGY

URTĖ SAMUKAITĖ-BUBNIENĖ

STUDY OF POLYPYRROLE BASED BIOSENSING SYSTEMS BY FLUORESCENCE METHODS

Doctoral dissertation
Physical sciences, Chemistry (03 P)

Vilnius, 2015

Doctoral dissertation was prepared at Vilnius University, Faculty of Chemistry and Center for Physical Sciences and Technology from 2010 to 2014.

Scientific supervisor − Prof. Dr. habil. Arūnas Ramanavičius (Vilnius University, physical sciences, chemistry – 03P).

VILNIAUS UNIVERSITETAS
FIZINIŲ IR TECHNOLOGIJOS MOKSLŲ CENTRAS

URTĖ SAMUKAITĖ-BUBNIENĖ

POLIPIROLU MODIFIKUOTŲ BIOLOGINIUOSE JUTIKLIUOSE NAUDOJAMŲ SISTEMŲ TYRIMAS FLUORESCENCIJOS METODAIS

Daktaro disertacija
Fiziniai mokslai, Chemija (03 P)

Vilnius, 2015

Disertacija rengta 2010 – 2014 metais Vilniaus universiteto Chemijos fakultete ir Fizinių ir technologijos mokslų centre.

Mokslinis vadovas − prof. habil. dr. Arūnas Ramanavičius (Vilniaus universitetas, fiziniai mokslai, chemija – 03P).

ACKNOWLEDGMENTS

Many people have contributed to the making of this work. Above all, I would like to express my genuine gratitude and many thanks to my supervisor prof. habil. dr. Arūnas Ramanavičius, for the guidance and development of the highest level work, and who was very generous with his time and knowledge.

I would like to thank the many honored scientists and specialists who generously took the time to share their experience, insights and comments. I am particularly grateful to dr. Almira Ramanavičienė, dr. Zbigniew Adamczyk, dr. Jaroslav Voronovič.

Many people read the manuscript at various stages of completion and offered insightful comments that improved the final result of this thesis; therefore I would like to thank dr. Renata Karpič, dr. Jurgis Barkauskas for the support.

I would like to gratefully and sincerely thank Birutė Bugelytė for her assistance, co-working and friendship.

Whole-heartedly gratitude goes to my family, whose patience and support made this thesis possible.

This work was performed at Vilnius University, Faculty of Chemistry, Physical Chemistry Department; Centre of Nanotechnology and Material Science (NanoTechnas); and Institute of Semiconductor Physics, State Research Institute Centre for Physical and Technological Sciences. Funding for this work was provided by the scholarship of Vilnius University and Research Council of Lithuania through all the years of study.

Table of Contents

List of Tables

List of Figures

Abbreviations and Symbols

Ab – antibody

Ab* – HRP-labeled antibodies

AFM – atomic force microscopy

AGID – agar gel immunodiffusion

AuNP – gold nanoparticles

BLV – bovine leukemia virus

BSA – bovine serum albumin

ChT – α-chymotrypsin

CRE – carbon rod electrode

DLS – dynamic light scattering

DLVO – Derjaguin, Landau, Verwey and Overbeek theory

ECP − Electrically conducting polymers

EIA – enzyme immunoassay

ELISA – enzyme-linked immunosorbent assay

ET – electron transfer

FAD – flavin adenine dinucleotide

FE-SEM – field emission scanning electron microscopy

GOx – glucose oxidase

gp51 – surface protein from BLV

HRP – The enzyme horseradish peroxidase

IFAT – indirect fluorescent antibody technique

Lyz – lysozyme

NP – nanoparticle

NSOM – near-field scanning optical microscopy

PAH – poly(allylamine hydrochloride)

PCR – polymerase chain reaction

Phe – aromatic amino acids residue phenylalanine

PPy – polypyrrole

RIA – radioimmunoassay

RSA – random sequential adsorption

SEM – scanning electron microscopy

Tyr – aromatic amino acids residue tyrosine

Trp – aromatic amino acids residue tryptophan

TMB – 3,3',5,5'-tetramethylbenzidine

UV-Vis – Ultraviolet to visible wavelength region

τ – fluorescence lifetime

Preface

Over the past decades, there has been intense research on the development of biosensing systems for the various ranges of analytes. The implementation of polymer technology achievements in the development of has biosensing systems designed a new generation of ultrasensitive biosensing devices. The effective combination of biologically active polymers and physical methods in biosensing systems may provide direct detection of wide range of analytes with great sensitivity and specificity.

Biosensing in general is showing special interest within polymer technology, because some polymers could provide significant advantages to biosensing systems, such as: low detection limits, high sensitivity, lower applied potential, reduction of background, efficient electron transfer, thermal stability, biocompatibility.

Electrically conducting polymers (ECP) are a promising new class of materials with the physical (electronic, magnetic, optical) performance, which in sme cases is close to that of metals and/or semiconductors. Therefore, ECPs are sometimes referred as 'synthetic metals'. Properties of ECP depend on their chemical composition and structure, therefore, their use can significantly improve either create a class of completely new intelligent materials and achieve amazing results. ECPs represent one of the main aspects of biosensing systems where ECPs can perform several very important functions: (i) as signal transducer,when the ECP combines the biologically active substance with electronic devices and transforms a signal received from the biological material to more easily recorded physical, i.e. electrochemical, signal; (ii) as immobilization matrices, such ECP-based matrices facilitate the recognition during the immobilization, through a variety of techniques, including non-specific physical adsorption, covalent as well as non-covalent coupling, electrostatic interactions (e.g. using negatively charged surfaces) and others, of biological materials; (iii) as a fluorescent tags, which are widely used in complex biological systems (cells, tissues) The advantage of such fluorescent

tags is a high quantum yield, narrow luminescence spectra and good photostability.

To date, a number of biosensing systems based on conductive polymers have emerged. The expectation of such biofunctional sensing systems is that the performance of specific functions will be better than purely organic or purely inorganic systems.

Fluorescence is used in biosensing systems as a non-destructive method of analyzing biological molecules at very low concentrations, by means of the molecule's intrinsic fluorescence (autofluorescence), or by attaching it with a extrinsic fluorophore, fluorescent dye. The fluorescence technology has been extensively applied mostly due to the high detection sensitivity. Additionally, the fluorophores display a variety of measurable properties (the emission intensity, orientation, waveform, lifetime, and the interrelationships between these properties) [1].

The occurrence of the spectrophotometric analysis methods greatly expanded fluorescent technology, therefore improvement of a fluorimetric methods for the biosensing analysis led to increase the sensitivity of the method more than 1,000 times. The effective combination of polymers and fluorescence methods in biosensing systems provides even more enhanced signal amplification.

Sensing using nanoparticles is taking added value in the field of biosensing systems. The properties of nanoparticles such as light absorption and dispersion are providing interesting sensing alternatives. However, adapting the nanoparticles in biosensing systems, the problem concerning energy distribution, which causes the particles agglomeration (adhesion), occurs. In order to avoid agglomeration of the particles, the nanoparticle surface can be modified with polymers. Successful insertion of the molecules in the organic system, such as polymer matrix, have attracted the attention of many scientists.

This thesis is built upon two key aspects – both the research of polypyrrole based biosensing systems, and the implementation of methods employed within the field, i.e. fluorescence.

The aim

To evaluate biosensing systems, in which polypyrrole is adapted as biomolecules immobilization matrix, by fluorescence methods.

The objectives of this thesis are the following:

• to evaluate the properties of glucose oxidase modified with polypyrrole by photoluminescence methods.

• to evaluate the electrokinetic properties of gold nanoparticles and to apply them for the modification of glucose oxidase and polypyrrole based system; to investigate resulting composites by photoluminescence methods.

• to evaluate the properties of immunosensors, in which polypyrrole is used as immobilization matrix, by photoluminescence methods.

Statements to be defended:

• the polypyrrole matrix can be used as a fluorescence quencher in the photoluminescent immunosensors, improving the selectivity of such sensors.

• the dissociation of flavin adenine dinucleotide cofactor from glucose oxidase significantly slowed down when enzyme glucose oxidase was entrapped within the polypyrrole matrix during "enzymatic" polymerisation.

• colloidal gold nanoparticles have a negative surface charge in a wide pH and ionic strength range and are suitable for the formation of polypyrrole layer.

• deposition of colloidal gold nanoparticles onto a solid surface is dependent on the diffusion, which depends on the initial particle concentration and ionic strength of colloidal nanoparticle suspension.

With respect to the aforementioned three objectives, **the major contributions** of this thesis are fourfold:

• Synthesis of polypyrrole by hydrogen peroxide formed in glucose oxidase catalyzed the reaction and self-incapsulation of glucose oxidase within formed polypyrrole layer.

• Polypyrrole matrix can be used as a quencher of fluorescence of non-specifically adsorbed materials that can enhance the selectivity of immunosensig systems.

• The electrophoretic mobilities and electrokinetic charge of gold nanoparticles were quantitatively evaluated in a broad range of pH and ionic strength. Particle deposition kinetics process was determined as diffusion controlled, with the initial rate proportional to the bulk concentration of gold nanoparticles.

1. Introduction

This chapter introduces the framework for the case study that comprises the main focus and key concepts of the research described in this thesis, reviewing the key elements involved in setting up qualitative study. This introductory chapter provides an overview of research on essential topic and presents basic principles of fluorescence and its methods used for biosensing system in general.

Context

Biosensing systems are widely used in various industries and bioscience fields both as diagnostic and analytical tools, general research. The motive to explore such systems is that these methods consolidated in biochemistry science and perfectly complement with substantial advantages: allows identifying materials that do not participate in the process and there are no enzymes to recognize them, meaning identification of materials extraneous to organism or system. It allows detection of all types of biological molecules at very low concentrations and quantities, large populations. This area of research includes biological molecules (hormones, peptides, specific proteins), drugs, viruses, cell research, which nowadays is a key area of interdisciplinary biosciences medium. Potential application of biosensing systems promises a breaking new era in analytical chemistry.

However, there has been intense research on the main limitations of such systems: indefinite color, stability changes over a sufficiently long period of time, inadequate detection sensitivity.

Nowadays, fluorescence is one of the most sensitive detection methods, due to its ability of signal multiplication and amplification, and therefore is widely used for immunoassay.

One promising approach in biosensing systems is to utilize the extraordinary properties of polymers and metal nanoparticles combined in a complex frame with enzymes and antigen-antibody systems.

Literature overview

The aim of this overview is to describe some of the early milestones in the study of important integrated subjects of this thesis and to give a deeper understanding of involved processes, materials and important aspects. This section starts with the most important issue luminescence and its complexions, paying particular attention to one of its most important form – fluorescence, and gradually describe significant facets of biosensing systems.

1.1 Luminescence

The origin of the term *luminescence* comes from Latin *lumen* = light and *escentia* = see. The term was first introduced by E. Wiedemann in 1888. Since then the description of this phenomena varied over time (G. G. Stokes, S. I. Vavilov concepts of luminescence) till the present steady definition: "Spontaneous emission of radiation from an electronically excited species or from a vibrationally excited species not in thermal equilibrium with its environment" [2]. However, overall definition of luminescence has failed to formulate, because of the conditions of investigation and various luminescence properties. The concept of term emphasizes one or the other luminescence parameters and in such way luminescence can be classified according to:

- the mode of excitation,
- the mechanism of energy conversion,
- the time characteristics of the luminosity.

Luminescence classified according to the mode of excitation:

- photoluminescence – excitation by light;
- chemiluminescence – excitation as a result of chemical reaction;
- biochemiluminescence – excitation of surplus energy transfer as a result of chemical reaction in biological systems;
- thermoluminescent – absorbed energy is re-emitted as light upon heating of the material;
- electroluminescence – excitation by an electric field;

- radioluminescence – excitation by penetrating radiation;
- cathode luminescence – excitation by an electron beam;
- ion luminescence – excitation by accelerated ions ;
- triboluminescence – excitation by mechanical stresses).

Two principal varieties according the duration of luminosity, fluorescence and phosphorescence (Fig. 1), are distinguished by the delay in reaction to external electromagnetic radiation: fluorescence – rapidly decaying luminescence, phosphorescence – prolonged luminescence, while a phosphorescent material does not immediately re-emit the radiation it absorbs. The slower time scales of the re-emission are associated with "forbidden" energy state transitions.

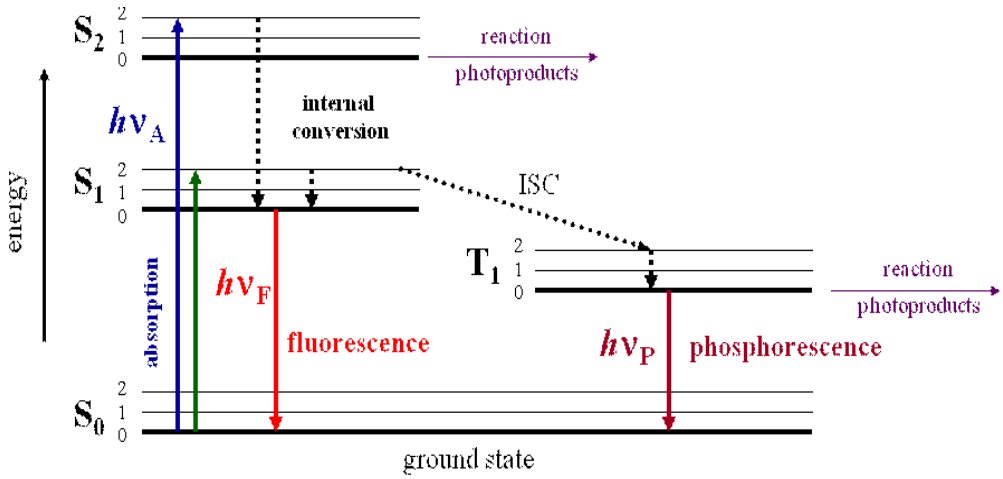

Fig. 1. *Jablonski's simplified diagram form illustrating the difference of fluorescence and phosphorescence according the duration of luminosity. S_0 is the ground state, S_1 and S_2 are excited singlet states; T_1 is an excited triplet state. 0, 1, 2 represent vibrational levels. Straight lines represent transitions involving photons, dotted lines represent vibrational or thermal transitions. (Picture's source http://chem.sci.utsunomiya-u.ac.jp/v13n2/22ALP_Nery/ALP Nery.html)*

In the mechanism of energy transfer a distinction is made among resonance, spontaneous, forced, and combinational luminescence.

Luminescence is the emission of light from any substance. It can result from the chemical reactions, electrical energy, subatomic motions, reactions in a crystals, stimulation of an atomic systems and the source influencing the appearance of luminescent process can be derived from various types of materials, such as:

- Atomic transitions;
- Organic light emitting materials;
- Inorganic light emitting diode materials (with colour conversion phosphors);
- Down-conversional materials;
- Powder materials;
- (Phosphor) Quantum dots;
- Upconversion nanoparticles (τ-Dots);
- Doped semiconductors and insulators (localized defects);
- Thin-film phosphor materials;
- Liquid crystals;
- Nanostructured materials.

Extraordinary interest and progress in the understanding of the basic principles of luminescence distinguishes luminescence forms fluorescence and electroluminescence covering a typical applications, including sulfide-based nanoparticles and color conversion phosphor materials [3].

Light emission process is very informative and from many luminescent parameter set it can be identified not only the objects, structures or individual molecules, but also their surrounding and processes taking place within the object.

Luminescence with its all mentioned forms has several significant advantages over other analytical techniques. Sensitivity, broad array of possible parameters to measure, real-time data acquisition, distant monitoring opportunity, relatively inexpensive instrumentation and the rapidly growing demand of luminescent assays make this technique very popular and

advantageous among scientists.

Luminescence is commonly used in natural sciences, biophysical sciences, environmental testing, speleology, hydrology, medical diagnostics, clinical research, and various industrial applications. Nowadays, many studies include the application of luminescence technology, which can be of service in modified nanoparticles research [4, 5] because nano-sized particles exhibit excellent photostability, tunable and narrow spectra, solubility, controllable size, are versatile to environmental conditions such as pH and temperature, and has extremely high surface area to volume ratio for anchoring targeting biomolecules; polymers [6, 7], which enabled, through the control of the chain structure, the fabrication of effective light-emitters with well-ordered molecular structures withal inter-molecular dipolar coupling resulting higher efficiency, and coordination polymers [8], named as next-generation luminescent materials for extremely sensitive and selective sensing [9]; antigen-antibody complexes within conjugates [10]; analysers based on enzyme assays [11-13] using enzymatic oxidation reactions during which oxygen or protons are consumed or produced and this can be easily monitored in various ways.

On the relevance of the subjects discussed this thesis is focused on these specific classes of materials, mentioned above – nanoparticles, polymers, enzymes, antigen-antibody complexes – and their applications in bioanalytical systems through luminescent technology.

1.2 Fluorescence

The term '*fluorescence'* first appeared in G. G. Stokes paper's "On the change of refrangibility of light" [14] footnote, when he described the phenomenon of *dispersive reflection,* from his experiments of fluorite and a glass of uranium able to change invisible light beyond the violet end of the visible spectrum into blue light.

Fluorescence, as mentioned earlier in this paper, is rapidly decaying luminescence. It's a process where a substance emits light as an effect of the

absorption of light of a shorter wavelength. The difference in wavelengths is called Stoke's Shift. Fluorescence typically occurs from aromatic molecules. A certain molecules pass a three-stage process responsible for the fluorescence and this can be illustrated using simplified electronic-state Jablonski diagram shown in figure 2.

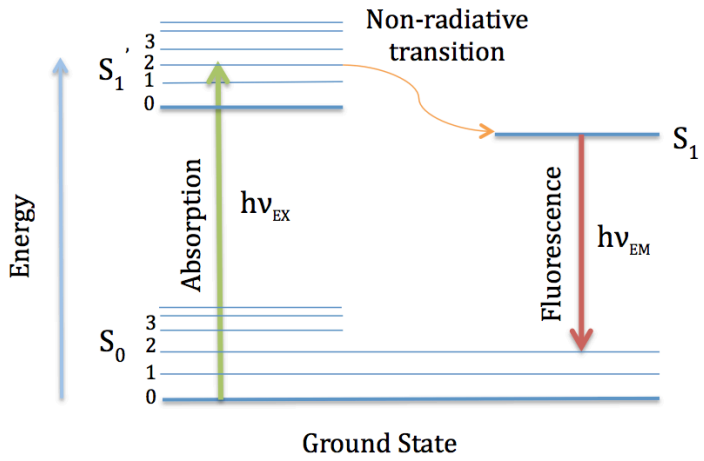

Fig. 2. *Simplified Jablonski's diagram form illustrating the processes involved in fluorescence (adapted from [15]).*

In excited singlet states, the electron in the excited orbital is paired (by opposite spin) to the second electron in the ground-state orbital. Consequently, return to the ground state is spin allowed and occurs rapidly by emission of a photon. The emission rates of fluorescence are typically 10^8 s^{-1}, so that a typical fluorescence lifetime is near 10 ns and typical lifetime for enzyme cofactor flavin adenine dinucleotide is 2.3 ns [15]. A photon of energy $h\nu_{EX}$ (were *h* is a fundamental constant of nature now known as Planck's Constant and *v* is the frequency of the particular photon) is supplied by an external source and absorbed by the fluorophore, creating an excited electronic singlet state (S_1').

Fluorescence can also be used as an analytical tool for the determination of concentrations [16], molecules binding processes [17], identification, detection and imaging of biologically important molecules [10, 18-20].

Fluorescence technology is highly interdisciplinary: numerous biophysical studies have revealed that most biological materials are colorless, making them difficult to quantify or locate by light microscopy [20]. Light-based technologies serve, in this contrast, as fluorescent contrast method, which provides visualization of the specific structures in cells. Without such contrast it is practically impossible to analyze biology derived investigation of cellular morphology and processes in cells in their full biological context [15].

Fluorescence quenching method serves as an advantage in fluorescence microscopy, while in the fluorescence intensity measurements, an increase is rarer compared with the decrease. The intensity is measured directly, without comparison with the reference beam, and in such way fluorescence measurements become more sensitive and precise. Concentrations as low as 10^{-10} to 10^{-12} M can be easily detected and measurement itself is nondestructive and noninvasive. The application of fluorescent agents, fluorophores, with fluorescence quenchers may enable shortening of time-consuming analysis and increase the selectivity and sensitivity of bioanalytical methods. Usually, such systems are based on increasing the fluorescence after separation of the quencher from the fluorescent agent. The combination of fluorescence agents and fluorescence quenching materials [21] has been successfully exploited in some bioanalytical formats, for example real-time polymerase chain reaction [22] and some fluorescence sensors [23]. Usually, such systems are based on increasing the fluorescence after separation of the quencher from the fluorescent agent [22] or amplification of fluorescence resonant energy transferred to the fluorescent agent [24]. Highly fluorescent conjugated polymers have been used for detection of electron-deficient aromatic molecules of trinitrotoluene by efficient fluorescence quenching [25-27].

Above all advantages, fluorescence measurements have some difficulties: fluorescence peaks usually are very broad and overlapping problem may occur in a limited measuring range. Interactions of other molecules, fluorophores may occur and change the signal. Changes of

biological environment or physical parameters (pH, dissolved oxygen) can also influence the measurement results.

1.2.1 Application of biochemical fluorophores in biosensing systems

Fluorescent molecules, also known as fluorophores, are the standard in many bio-sciences, because of their versatility, sensitivity, and quantitative capabilities. Fluorophores are expected not to be inert but rather to respond to their micro-environment or to a chemical species (ion, pH or oxygen). The instrumental properties needed to perform fluorescence measurements are determined by the spectral properties of the fluorophores.

Fluorophore can be divided into two groups: internal (intrinsic, i.e. flavins) that exists naturally and external (extrinsic, i.e. rhodamine), which is added to the sample that does not display desired spectral characteristics. Intrinsic protein fluorescence originates from three aromatic amino acids residues – tryptophan (trp) with excitation and emission maxima of about 280 and 348 nm, tyrosine (tyr) with excitation and emission maxima of about 275 and 303 nm, and phenylalanine (phe), with excitation and emission maxima of about 255 and 282 nm [28], UV-Vis chromophores. In proteins that contain trp as well as one of these other fluorescent amino acids, it is common for the energy absorbed by phe and tyr to be transferred to trp and emit fluorescence around 350 nm [28]. The predominant protein's chromophore is amino acid tryptophan indole group, while phenylalanine has a very low quantum yield, and emission by tyrosine in native proteins is often quenched due to its interaction with the peptide chain, hydrogen bonding to the hydroxyl group, or energy transfer from tyrosine to tryptophan. Indole absorption maximum is at 280 nm and emission - at 340 nm. Indole emission spectrum is highly dependent on the solvent polarity [15]. UV-Vis absorbing chromophores are very useful for chemical reaction following. Denaturation of proteins frequently results in increased tyrosine emission. Tyrosine is the only one of the aromatic amino acids with an ionizable side chain. Tyrosine is one of three hydroxyl containing amino acids. In extrinsic fluorescence proteins can be

covalently labeled with fluorophores, thus producing fluorescent protein conjugates. Labeling proteins with chromophores which has longer excitation and emission wavelengths, is more desired than the aromatic ring acids with absorbance of ultraviolet light (ca. 280 nm) [15]. Fluorescent probes are much more sensitive than UV-Vis absorption chromophores.

The choice when choosing a fluorophore used for biosensing systems mainly depends on:

- Excitation/emission wavelength of the fluorescent product;
- Relative solubility in aqueous environment;
- The interface from pH, solvents or other experimental conditions;
- The chemical-, thermal- and photostability;
- Laser source;
- Filters.

Immunofluorescence can be performed either direct or indirect methods. The conjungation of the primary antibody with the fluorophore (e.i. rhodamine (tetramethyl rhodamine isothiocyanate, TRITC)) is applicable in direct methods. Direct labeling has two major advantages [29]:

1) a single incubation with the labeled reagent is required,
2) provides minimal nonspecific staining and less background.

Additionally, the direct labeling technique allows the use of two or more primary antibodies of the same species or isotype, avoiding the problems with secondary antibody staining [29]. Indirect methods covers primary antibody that is detected by a secondary antibody (which is fluorescence-labeled) that is directed against the first antibody. While it is easier to label secondary antibodies and more than one molecule of the secondary antibody can bind to the primary antibody resulting in an amplified signal, indirect method is more sensitive and more commonly used [30]. The signal obtained in direct methods is weaker when compared to indirect methods, as signal amplification provided by the use of secondary antibodies does not occur.

1.2.2 Properties of fluorescence spectra.

Solution spectra strongly depend on intramolecular interactions. Due to interaction between molecules of specific solution and dissolved substance (formation of complexes, intramolecular transfer of charge) molecular structures with new electronic gallop occur. New stripes that are uncharacteristic for solution-forming substances occur in absorbed spectra and spectra of emission. When interaction between molecules is weak, a solution affects a position and structure of electronic stripes, however form of spectrum remains. Molecules of dissolved substances remain the centres of absorption and emission, and influence of manifests as certain disturbance. Such interactions are called universal. Shifts of stripes originate due to interaction of dipole moments of fluorophores with a field of surrounding solvent and due to specific interaction of fluorophore with one or several molecules of solvent. Changes of dipole moments of fluorophores at the time of excitation require refocusing of surrounding molecules of solvent [31].

Spectra of molecules in nonpolar solvents are similar to steam spectra. Position of stripes and intensity vary slightly. Shift of stripes and spread of oscillatory structure is observed in polar solvents. Effect of solvent on position of stripes and shape depends on the nature of bounces that determine stripes. After replacement of nonpolar solvent with polar, $\pi\pi^*$ stripes move to the side of long waves, whereas $n\pi^*$ move to the opposite side. Shift of $n\pi^*$ stripes to the side of short waves in polar solvents with a group of hydroxyl is explained with formation of hydrogen bonding between molecules of solvent and dissolved substance. Therefore energy of n level decreases. Polar solvents usually form a stronger hydrogen bond with molecules that are in the main state, not in the induced $n\pi^*$ state, therefore an energy of the main state decreases more, an energy of $n\rightarrow\pi^*$ bounce increases and $n\pi^*$ stripes move to the side of short waves. It is convenient to identify the stripe‘s nature in accordance with this shift. However, this feature is not unambiguous, e.g.

when solvent gentility increases, benzoic and petroleum ππ* absorbed by stripe also move to the side of shorter waves [31].

Solvent also affects photoluminescence of organic compounds. In some cases shift of stripes is observes, moderate changes of productivity and duration, in other cases – qualitative changes of fluorescent properties of dissolved substance.

Solvation phenomena usually are observed in solvents. In non-stimulated state molecule is in balance with solvent shell – surrounding molecules of solvent. Stimulation of molecule is very rapid process and solvent shell does not have enough time to adapt to new state of molecule. During stimulation redistribution of electronic density occurs, dipolar moment of stimulated state differs respectively from the main state. Molecular geometry and lengths of interatomic bonds also can vary in the stimulated state. Certain time that depends on physical and chemical characteristics of solvent is required for reorientation of molecules of solvent: temperature, viscosity, polarity, etc. Stimulated molecule reaches a balance with solvent when solvent shell adapts to the state of stimulated molecule. Analogous processes happen in solvent after dis-activation of molecule. Solvent shell reorients and readjusts to the main state of molecule. Stokes shift of molecular fluorescence spectrum depends on time of solvent relaxation. Such dependency is particularly noticeable in spectra of polar molecules. Information about stimulated molecular state, its geometry can be obtained during analysis of solvents influence on absorption and fluorescence spectra, also dipolar moment can be evaluated [31].

Stokes shift of fluorescence is sensitive to solvent polarity. As bigger is dipolar moment of solvent and indicative polarizability, as more intense is Stokes shift. Therefore measurements of fluorescence spectra are often used for the evaluation of the polarity of fluorophore surrounding environment.

1.2.3 Measurements of time-resolved fluorescence

Time-resolved measurements are widely used in fluorescence spectroscopy. Time-resolved measurements contain more information than steady-state data, while these measurements indicates interactions with the substrate or the surrounding of each acting agent or its residues and spectral overlap of absorption and emission does not occur, time-resolved data may be separately revealed [15]. Also, fluorescence lifetime measurements are typically independent of the probe concentration, that is very important while measuring probes with possible changes in concentrations, due to washouts, photobleaching, alterations of optical conditions and other factors.

Fluorescence is described by its lifetime τ. When a fluorescent substances (fluorophores) are excited, the fluorescent light is not instantaneously emitted, but decays over a period. Scattered light and background from sources are allowed to decay over time before a selected part of sample's decay curve is integrated and in such way getting more precise information about investigative. Fluorescence lifetime measurements are very useful for compound identification and complex environment measurements because fluorophore lifetime is independent upon intensity, adsorption or scattering effects.

The decay of the excited state of a molecule to the ground state can be described by the equation:

$$I(t) = I_0 \exp(-t / \tau)$$

where, I_0 is the intensity at time zero (upon excitation) and τ is the lifetime. Although this equation is based on the first order kinetics, usually many fluorescence decays are multi- or non- exponential. This can be attributed to molecules environmental influence or quenching processes.

The study on time-resolved FAD of immobilised GOx [32] have revealed that FAD fluorescence emission of sol-gel immobilized GOx exhibits a three-exponential decaying behavior, each one being dependent on the conformational states of FAD cofactor. This study indicated that time-resolved

fluorescence could be extremely useful for better understanding of processes, which are involved into biocatalysis.

1.3 Glucose oxidase

The discovery of glucose oxidase (GOx) is attributed to Müller. The GOx, also known as notatin (penicillin A), is a homodimeric flavoprotein found predominantly in fungi. Certain fungal species such as *Aspergillus niger, Botrytis cinerea, Penicillium notatum* and *Phanerochaete chrysosporium* have the ability to produce glucose oxidase. The molecular weight of GOx ranges from ~130 kDa to 175 kDa. The GOx enzyme is composed of two identical subunits (the molecular weight of each subunit is aproximatelly 80 kDa) joined together by disulfide bonds. Each subunit carries one molecule of tightly non-covalently bond coenzyme flavin edenine dinucleotide FAD ≈15Å per monomer below the surface. Dissociation of subunits is possible only under denaturing conditions and is accompanied by the loss of the coenzyme FAD [33]. The monomer with approximate dimensions of 60×52×37 Å contains 583 amino acid residues, 17 α-helices and 30 β-strand structures, and consists of two separate structural domains. The cofactor FAD is situated in the first domain. The main FAD interactions with configuration are 23 potential hydrogen bonds, mostly involving the ribose and pyrophosphate groups. Glucose oxidase contains 1 mol of FAD/mol of proteinic enzyme, although some differences are observed in GOx obtained from different fungal species [34].

Femtosecond dynamics of flavoproteins studies have recently been reported [35] and electron transfer (ET) reactions of FAD in glucose oxidase enzyme were described in detail. Study report the charge recombination in GOx takes place in 30 ps and nanoseconds, electron transfer from FAD to tryptophans (Trp)/tyrosines takes two - 1.8 ps (75% component) and 10 ps (25% component) – reaction times. All fluorescence quenching dynamics are attributed to an ultrafast electron transfer between flavins and the aromatic residues, tryptophans and tyrosines, by a one-electron half-reduction reaction of the flavins. The observed decay of the excited-state of flavins is the result of the

electron transfer between isoalloxazine ring and aromatic residues in the protein to form anionic semiquinone (blue neutral form) flavin and cationic residues [35].

D-glucono-δ-lactone is an inhibitor of GOx [36]. GOx protein is catalyzed by beta-D-glucose oxidation of D-glucono-1,5-lactone, which is then hydrolyzes to the gluconic acid. In order to act as a catalyst for GOx, GOx enzyme must hold FAD cofactor (as redox reaction element). During the oxidation-reduction (redox) reaction, bonding and release of the electrons proceeds, while a substance oxidation (electron loss) always is associated with other materials reduction (electron bonding). In GOx catalyzed redox reactions, FAD is reduced to $FADH_2$ and in such way FAD and $FADH_2$ forms a redox couple. Then the reoxidization of $FADH_2$ to FAD occurs owing to molecular oxygen (O_2), and hydrogen peroxide (H_2O_2) is produced as a subproduct (equations 1.1. and 1.2.). GOx (primary form) may again react with a greater glucose amount.

$$\text{Glucose} + \text{GOx-FAD} \rightarrow \text{gluconic acid} + \text{GOx-FADH}_2 \qquad (1.1)$$

$$\text{GOx-FADH}_2 + \text{O}_2 \rightarrow \text{GOx-FAD} + \text{H}_2\text{O}_2 \qquad (1.2)$$

Molecular oxygen is a natural electron acceptor in glucose oxidase-catalyzed reactions, although many other electron acceptors are also able to react in GOx oxidation processes [37, 38]. In the paper [39], the oxidizing substrates were divided into molecular oxygen, quinones, and one-electron acceptors. Generically, two large groups can be defined: the electron donors in the reductive half-reactions, and the electron acceptors in the oxidative half-reaction. Numerous sugars (electron donors) and derivatives of d-glucose are potential substrates of GOx, but that β-D-glucose is by far the best [39]. The second group of electron acceptors involves benzoquinones and naphthoquinones, which indicates that both the two-electron acceptors and molecular oxygen are good substrates of GOx [39].

The catalytic cycle can be divided into two half-reactions (considering the reaction of the oxidized and reduced enzymes studied separately), referred

as the reductive and the oxidative half-reactions. The mechanism of proposed reaction could be represented hereinafter in figure 3:

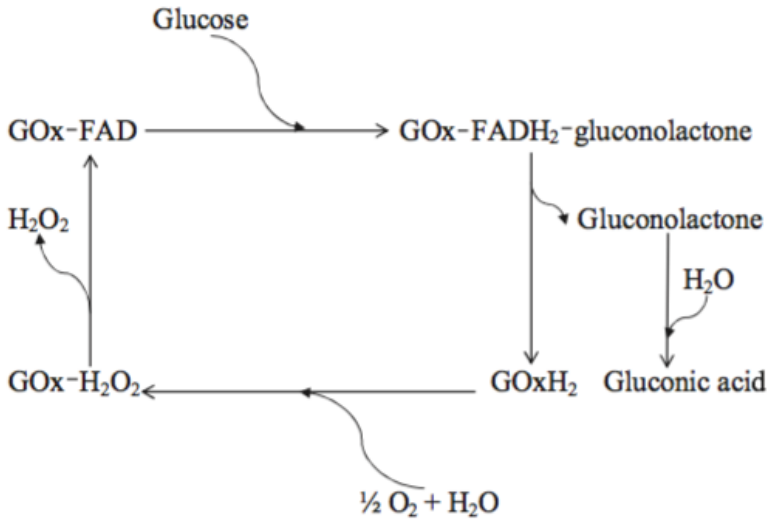

Fig. 3. *Scheme of GOx enzymatic reaction [40].*

The GOx overall catalytic reaction, depending on the enzyme and substrates, proceeds through a *ping-pong bi-bi*, nomenclature proposed by Cleland [41], mechanism (i.e. substitude-enzyme ternary-complex mechanism in two-substrate, two-product case) [39, 42]. And even inactivation of GOx with the removal of FAD cofactor, the resulting apo-glucose oxidase still binds glucose [43] and this can be applied as a method of glucose sensing based on inactive form of GOx.

The most common enzyme used in various interdisciplinary sciences is glucose oxidase and since the first report by Müller [44] in 1928 and a review of chemical mechanism by Bentley [45] in 1963 made a profound change in our knowledge about GOx and numerous possibilities of applications started to expand.

1.4 Flavin adenine dinucleotide

Flavin adenine dinucleotide (FAD) belongs to a very important group of flavins that are highly versatile and are involved in a wide range of biological processes, catalyzing reactions ranging from redox catalysis to photochemistry, from DNA

repair to light emission. Flavoproteins can function with cofactors for catalytic reactions such as glucose oxidase. Flavins are the most frequently exploited organic redox coenzymes in nature. They exist in three redox states that are flavoquinones (fully oxidized state), flavosemiquinones (one-electron reduced state) and the flavohydroquinones (fully reduced state). Flavins are known to be electron transport cofactors on organisms and can undergo electron and proton-coupled electron transfer reactions, which are involved in one-electron and two-electon transfer reactions [46, 47], see figure 4.

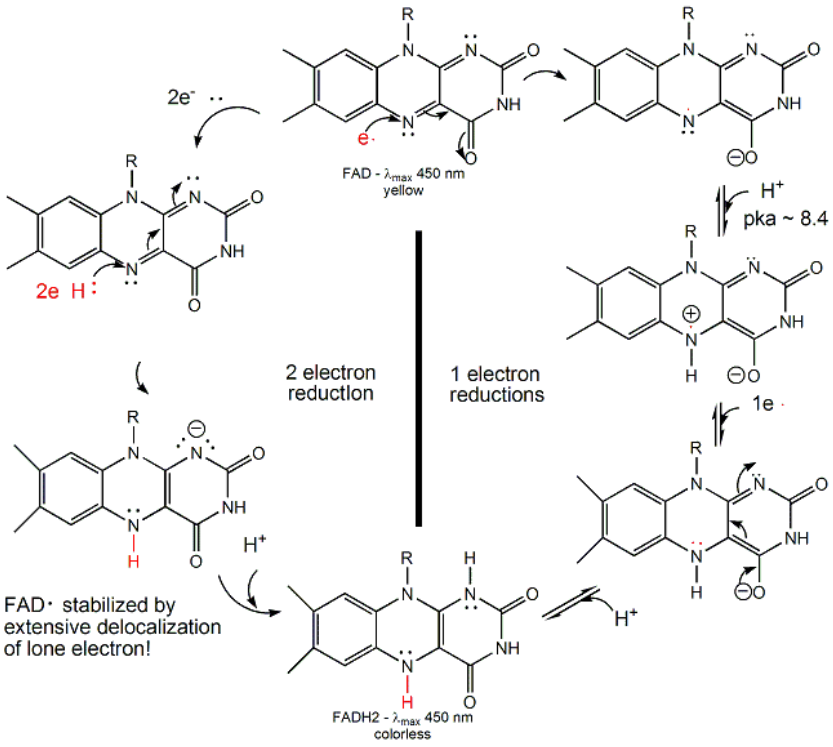

Fig. 4. *The lipophilic electron carrier, ubiquinone. (Picture's source http://employees.csbsju.edu/hjakubowski/classes/ch331/oxphos/fad1or2e.gif)*

Flavins excitation and emission maxima are around 450 and 520 nm, respectively, in aqueous solutions, but with a red-shifted emission peaked at 560 nm for dried flavins [28].

FAD is an autofluorescent metabolic cofactor used to oxidize a substrate. FAD is involved in the catalysis of many different redox-sensitive reactions of physiological importance. As its name indicates, it is a

dinucleotide in which one of the heterocyclic components is flavin and the other is adenine. The fluorescence originates from the isoallaxazine ring group (the isoalloxazine ring is amphipathic – xylene portion is hydrophobic, pyrimidine moiety is hydrophilic) that is in close contact with four aromatic residues of Tyr-515, Trp-426, Tyr-68, and Trp-111 of the molecule. The observed fluorescence quenching of the FAD is due to its interactions with these residues [35]. Also, the redox property of flavin and Trp drives the electron transfer reaction [35]. FAD decaying kinetics depends highly on the interaction with the neighboring adenine group and microenvironment [48]. The fluorescence emission of FAD also depends on solvent polarity, as evidence by the Stokes shift.

FAD is a reducing agent and when it oxidizes a substrate, the coenzyme is reduced to $FADH_2$ (Fig. 5).

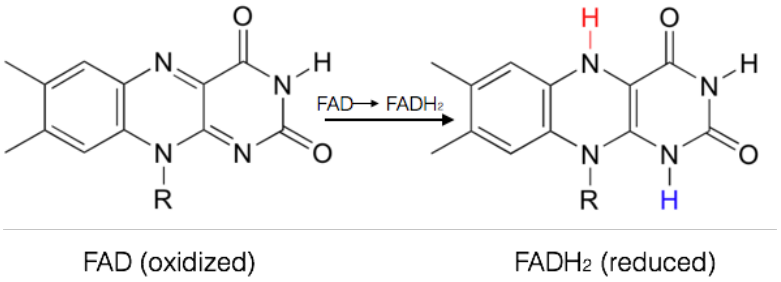

Fig. 5. *Oxidized and reduced (hydrogenated) forms of FAD.*

FAD exists in two conformations – an extended, open conformation, and a closed one, stacked conformation and when interpreting the fluorescence lifetime measurements, three ranges can be assumed to characterize decay: long (about 2 – 3 ns), intermediate (about 300 ps), and short (less than 10 ps) lifetime, that can be ascribed to open, intermediate and close configurations [32].

The dependency on sensitivity of internal interactions and microenvironment makes FAD fluorescence kinetics an excellent tool for the characterization of biochemical reactions.

1.5 Bovine leukemia virus and its surface glycoprotein *gp*51

Bovine leukemia is contagious, worldwide common chronic viral disease caused by bovine leukemia virus (BLV), which was formerly isolated in culture in 1969 [49]. BLV, a deltaretrovirus, causes B-cell leukemia/lymphoma in cattle and is prevalent in herds globally.

The virus infection is spread horizontally among animals in contact. More than a half BLV-infected animals are asymptomatic carriers of the virus during their entire life. In these animals, neither clinical signs on organs, nor any visible symptoms are evidenced. However, almost all these animals have detectable antibodies, which can be identified by the presence of anti-BLV antibodies and/or of proviral DNA [50], found, because of the infected lymphocytes, in the body fluids (blood, milk, saliva, urine, nasal secretions). BLV is a major animal health problem worldwide causing important economic losses.

Bovine leukemia is also potentially a public health hazard, because BLV belongs to the same oncogenic retrovirus family, which belongs to the deltaretrovirus genus and is structurally and biologically closely related to the human T leukemia, T-lymphotropic type and lymphoma I and type II viruses (HTLV-I, HTLV-II) [51], old world monkey Simian T-lymphotropic viruses (STLVs), human immunodeficiency I and type II viruses (HIV-I, HIV-II), primates, cats and bovine immunodeficiency viruses [52]. The virus particle is spherical and enveloped with surface glycoprotein projections. The viral envelope is formed by a cell-derived lipid bilayer with inserted proteins, specifically, a transmembrain protein (*gp*30) and s surface protein (*gp*51). The *gp*51 protein ensures the recognition of the cellular viral receptor. A schematic representation of a typical structure of retroviruse is presented in figure 6.

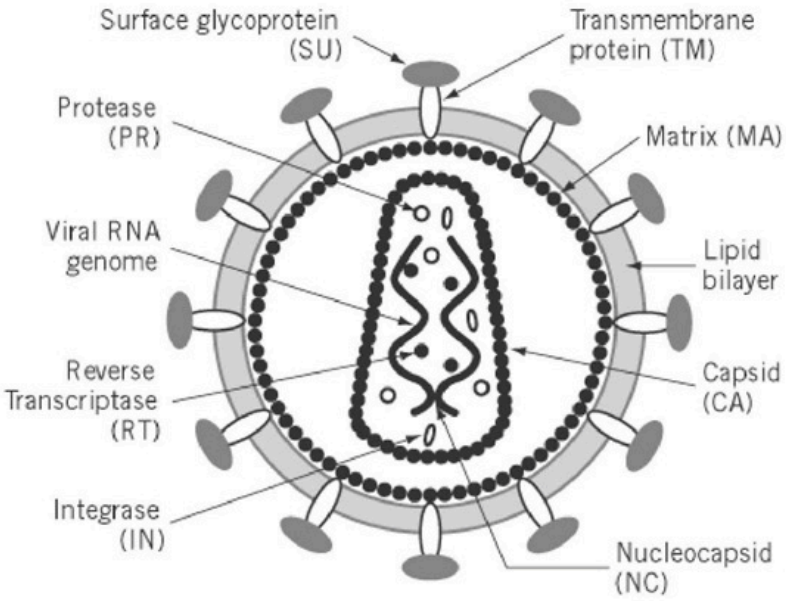

Fig. 6. *Schematic representation of a typical retrovirus virion, illustrating structural and enzymatic proteins [53].*

Globally, these epidemiological studies receive special attention, because in some regions the leukemia's morbidity of people and bovine is significantly higher [54].

Clarifying epidemiological situation of bovine viral diseases, diagnostic tools for these diseases can be more effectively applied in order to strengthen the prevention and eradication means. As cattle may be infected at any age, including the embryonic stage, it is very important to have early diagnosis.

For BLV detection, indirect (serological) methods are still dominant and typical investigation is based on signals generated by the formation of antigen-antibody complex. Several methods have been used to detect and to visualize antigens with the use of antibodies. Detection of the BLV specific antibodies through agar gel immunodiffusion (AGID) reaction, an indirect enzyme-linked immunosorbent assay (ELISA), polymerase chain reaction (PCR), indirect fluorescent antibody technique (IFAT) and immunoblotting are the most commonly used methods. Serological diagnosis of enzootic bovine leucosis (EBL) is mainly based on the screening of the samples for *gp*51 antibodies. If the cattle is infected by BLV 1IgY-class antibodies against viral structural

proteins response to an infection is generated.

Enzyme-linked immunosorbent assay method. Enzymes as immunometric tags have the largest share in immunometric methods and they must have several important characteristics to be used for antibodies and antigens tagging: high catalytic constants; the enzymatic reaction products must be easily identifiable; substrate and product cannot affect antibody antigen interactions; enzyme must remain stable. An indirect ELISA method is the most common type of amperometric immunosensors. In retroviral infections, ELISA has been used mainly as a screening test. The aim of ELISA test is to detect antibodies in serum *via* the antigen-antibody complexes. Various types of ELISA (indirect, sandwich, competitive, multiple and portable) have been employed with modifications. The key step of ELISA methods is the detection of antigen by adhering or immobilizing the antigen or antigen-specific antibody directly onto the surface. This method provides quantitative results and is sensitive, highly reproducible and less time-consuming than the conventional AGID test.

ELISA for EBL is mostly based on the use of partially purified BLV *gp*51.

Agar gel immunodiffusion. The AGID test was developed in the 1970s and has become the first serological test for serodiagnosis of enzootic bovine leucosis. It is a passive diffusion of soluble antigens and/or antibodies toward each other leading to their precipitation in a gel matrix. Although the AGID test is less sensitive and specific than ELISA, AGID test has been widely used mainly for the routine diagnosis of serum samples because of the simplicity, low requirements for reagents quantity, and these tests are used to detect antibodies to all subtypes. In the study [55], a recombinant protein was used for detection of antibodies in sera of BLV-infected cattle as AGID antigen. The AGID results using recombinant BLV *gp*51/*gp*30 were reproducible and consistent, and there were no significant variations in repeated tests [55].

Polymerase chain reaction. Detection of BLV by polymerase chain reaction was described in numerous papers [56-58]. However, the PCR has

some limitations in the detection concerning variability in the BLV genome and highly mutable RNA genome, were some isolates are hardly detectable [59]. In the study [60], a substantial number (more than 100) of various infected cattle from different areas (to cover diverse infected animals with different strains of BLV) were used. A real-time PCR with molecular beacons and nested PCR assays to detect BLV in milk and blood were investigated. 3 primer pairs from 3 different genomic regions (*pol, env, gag*) were evaluated by nPCR and primers from the *pol* region were further evaluated in a real-time PCR. Although real-time and nested PCR methods are not designed to replace traditional antibody assays, they can provide a useful supplement for the early detection of BLV (infection can be detected from 2 to 4 weeks earlier when using serology [58]) and for confirming BLV infection from blood and milk specimens [60].

Indirect fluorescent antibody technique. A form of fluorescent antibody technique commonly used to detect serum antibodies and immune complexes in infected tissues by formation of antigen-antibody complex which is then labeled with fluorescein-conjugated anti-immunoglobulin antibody. Indirect fluorescent-antibody technique (IFAT) for serological diagnosis was described in [61, 62]. The studies showed that IFAT is remarkably sensitive in the detection of acute-phase antibodies, is inexpensive, readily adaptable to clinical settings possessing immunofluorescence. Another study [63] on IFAT and ELISA for diagnosis of BLV concluded, that The percentage of BLV-infected animals detected with the employed FAT was greater than that obtained with the ELISA. The lack of detectable specific antibodies in BLV-positive animals may also be caused by mutations within the *env* gene. The FAT indirect reaction applied in the present study allows for the detection of viral proteins directly in varied cells of an infected organism, regardless of the infection phase, concomitant diseases, animal age, pregnancy, and lactation month. Therefore, it is possible to detect BLV even in early infection phases when *gp*51 antibodies are not yet synthesized or when their level is low and below the detectability with the ELISA [63].

Immunoblotting (western blotting). The immunoblotting technique provides information about the presence or concentration of an antigen by combining protein separation *via* gel electrophoresis in a carrier matrix with specific recognition of antigens by antibodies. Immunoblotting is useful when the antigen of interest is insoluble or readily. Western blotting (WB) usually serves as reference conformatory assay or supplemental test in retroviral infections. Western blot assay should not be used as a screening test and if the protein degradates quickly, WB won't detect it well.

Piezoelectric systems, electrochemical detection systems, surface plasmon resonance technique might be applied to simplify and improve upwards mentioned methods.

Piezoelectric systems. The main part of piezoelectric immunosensor's is a resonator with the functionalized transducer, which usually is covered with an antibody or an antigen. An obvious advantage of such immunosensors is the direct registration of biochemical interaction without the need of additional labels. During the initial studies on immobilized BLV envelope protein *gp*51 [64], piezoelectric immunosensor response was monitored as the control of mass transport to/from the electrode. A quartz crystal microbalance (QCM), which is high-frequency transducer, has been used to register interaction of *gp*51 with specific antibodies from the blood serum of BLV-infected cattle. Protein *gp*51 was cross-linked with glutaraldehyde on the platinized surface of quartz crystals to prevent fast desorption. The application of piezoelectronic sensors for determining bacterial and viral antigens has apparent advantage while there is no need of biochemical markers for the registration of binding [65].

Electrochemical detection systems. Electrochemical detection systems (EDS) transform electrochemical information into analytically useful signals. EDS usually consists of two basic parts – chemical recognition systems and transducer. EDS has low detection limits, wide linear response range, good stability, and reproducibility. Electrochemical impedance spectroscopy (EIS) measurements were applied in the research on bovine leukemia virus (BLV)

protein (*gp*51) entrapped within electrochemically synthesized polypyrrole (Ppy/*gp*51) [65]. This study showed that EIS based studies can provide a method to follow the antigen–antibody interaction at antigen or antibody modified electrode surfaces and EIS based immunosensing features advanced quantifying of the interaction between antibody and antigen in real-time measurements [65].

Surface plasmon resonance. Surface plasmon resonance is a technique for detecting changes in refractive index occurring at the metal surface upon interaction between the two biospecific partners (by immobilizing one of the partner of the pair on a metal surface, allowing the other partner to flow in excess over that surface). SPR was introduced in the early 1990s as the underlying technology in affinity biosensors for biomolecular interaction analysis. SPR method can be applied for the precise determination of analytes while method uses immediate analyte interaction with immobilized bio-material and detection in real-time, which allows detailed investigation of these substances interaction kinetics.

The SPR method was applied for the determination of protein *gp*51 in several studies [66, 67]. An immunosensor for the determination of bovine leukemia virus antigen (*gp51*) was developed using SPR-chip coated with gold. It has been demonstrated the successful application of frag-anti-*gp*51 for the design of SPR-immunosensor for *gp*51 detection. Developed immunosensor is sensitive and able to interact with a larger amount of analytes [66]. In the work [67] the SPR sensor was used for the detection of the level of anti-*gp*51 in the blood serum and it was shown such methods are more sensitive, rapid and simple that compared to AGID methods.

However, serological tests have a disadvantage – antibodies may not be produced until approximately 14 weeks after the infection of bovine. Meanwhile, the animal could transmit the virus to others. Confrontation of various methods might be useful to improve detection of serological diseases.

1.6 The enzyme horseradish peroxidase

The term *peroxidase* first was mentioned by Linossier in 1898. Peroxidases catalyse the oxidation of electron donor substrates by H_2O_2. The reaction consists of three-step process – the enzyme is first oxidized by H_2O_2 and then reduced back by two steps to the native form, with formation of two intermediates. Horseradish peroxidase (HRP) is among the most intensively studied peroxidases. It is a heme protein with 308 amino acid residues and has a single chain polypeptide containing four disulfide bridges. HRP contains two different types of metal center – single iron(III) protoporphyrin IX and two calcium atoms. Both are essential for the structure and functional integrity of the enzyme [68]. HRP catalyzes the transfer of two electrons from a substrate to hydrogen peroxide to produce an oxidized substrate and water. For bio-detection, these HRP substrates generate a fluorescent signal upon oxidation. HRP is generally used as a label enzyme in biosensing systems. The suitability of HRP for labeling is due to its small molecular weight (~44 kDa, ~ 18% of the molecular mass is due to 8 covalently linked carbohydrate chains), while small size allows greater penetration into sample tissues, and stability to chemical modification [69-71]. Labeling of immune reagents with HRP requires covalent linking to the selected reagent. Improved coupling methods is suggested in [72]. Immunoglobulin G (IgG) with HRP using cyanuric chloride (2,4,6-trichloro-1,3,5-triazine, CC) as a bridging molecule was used and gave comparable sensitivity in competitive ELISA. The principal advantage of this method is that the first chlorine in CC is reactive toward both amino and hydroxyl groups in HRP molecule [72]; the lack of free amine groups in HRP molecule in such way become an advantage. The high titre values (1/40,000 to 1/70,000) demonstrated the efficiency of this coupling method.

Polymers have attracted a strong interest to apply them for fabricating enzymes functional systems. Various methods to improve HRP functionality are proposed: chemical modification, stabilizing additives, derivatization, crystallization, genetic engineering, and immobilization.

Immobilizing HRP on electrodes modified with conducting polymers improves the properties of the electrodes: (i) increases and facilitates the response towards H_2O_2, (ii) increases linear range of response, (iii) reduces detection limit, (iv) offers excellent enzymes electrocatalytic activity, (v) provides good sensitivity and selectivity, (vi) guaranties the simplicity of the analytical method in the application [73-75].

1.7 Conductive polymers and their application in biosensing systems

With the invention of conductive polyacetylene in the 1970s, conducting polymers have received significant attention. The 2000 Nobel Prize to Alan J. Heeger, Alan G. MacDiarmid, and Hideki Shirakawa for their discovery and development of electrically conductive polymers was a breakthrough in the field of polymers. The scientific and engineering interest is due to electrical and optical properties of metals and semiconductors, processing advantages, mechanical flexibility and high thermal stability.

Conducting polymers can be attributed as electroactive biomaterials [76].

There are three main groups of conducting polymers:

- Electron-conducting polymers,
- Proton-conducting or inherently-conducting polymers,
- Ion-conducting polymers.

The most studied conductive polymers are the π–π conjugated polypyrrole (Ppy). Conjugated polymers have alternating saturated and unsaturated bonds along the main-chain backbone. Saturated single bonds have σ–bonds while unsaturated double bonds have a combination of σ–bond and π–bond.

Conjugated polymers may act as electronic conductors, and redox switching further controls this property.

Polypyrrole (Ppy) is an organic polymer formed by induction of polymerization of pyrrole. Although polymerization can be reached by

different ways (chemical initiation by oxidative agents, electrochemical activation, photo induced current), usually the PPy is produced by electrochemical and chemical reaction, though other not mentioned here polymerization methods could be applied also.

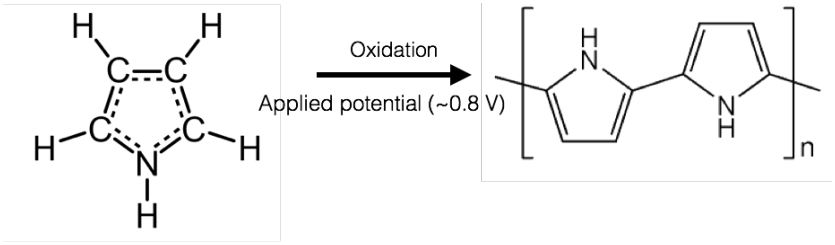

Fig. 7. *Polypyrrole and its derivatives can be prepared by (I) chemical or (II) electrochemical oxidation of pyrrole.*

Chemically synthesized conjugated polymers are initially insulators in a neutral state. Ppy's backbone in the reduced state is neutral and in the oxidized state – positively charged. Chemical methods have some advantages such as easy preparation of Ppy particles of controllable size, possibility to uniformly perform overoxidation of polymer, ability to produce appropriate Ppy structures (nanoparticles, coatings). However, there are some disadvantages of using chemical synthesis method: a little amount, compared to the bulk solution, is covering the surface of interest (the surface coverage is ineffective), Ppy is almost insoluble in usual solvents and poorly adhesive to the most of surfaces.

In electrochemical synthesis the deposition of Ppy on electrodes and the growth of the Ppy film depends on electrical characteristics of non-conducting Ppy growth, which is self-limiting although by contrast inherent conductivity and charge connectivity between anode and Ppy makes their growth virtually unlimited [77]. Thickness and morphology of deposited Ppy layer might be controlled (yield od formed polymer in the term of through the electrochemical system passed charge is close to 100%), and various solvents might be applied.

This aspect is very important when using biomaterials for their entrapment by Ppy, while usually their environment concerns water solutions at neutral pH. Electrochemically synthesized polypyrrole features good conductivity, high surface coverage.

In summary, chemical synthesis is used when large quantities of material are required and involves strong oxidizing agents; electrochemical synthesis is used when control over material thickness, geometry, location and good quality of films are required [77].

Also Ppy can be produced by UV-catalytic reaction induced by H_2O_2 [78, 79]. As an oxidant under UV irradiation, H_2O_2 can be used to induce the polymerization of pyrrole. Photolysis of H_2O_2 led to the formation of hydroxyl radicals, which then initiated the oxidative polymerization of pyrrole. This approach avoids the issue of metal residue in the polymer caused by metal oxidants, whereas the reaction efficiency is low [78].

An electrically conducting materials based on π–π conjugated polymers are often used as synthetic electrocatalysts or immobilisation matrix for different biomolecules. Moreover, conjugated polymers provide effective immobilisation basement for biomolecules on different substrates [80]. Ppy could be also used as a matrix for the immobilization of enzymes, which enables biological recognition of the analyte, and as a fluorescence quencher, which increases the selectivity of fluorescence-based detection [81]. Ppy has been shown as one of the most suitable matrixes for electrochemical immunosensors [22]. The Ppy is conductive, has biocompatibility in combination with biomaterials [23], exhibit unique affinity properties [82], has outstanding biocompatibility in vivo [83], and features redox activity [84]. Ppy is thermally stable [85] and perfectly stable at room environment [23]. Thermal degradation occurs when loosing or with the decomposition of dopant, and depending on the dopant ion the degradation occurs only above 150 – 300°C. To enhance its biological recognition functions, Ppy is easily modified by proteins [26], and molecular imprints of high [27, 85] and low [25] molecular

weight. These properties make the Ppy extremely useful for the design of a variety of biosensors.

In this thesis, in the research on BLV proteins *gp*51 and horseradish peroksidase (HRP) the Ppy was used as a matrix for immobilization of these proteins, which enables biological recognition of the analyte, and as a fluorescence quencher, which increases the selectivity of fluorescence-based detection. In the work with GOx, the enzyme was coated by a (Ppy) shell (GOx/Ppy-nanoparticles) and the ability of Ppy to decrease the unfolding process of the enzyme was investigated.

1.7.1 Some aspects of applications of polypyrrole for the immobilization of enzymes

The way by which enzymes are immobilized is crucial in development of enzymatic biosensors. Various techniques, i.e. adsorption, covalent binding, entrapment, encapsulation, cross-linking, self-assembly, were applied for the immobilization of enzymes to preserve their activity. The immobilization of enzymes within polypyrrole matrice provides very convenient and stable biocatalyst interface preserving high level of enzymes activity. Electropolimerized Ppy matrix acts as an interface for direct electron transfer between enzyme and electrode. To facilitate direct electron transfer the Ppy backbone should approach the redox site of enzymes.

The direction and speed of electron transfer from enzyme occurs principally by adjusting the distance between redox cofactors [86]. Marcus theory states that electron transfer decays exponentially with increasing the distance. Distance between redox centers and driving force (e.g. the potential difference) control of electron transfer reactivity is crucial in enzymatic reactions. Accordingly, to provide fast and direct electron transfer from immobilized redox enzyme to the transducer, the distance should be as short as possible and the orientation of immobilized enzyme should be the most suitable for electron transfer. From this point of view, enzymes entrapment within conducting polymer matrixes has some disadvantages.

A rotating ring- and/or disk-electrodes in which the platinum disk- or ring-shaped electrodes were coated with a polypyrrole/glucose oxidase film deposited by electrochemical polymerization, has been used to characterize the Ppy/GOx electrode [87]. From this study, it is clearly apparent that the biotransformation of glucose takes place mainly at the polypyrrole film/solution interface independently on electrode rotation speed and that the catalysis is not limited by oxygen only. Glucose oxidase catalyzes the oxidation of substrates by electron transfer to the oxygen and in this process the H_2O_2 is formed. However, it is difficult to interpret influence of the reaction of hydrogen peroxide and polypyrrole. There was a suggestion [87] that such reaction decreases the electrical conductivity. Reaction of Ppy with H_2O_2 leads to oxidative charge transfer as well as oxidative degradation and in such processes unfortunately reduces charge carrier mobility.

A study [88] of immobilization of glucose oxidase enzyme in thin polypyrrole films investigated influence of polymerization conditions and film thickness on the activity and stability of the immobilized enzyme. Study showed that concentration of pyrrole monomer, which polymerizes and forms polypyrrole, is important factor for the control of thickness of the polymer film and the amount of enzyme, which can be immobilized in the films. Above a thickness of 1.0 μm, the apparent activity of the immobilized enzyme increases linearly with increasing film thickness. After the loosely entrapped enzyme is leached from the polymer film, the rate of loss in activity is very low indicating that the well-entrapped enzyme, as well as the polypyrrole films, exhibit good stability and the reproducibility of the immobilization technique is excellent [88].

1.8 Some aspects of catalytic biosensors based on conducting polymers

The quantitative analysis of selected compound samples usually has been achieved by highly sophisticated chromatographic and spectroscopic techniques. The demand for fast response time, high specificity, rapid and continuous measurements and that can be easily integrated into technology

created a new type of sensors – biosensors. Enzyme based biosensors are the earliest biosensors, introduced by Clark and Lyons in 1962. Enzymatic (catalytic) biosensors rely on the enzyme-catalyzed conversion of a non-detectable substrate into a detectable product. Enzymes are very efficient catalysts and the most important aspect while creating catalytic biosensor is the immobilization of the bio-catalyst. Conducting polymers as immobilization materials perfectly fits with this aspect. Number of papers [89-92] reported various immobilization techniques (i.e. adsorption, covalent binding, entrapment, encapsulation, cross-linking, self-assembly) onto and/or within conducting polymer based materials during the development of catalytic biosensors. Most often polypyrrole is used for the development of catalytic biosensor as immobilization material. From the catalytic perspective, Ppy has very important advantages such as being a catalyst support; biocompatibility to working environment; electrocatalytic activity; a biomolecules stabilizing material; enhanced catalyst activity reaction.

Ppy immobilization matrix effectively serves as coupling of enzyme to electrode material. Such method is very attractive due to its simplicity and the empowerment to control the enzyme layer thickness and enzyme loading. A simple electrode preparation procedure allows quick electrode renewal. Also Ppy coating is found to be an effective barrier to the electroactive interferents [93].

Glucose oxidase and horseradish peroxidase are the most widely used enzymes for catalytic biosensing systems that has been reported in literature [40, 94-97]. Such system is very attractive, while formation of biologically active layer can be performed by "one step" procedure and prepared on miniaturized materials. The detection of analyte is based on specific catalytic conversion by bio-catalyst interacting with appropriate signal transducer. Biological element combines with the analyte of interest and does not change it chemically, but converts to an auxiliary substrate. These specific interactions of analytes with bio-recognition elements results in changes of physicochemical properties that can be detected and measured.

1.9 Gold nanoparticles in biosensing systems

Gold nanoparticles have received considerable attention due to their attractive physical and chemical properties such as: redox activity [98], advanced conductivity [99], high thermal conductivity, high resistance to oxidation [100], and advanced optical properties [101]. Therefore, they have been extensively explored due to their diverse applications in photonic and antireflective materials [102], catalysts [103], analytical sensors in SERS spectroscopy [104, 105] and biological probes or markers [106, 107]. Moreover, gold nanoparticle monolayers formed on solid substrates have found various applications for example as new substrates for surface enhanced spectroscopy [108]. These thin films are usually produced *via* physical and chemical methods such as: sputtering [109], evaporation [110], chemical vapor deposition (CVD) [111] and self-assembly of metal colloids [112]. Increasing attention is paid to preparation of gold mono- and multi-layers using simple and reliable methods [113]. Many works concerning the issue have been devoted to investigations of citrate-stabilized gold nanoparticle deposition on positively charged anchored monolayers of polyelectrolytes, dendrimers and silanes [114-120].

AuNPs are proposed as biolayer for immunosensors to amplify the signal and increase the number of active sites on the selective surface. Gold nanoparticles are ideal for developing novel sensing strategies, because of their excellent possessing features [121]:

- Straightforward synthesis;
- High stability;
- Unique physicochemical properties which are geometrically dependent;
- High surface-to-volume ratio;
- Excellent biocompatibility using appropriate materials;
- Properties of AuNPs can be easily tuned by varying their size, shape, and the surrounding chemical environment;
- AuNPs platforms are very suitable for multifunctionalization with a wide range of organic and biological substrates.

These attributes led to develop unique sensing strategies with improved sensitivity, stability, and selectivity, handling large volumes and low-concentrations samples [122].

The scientific synthesis of colloidal gold dates back to Faraday's work in 1857. The breakthrough came with the Turkevich approach for the gold nanoparticles synthesis, using citrate reduction of chloroauric acid in water, in 1951. Citrate caped gold nanoparticles are very suitable for biosensing systems, while their surface of weekly bound citrate coating is negatively charged and can be easily exploited for electrostatic interactions with various positively charged biomolecules like antibody, enzymes, proteins. In most cases, AuNPs are conjungated directly to the proteins and other biomolecules due to early mentioned electrostatic and hydrophobic interaction compatibility. The presence of sulfhydryl groups of proteins form strong bonds with the gold material [123]. Moreover, AuNPs do not affect the functional consequences after the large protein (150 kDa) immobilization [123] and can be used for the detection of target analyte specifically, improving enzymes's activity and stability [124]. However, tighter binding and smaller protein systems may affect protein structure and function [123] and overall bio-reactivity of nanoparticle. Depending on the specific properties of nanoparticle surface and dimension, the environmental conditions and actual protein characteristics, NPs either affect or does not have an impact on proteins structure and functions [125, 126].

Another positive feature is the nanoparticle-curved layouts. The surface-chemical properties of nanoparticles provide flexibility and enhanced surface area to adsorbed biomolecules, compared to those with adsorption on planar surfaces [127]. NP surface can modify the structure and function of the adsorbed protein and mediate biological effects [126]. Gold NPs were shown to influence the structure and processes of proteins. The study of citrate-caped AuNPs on the amyloidogenic protein [128] introduces with common process of protein, fibrinogenesis, influenced by interaction with NPs. Authors present detailed structural characterization of the interaction between a fibrillogenic protein, β_2-

microglobulin, and a 5 nm hydrophilic AuNP. Experiments show that the protein-nanoparticle interaction is week in the physiological-like conditions and do not induce protein fibrillation [128]. Another paper described the effect of AuNP morphology on adsorbed protein structure and function [129]. Adsorbed enzymes, lysozyme (Lyz) and α-chymotrypsin (ChT), onto synthesized gold nanospheres and gold nanorods have been investigated. In the case of Lyz, adsorption on gold nanospheres and gold nanorods resulted in a 10% and 15% loss of secondary structure, respectively. ChT retained most of its secondary structure and activity on gold nanospheres and gold nanorods. Adsorption of ChT on the gold nanorods surface allowed the conjugates to recover activity and remain stable. This paper [129] demonstrated, that protein adsorption is affected by AuNP morphology, though the extent of the effect is protein-specific [129].

In this thesis, AuNPs electrokinetic properties were investigated in detail for a future perspective to form Ppy layer on their surface.

2. Experimental

Materials and methods

In this chapter the technologies of preparation of glucose oxidase and conducting polymer used for investigation of fluorescence is presented. Preparation of detailed report gives account also of the preparation of monolayers for gold particles deposition investigation. This section gives a detailed description of the procedures that was followed in completing the experiments discussed in chapter 3.

2.1 Materials

All chemicals were of analytical grade and were used without further purification.

The solutions were prepared in ultrapure water. The trisodium citrate dihydrate (ACS) P.A. was purchased from POCH S.A., (Gliwice, Poland). The hydrogen tetrachloroaurate, sodium chloride, sodium hydroxide and hydrochloric acid were commercial products of Sigma Aldrich.

The poly(allylamine hydrochloride) (PAH), an organic cationic polyelectrolyte, was used for mica surface modifications. PAH, having an average molecular weight of 70 000 Da, was purchased from Polysciences, Inc. (Warrington, US). Natural ruby mica sheets were supplied by Continental Trade Ltd. (Warszava, Poland). Mica sheets were freshly cleaved and used without any pre-treatment.

Ultrapure water, used throughout this investigation, was obtained using the Milli-Q Elix&Simplicity 185 purification system from Millipore SA (Molsheim, France).

GOx (E.C. 1.1.3.4.) from P. vitale (130 units/mg) was purchased from BIOTUL (Kiev, Ukraine). Glucose was obtained from Carl Roth Gmbh (Karlsruhe, Germany). Pyrrole and other chemicals were purchased from

SIGMA–ALDRICH CHEMIE GmbH (Steinheim, Germany). Unless otherwise stated, reagents were of analytical grade and used as received.

Pyrrole, HRP, rhodamine B (rhoda- mine), and fluorescein-5(6)-isothiocyanate (fluorescein) were obtained from Sigma (St Louis, USA). The Ppy was further purified by passing it through a 5 cm length column packed by Al_2O_3. Before use, rhodamine B and fluorescein were dissolved in 96% ethanol and the solution was then added to 50 $mmolL^{-1}$ phosphate buffer, pH 7.2. The final concentration of both solutions was 12.5 $\mu molL^{-1}$. Purified and lyophilized bovine leukemia virus (BLV) protein gp51 and blood serum of BLV-infected cattle containing antigp51– Ab were obtained from Biok (Kursk, Russia). The secondary antibodies, which were labeled by HRP (Ab*), were obtained from the institute of Pourquier (Montpellier, France).

2.2 Preparation of glucose oxidase self-encapsulated within polypyrrole for fluorescence measurements.

2.2.1 Preparation of chemicals

Analytical grade chemicals were used for the preparation of buffers. All solutions were prepared in HPLC-grade water purified in a Purator-B Glas Keramic (Berlin, Germany). Pyrrole was purified by passing 1.5 mL aliquots through a neutral Al_2O_3 column (5.0 cm length and 0.4 cm diameter) to remove all coloured compounds. Glucose stock solutions were prepared at least 24 h before use to allow glucose to mutarotate and reach equilibrium between its α and β forms. When needed the GOx solution (1.35 $mgmL^{-1}$) in 0.05 M sodium acetate (Na-acetate) buffer, pH 6.0, was freshly prepared from powder of the enzyme. All solutions were stored and all measurements were performed at 20 °C.

The samples were prepared as polymerization solutions in 0.05 M Na-acetate buffer, containing 1.1 $mgmL^{-1}$ of GOx, 16 mM of glucose and 236 mM of pyrrole, within pH values varying in the range from 1.0 to 9.0. Fluorescence dependence on pH and some other parameters were investigated.

2.2.2 Investigation of fluorescence

Fluorescence was measured by a detection system based on a low-stray-light double monochromator (JY HRD1) and a photomultiplier (Hamamatsu R1463P) operating in the photon- counting mode. A 325 nm He–Cd laser was applied for optical excitation of the samples.

2.2.3 Investigation of time-resolved fluorescence

Time-resolved measurements were performed by using the Jasco V670 spectrophotometer for absorption spectra of investigated glucose oxidase (GOx) samples. PMMA cuvettes with 1 cm length optical path were used for all optical measurements. Fluorescence spectra and fluorescence decay kinetics were measured with a time-correlated single photon counting spectrometer Edinburgh-F900 (Edinburg instruments, United Kingdom). A picosecond pulsed diode lasers EPL-375 emitting picosecond duration pulses was used for the excitation at 375 nm with an average power of 0.15 mW/mm^2. The pulse repetition rate was 2 MHz and the time resolution of the setup was about 100 ps taking into account temporal deconvolution procedure. All fluorescence spectra were corrected for the instrument sensitivity.

2.2.4 Electrochemical investigations

Electrochemical (amperometric) investigations were performed in order to evaluate the stability of GOx/Ppy-nanoparticles and to compare it with the stability of native GOx in similar solution. For this the GOx/Ppy-nanoparticles were prepared by GOx-induced polymerization in 0.05 M Na-acetate buffer, pH 6.0, containing 1.1 $mgmL^{-1}$ of GOx, 16 mM of glucose and 236 mM of pyrrole. After 24 h of polymerization, the GOx/Ppy-nanoparticles were removed by centrifugation and then they were washed by water a few times to remove unreacted pyrrole, glucose and non-encapsulated GOx. After this, GOx/Ppy-nanoparticles were again resuspended in the same amount of 0.05 M Na-acetate buffer, pH 6.0, to obtain a concentration of GOx/Ppy nanoparticle

similar to concentration before centrifugation.

For amperometric detection, two types of modified carbon rod electrodes: (i) modified with GOx (GOx-Electrodes) and (ii) modified with GOx/Ppy-nanoparticles (GOx/Ppy-Electrodes) were designed according to a previously published protocol [130]. Carbon rod electrodes (CREs) "Ultra F purity" 3.0 mm in diameter were obtained from Ultra Carbon Division of Carbon, USA, RAVEN-M. The CREs were sealed into epoxy to prevent contact of the electrode side surface with the solution. Then the CREs were polished with fine emery paper and then by Al_2O_3 slurry (grain size 0.1 μm), followed by rinsing the electrode surface with ethanol and distilled water; then the electrodes were dried at room temperature before coating with enzyme or GOx/Ppy. For the preparation of GOx-Electrodes, 3.0 μL of 1 $mgmL^{-1}$ of GOx solution were deposited on the electrode surface and then water was evaporated at room temperature under intensive ventilation; the deposition/evaporation procedure was repeated five times. Then the electrodes were kept for 20 h over 5% solution of glutaraldehyde at 4°C in a closed vessel as previously described [131]. For the preparation of GOx/Ppy modified electrode, 3.0 μL of GOx/Ppy suspension, which was shaken before use, was deposited on the electrode and then water was evaporated at room temperature under intensive ventilation; the deposition/evaporation procedure was repeated five times. As GOx electrodes, GOx/Ppy electrodes were kept for 20 h over 5% solution of glutaraldehyde at 4 °C in a closed vessel. After this preparation step, both types of electrodes (GOx-electrodes and GOx-Ppy-electrodes) were thoroughly washed with distilled water to remove non-immobilized enzyme or non-immobilized GOx/Ppy-nanoparticles.

The amperometric signal was detected by using three electrode circuit in phosphate buffer, pH 7.0, with 2.0 mM of phenasine methosulphate and different glucose concentrations at +300 mV versus Ag/AgCl/KClsat; a speed rate of 120 rpm for mixing of the solution in an electrochemical cell was applied. Potentiostat PGSTAT 30 Echochemie/Autolab (Ultrech, Netherlands) was used for all electrochemical experiments. The modified electrodes were

used as working electrodes and a 2 cm^2 Pt electrode was used as an auxiliary one. During stability tests, the GOx solution and GOx/Ppy suspension both were kept at 20°C and GOx- and GOx/Ppy-electrodes were developed immediately after preparation of GOx and GOx/Ppy solutions and then again after incubation of GOx and GOx/Ppy solutions 3, 6 and 14 days.

2.3 Preparation of monolayers for gold particles deposition investigation

2.3.1 Preparation of gold nanoparticles

The standard method, described by J. Turkevich et al. in 1951 and refined by G. Frens in the 1970s [132, 133] was used to produce size-defined spherical gold nanoparticles through chemical reduction. The colloidal gold suspension was prepared by standard citrate reduction procedure [134] with some modifications. Typically, 100 mL of 1 mM hydrogen tetrachloroaurate ($HAuCl_4$) aqueous solution was heated up to 88°C. Afterward, 10 mL of 38.8 mM sodium citrate was quickly added, while stirring vigorously at 300 rpm, resulting a in colour change of the originally yellow solution to burgundy red (colour change indicates the presence of colloidal gold nanoparticles). The mixing rate effect on nanoparticle size is an important factor in the reduction process while particle size and size distribution is also affected by mixing rate [135]. The mixture was kept at 88°C for a defined time (normally 15 min) while stirring continuously and hereafter cooled to room temperature.

The reaction mixtures were purified of excess ions using a stirred membrane filtration cell (Millipore, model 8400) with a regenerated cellulose membrane (Millipore, NMWL: 100 kDa). The washing procedure was repeated until the conductivity of the supernatant solution stabilized at ca. 15 - 20 $\mu S\ cm^{-1}$.

2.3.2 Deposition of nanoparticles on selected substrates

The procedure for gold nanoparticle deposition on PAH modified mica sheets was analogous to that described in paper [136]. A saturated PAH monolayer on

mica was deposited under diffusion-controlled transport conditions. In order to perform this procedure, freshly cleaved mica sheets were placed into the PAH solution, having a concentration of 5 mg L-1, I=10^{-2} M NaCl and pH 4, for 15 minutes. Afterwards mica sheets, which were covered by the polyelectrolyte monolayer, then were rinsed with water and after this were immersed in the gold suspension. The progress of PAH adsorption was monitored *in situ* by the streaming potential measurements performed according to previously described methodology [137, 138].

The sheets were used for the deposition of gold nanoparticles under diffusion-controlled transport conditions from suspensions containing various AuNPs concentrations (5, 10, 20, 50 mgL^{-1}) in the bulk at pH 6 and various ionic strengths varying between 10^{-4} and 3×10^{-2} M. The deposition time was varied between wide limits in order to obtain gold monolayers of a desired surface concentration (surface coverage). After the deposition, the samples were rinsed with ultrapure water and air-dried. Gold nanoparticle monolayers were analysed *ex-situ* by atomic force microscopy (AFM) and scanning electron microscopy (SEM). The number of particles per unit area of the substrate was determined from these AFM or SEM images using 'MultiScan' image analysis software.

2.3.3 Characterization of materials

Characterization of the gold particle suspension and the monolayers on PAH covered mica was carried out using the following techniques: (i) the bulk extinction spectrum was measured using spectrometer Shimadzu UV-1800 from Shimadzu, Corp. (Tokyo, Japan); (ii) the weight concentration of the particle suspension was determined using the high precision densitometer DMA 5000 M from Anton Paar, GmbH (Graz, Austria). The electrophoretic mobility as a function of ionic strength (I) and pH was determined using the Zetasizer Nano ZS from Malvern, Ltd (Malvern, UK). SEM measurements were conducted using electron microscope JEOL JSM-7500F from JEOL, Ltd (Tokyo, Japan) at 15 kV. To ensure sufficient conductivity of sample it was

covered with a thin layer of chromium before the measurement. Additionally, the surface concentration of gold nanoparticles on the mica substrate was determined using atomic force microscope NT–MDT equipped with the SMENA B scanning head both from NT MDT, Co. (Moscow, Russia). Imaging was performed in semi-contact mode using composite probes possessing a silicon body, polysilicon layers, and silicon high resolution tips. Additionally, the JEOL JSM-7500F microscope working in transmission mode was used. Samples for this examination were prepared by dispersing a drop of the gold colloid on a copper grid, which was covered by a carbon film.

The weight ratio of the purified gold suspension was determined using a densitometer. It was calculated using the formula:

$$w = \frac{\rho_p(\rho_s - \rho_e)}{\rho_s(\rho_p - \rho_e)}$$

Where ρ_p= 19.3 g cm^{-3} is the specific density of gold nanoparticles, ρ_s is the density of stock gold suspension and ρ_e is the density of supernatant solution, acquired by membrane filtration and measured by a high precision densitometer as previously described in literature [136, 139].

It was determined that gold concentration in stock suspension after purification was equal to 127 ppm.

2.4 Preparation of conducting polymers as fluorescence quenching matrixe

2.4.1 Synthesis and modification of Ppy layers

The Ppy was synthesized electrochemically on a pretreated platinum surface. A potentiostat–galvanostat “Pgstat 30” (Echochemie/Autolab, Utrecht, The Netherlands) was used for electrochemical deposition of Ppy. A three-electrode electrochemical cell consisting of:

1. a 1.0 mm diameter platinum working electrode as a substrate for deposition of Ppy;
2. a platinum-wire as auxiliary electrode;
3. an Ag/AgCl/(in saturated KCl) (Ag/AgCl) reference electrode

was used for deposition of Ppy. During the pretreatment phase the platinum-based working electrode was immersed in an ultrasonic bath with concentrated HNO_3 for 10 min; after this treatment it was rinsed with water and subsequently polished on a polishing cloth using aluminum paste with 3.0, 1.0, and, finally, 0.3 μm grain size. The electrodes were then rinsed with water, and ultrasonicated in a 10 $molL^{-1}$ solution of NaOH then in a 5 $molL^{-1}$ solution of H_2SO_4 for 10 min. Electrochemical synthesis of Ppy was performed in a low-volume electrochemical cell which enabled polymerization at low polymerization solution volume [140].

Water purified by use of a "Purator-B" (Glass Keramic, Berlin, Germany) was used for preparation of all solutions. All solutions used for synthesis of Ppy were prepared and used under rigorous exclusion of oxygen by argon.

After the electrode pretreatment steps mentioned, electrochemical potential cycling in 0.1 $molL^{-1}$ H_2SO_4 at sweep rate of 100 mVs^{-1} in the range from –300 to +1200 mV was performed. The platinum electrode was then modified by platinum-black by means of five potential cycles between +500mV and –400 mV vs Ag/AgCl at sweep rate of 10 mVs^{-1} in a solution of 0.1 $molL^{-1}$ KCl containing 0.8 $mmolL^{-1}$ of H_2PtCl_6. Electrochemical formation of the gp51-doped Ppy (gp51/Ppy) film was carried out in solution containing 50 $mmolL^{-1}$ pyrrole, 100 $mmolL^{-1}$ KCl, and 10 $mgmL^{-1}$ gp51. Electrochemical formation of gp51 doped Ppy films was performed by means of a sequence of 20 potential pulses of +950 mV for 1 s and +350 mV for 10 s [141]. Oxygen-free solutions were used for polymerization of pyrrole. Control electrodes modified with blank Ppy were prepared according the same

pretreatment/deposition procedure, but in the absence of gp51 during last step of preparation.

Secondary antibodies labeled with HRP were used for indication of antigen–antibody (gp51/anti–gp51–Ab) complex formation. The Ppy/gp51-modified Pt substrate was incubated for a 30 min in sera from healthy or BLV-infected cattle until steady-state conditions in formation of gp51/anti-gp51–Ab were achieved [142, 143]. This was followed by incubation in Ab* solution for 30 min. When the Ppy/gp51 layer was incubated in blood serum of BLV-infected cattle containing anti-gp51–Ab antibodies formation of an immune-complex based on antigen–antibody (HRP-labeled secondary anti-body) complexes (gp51/anti-gp51–Ab/Ab*) was achieved.

2.4.2 Determination of fluorescence

Before spectrophotometric measurements, modified substrates were thoroughly washed in 50 $mmolL^{-1}$ phosphate buffer, pH 7.2, for 30 s and then dried at room temperature under intense ventilation for 10 min. Modified substrates were placed in the fluorescence detection system and a laser beam used for excitation of fluorescence was focused on to the middle of substrate. To verify attachment of Ab* to gp51/antigp51–Ab complex, HRP-catalyzed reaction substrate consisting of 10 $mmolL^{-1}$ hydrogen peroxide and 1.0 $mmolL^{-1}$ 3,3',5,5'-tetramethylbenzidine (TMB) was added. This addition resulted in the formation of a product with much more intense fluorescence than Ab*. The same procedure was used for investigation of substrates modified by a bare Ppy layer. A homemade luminescence spectrometer was used for detection of fluorescence. A continuous wave He–Cd laser (8 mW, 325 nm) was used for excitation of fluorescence. Collected light was dispersed by a double monochromator (Jobin Yvon Model HRD-1).

A cooled photomultiplier (Hamamatsu R1463P) connected to a photon-counting system was used to monitor fluorescence intensity. Fluorescence measurements obtained before and after each interaction step were collected,

compared, and the differences interpreted as analytical signals. Each measurement was performed at least for three times at room temperature and the average signals are presented in all figures. The reproducibility of measurements at l_{max} was within 95%. All measurements were carried out under ambient air conditions.

3. Results and discussion

3.1 Immunosensor based on fluorescence quenching matrix of conducting polymer polypyrrole.

Immunosensors are one of the most promising lines in the development of biosensing devices due to immune system capacity to develop biomolecules (antibodies), which are sensitive to number of analytes. Fluorescence is one of the most widely employed methods in immunosensors design due to remarkable properties and opportunities fluorescence technique, which significantly enhances the sensitivity of biosensor. Proteins have been modified with polymers in diverse manner over the past 35 years. However, protein bioactivity can be either positively or negatively influenced by polymer conjugation. Construction of any type of immunosensor needs immobilization of a "receptor site" (mostly antibodies are applied for this purpose), which selectively recognizes the analyte [26]. Polypyrrole (Ppy) has been shown as one of the most suitable immobilization matrixes for electrochemical immunosensors [22].

3.1.1 Principle of action of immunosensor based on fluorescent protein and fluorescence-quenching polymer

This immunosensor was based on bovine leukemia virus (BLV) protein *gp*51, which was immobilized within Ppy. The *gp*51 forms an immune-complex with antibodies against *gp*51 proteins (anti-*gp*51–Ab) [144]. The anti-*gp*51–Ab is present at high levels in the blood serum of cattle infected by BLV. Affinity sensors are usually based on ligand-receptor interactions [25, 26] including antibody-antigen complex formation [26]. Hence, a biological recognition system for this fluorescence immunosensor model was based on Ppy with entrapped BLV proteins gp51 (Ppy/*gp*51). This Ppy/*gp*51 layer was used for the detection of anti-*gp*51Ab, as it was proved by electrochemical impedance spectroscopy in the study [65]. Secondary anti-bodies against anti-gp51Ab, which were labeled with HRP (Ab*), were used as fluorescence-detectable

labels that are able to specifically recognize and interact with the complex of *gp*51 proteins and anti-*gp*51–Ab antibodies (*gp*51/anti-*gp*51–Ab). It was demonstrated that fluorescence of nonspecifically adsorbed Ab* was almost completely quenched by the conductive Ppy substrate. In addition, the enzymatic activity of HRP was exploited as a traditional reference method for verification of the formation of immune complex *gp*51/anti-*gp*51–Ab/Ab*. Enzymatic activity of HRP in this complex was proved by chrono-amperometry and spectroscopy [145].

Figure 8 illustrates a schematic diagram of the principle of action of the immunosensor proposed in this research. The Ppy layer was used for several purposes:

1. as an immobilization matrix for gp51;
2. as a nonfluorescent background;
3. as a fluorescence quencher of Ab*, which is non-selectively adsorbed on the Ppy surface.

As is demonstrated in Fig. 8, the Ppy layer quenches the fluorescence of nonspecifically adsorbed fluorophores and other fluorescent materials. In this way the quenching of the fluorescence signal, which could be generated by non-specifically adsorbed fluorophores, increases the selectivity and sensitivity of the immunosensor proposed here.

The Ppy matrix quenches the fluorescence of not specifically adsorbed fluorophores, which are close enough to the surface of the conducting polymer, i.e. the Ppy. The quenching becomes weaker after spatial separation of the fluorophore from the Ppy surface by formation of large protein-based complexes (Fig. 8.).

The autofluorescent HRP is covalently attached to secondary antibodies, which are selectively bound to the target system based on anti-gp51–Ab antibodies. Therefore the fluorescence signal of HRP corresponds to the surface concentration of gp51/anti-gp51–Ab/Ab*. Selective binding of specific secondary antibodies labeled with fluorescent agent and target system

gp51/anti-gp51–Ab results in the formation of large protein complexes— gp51/anti-gp51– Ab/Ab*.

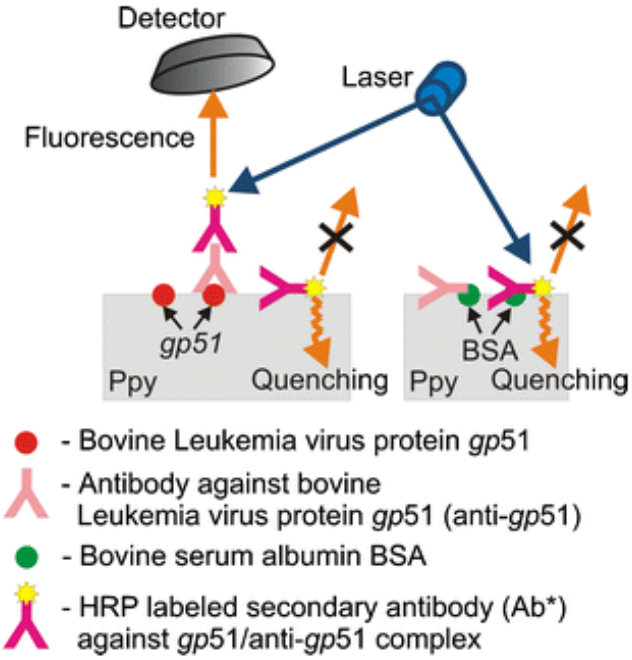

***Fig. 8**. Schematic diagram of the principle of the Ppy-based fluorescence immunosensor.*

The formation of such large complex results in an increase of the distance (15–40 nm) between the fluorophore (in this case HRP) and the Ppy surface [146], this distance is long enough, and for this reason the fluorescence quenching becomes weaker. Therefore, the formation of the antigen-antibody-(secondary antibody) complex (*gp*51/anti*gp*51–Ab/Ab*) [146] enables the distance to be exceeded, which is required for the energy transfer and guarantees efficient fluorescence [147]. In contrast, fluorescent labels, which are nonspecifically adsorbed on the surface of Ppy, become close to the conductive Ppy layer after evaporation of the water. The excitation energy transfer to the delocalized π–π electron states of the conjugated backbone of Ppy enables efficient fluorescence quenching of such nonspecifically adsorbed fluorescent agents.

3.1.2 Fluorescence quenching by polypyrrole

The first stage of the presented research was evaluation of fluorescence quenching of widely used fluorescent dyes (fluorescein and rhodamine B) by Ppy as a nonfluorescent matrix. The Ppy layer was deposited over Pt substrate and modified by protein *gp*51 (Ppy/*gp*51). The fluorescence properties of Ppy/*gp*51 were investigated before and after treatment with fluorescein solution and are presented in figure 9A. Similar experiments were performed with a Ppy/ *gp*51 layer, which was treated with a solution of rhodamine B (Fig. 9b). The recorded fluorescence signal of the Ppy/*gp*51 layer before incubation was close to the noise level; this was attributed to scattered light (Fig. 9, column 1). Further the fluorescence signal was recorded after incubation in fluorescein solution for 30 min and with a drop of fluorescein solution deposited on the Ppy/*gp*51 layer (Fig. 9A, column 2). The sample with the drop of fluorescein solution had high fluorescence intensity (Fig. 9A, column 2). A similar fluorescence increase was observed if the drop of rhodamine B solution was deposited over the Ppy/*gp*51 layer (Fig. 9b, column 2). The fluorescence signal of the same concentration of fluorescein was higher than that of rhodamine B (Fig. 9, columns 2). The difference between the fluorescence signals corresponds to variation in the quantum yield of these materials—95% for fluorescein and 65% for rhodamine B [15, 148]. The Ppy/ gp51 layer was then dried for 10 min at room temperature and the fluorescence of sample was investigated after evaporation of the water. The fluorescence intensity of the dried Ppy/gp51 layer was low (Fig. 9A, column 3), and close to the signal recorded for the bare Ppy/gp51 layer (Fig. 9A, column 1).

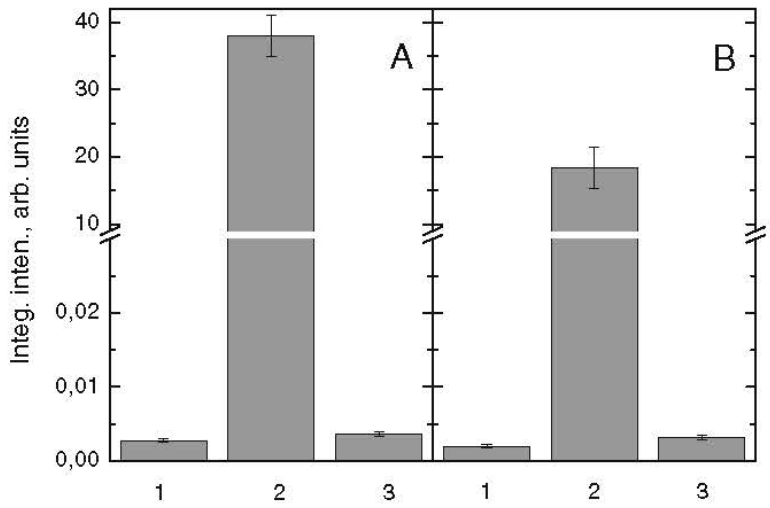

Fig. 9. *Integrated intensity of fluorescence spectra of the Ppy/gp51 layer treated with (A) fluorescein and (B) rhodamine B: column (1) before treatment; column (2) after incubation for 30 min with a drop of fluorescein or rhodamine B solution; column (3) after Ppy/gp51 layer was dried.*

Note, that the fluorescence of the dried specimen can be partially reduced by self-quenching of dye molecules by the formation of aggregates and enhanced exciton migration. The low concentrations of fluorescein used are the most suitable for fluorescence measurements in the absence of resonance energy transfer. Additionally the preparation of thin samples enables avoidance of energy transfer and reduction of the self-quenching effect. The fluorescence of the moiety in our case can, therefore, be partially reduced because of self-quenching [149]. The results clearly showed fluorescence quenching of fluorescein and rhodamine B by the π–π conjugated backbone of Ppy. Similar fluorescence quenching of fluorescein and rhodamine B was observed for the Ppy layer without entrapped protein *gp*51. The experimental results prove that the conductive Ppy layer is an efficient quencher of fluorescing molecules, which are close enough to the surface of Ppy layer. Efficient fluorescence quenching at the surface of Ppy layer is possible because of delocalization of π–π electrons in the conjugated backbone along the polymer chain and the possibility of exciton migration via the conjugated

polymer chain [22].

The main purpose of the detection systems used in biosensors is to provide high selectivity and sensitivity toward the analyte. Most fluorescence sensors are based on the increase of the fluorescence signal caused by an increase of the analyte concentration [22]. However the sensitivity of sensor depends on the signal-to-noise ratio and, in fluorescence-based sensors, noise is increased substantially by nonspecifically adsorbed fluorescence labels [147]. Moreover, in conventional fluorescence-based sensors there is some level of background fluorescence, which can result in a distorted analytical signal. Therefore a low fluorescence background (residual fluorescence) of the system (ideally closed to zero) can increase signal-to-noise ratio and in this way it can improve the sensitivity of the sensor. In this respect the Ppy seems to be a very suitable substrate for fluorescence sensor design, because the fluorescence background of this polymer is minimal (Fig. 9A and B, columns 1); in addition, the Ppy resulted in efficient fluorescence quenching (Fig. 9A and B, columns 3). On the other hand, Ppy is a polyelectrolyte and in addition it could be doped by ionic compounds; this ionic nature of Ppy might be successfully exploited in designing new fluorescence sensors. The desired property of Ppy is the fluorescence quenching in the dry state, which quenches the fluorescence generated by fluorescence agents nonspecifically adsorbed on the Ppy layer. However the Ppy can also reduce fluorescence signals coming from the fluorescence label; this is undesired because it reduces the sensitivity of bioanalytical system. Therefore, fluorescence agents that are not susceptible to self-quenching should be applied in the above described sensor design. One of many such agents is HRP, which as cofactor has autofluorescent moieties—hemes-c [150]. The polypeptide-based shell of HRP prevents hemes-c from self-quenching if two or more HRP molecules come close to each other and thus it still prevents the energy transfer even after evaporation of water. Moreover HRP is often used as a fluorescent label in immunoanalytical systems including enzyme-linked immunosorbent assay (ELISA) and electrochemical immunosensors in the form of its conjugates with antibodies

recognizing analyte-based complexes [145]. HRP has significantly lower fluorescence than organic fluorescence agents such as fluorescein and rhodamine B [151], but in addition to fluorescence detection spectrophotometric and/ or amperometric detection of HRP enzymatic activity could be exploited as the reference detection method suitable for verification of *gp*51/anti-*gp*51–Ab/Ab* complex formation [145]. Owing to these advantages HRP was selected as the fluorescence agent for this research.

Fluorescence quenching of HRP and HRP-labeled antibodies (Ab*) adsorbed on the surface of the Ppy/*gp*51 layer was investigated in the second part of this research. The emission peak in the range 410–420 nm was observed in the spectra obtained from Ab* solution (data not shown). This is attributed to the emission of heme-c present in the HRP structure [145]. Figure 10 shows the integrated intensities of fluorescence spectra of the Ppy/*gp*51 layer, which was treated several times with HRP (A) or Ab* (B) solution. At first, fluorescence of the Ppy/*gp*51 layer was measured before any treatment (Fig. 10, columns 1) and in this case the Ppy/*gp*51 layer generated a very low fluorescence signal only. The fluorescence intensity of the Ppy/*gp*51 with a deposited drop of the HRP solution before evaporation of the solvent was significantly higher (Fig. 10A, column 2) than the fluorescence intensity of dried Ppy/*gp*51 layer (Fig. 10A, column 3). Correspondingly the fluorescence signal of the Ppy/*gp*51 layer with the drop of Ab* solution before evaporation of the solvent was significantly higher (Fig. 10B, columns 2 and 4) than the fluorescence signal of dried Ppy/*gp*51 layer after evaporation of the solvent (Fig. 10B, columns 3 and 5).

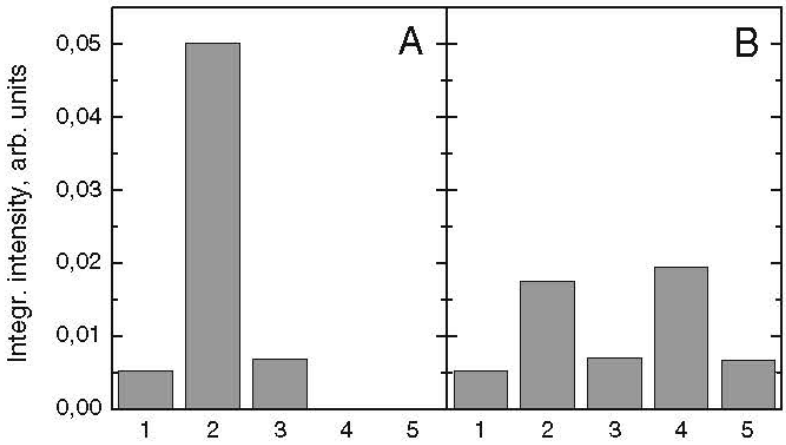

Fig. 10. *Integrated intensity of fluorescence spectra of the Ppy/gp51 layer after different treatments with fluorescent HRP agent. (A) Treatment with free HRP: column (1) before treatment; column (2) with 2 μL drop of HRP solution; column (3) after the solvent was evaporated. (B) Treatment with HRP bound to secondary antibody: column (1) before treatment; column (2) with 2 μL drop of Ab*HRP solution; column (3) after the solvent was evaporated; column (4) after a second addition of a 2-μL drop of Ab*HRP solution before the Ppy/ gp51 layer was dried; column (5) after the solvent was evaporated for the second time.*

The recorded fluorescence signal was slightly higher after the second addition of the drop of Ab* solution, in both the unevaporated and in dried states (Fig. 10, column 5 compared with column 3 and column 4 compared with column 2). The Ab* from the first addition was not removed from the surface and subsequently partially dissolved in the second drop and again it was re-deposited when the second drop was dried. Results from HRP deposited on the Ppy/*gp*51 (Fig. 10A) and results from HRP-labeled antibodies deposited on a similar Ppy/*gp*51 layer (Fig. 10B) show efficient fluorescence quenching of the HRP by the conducting Ppy layer. The fluorescence quenching phenomenon described here is very beneficial for the design of fluorescence-based immunosensors. Presented and discussed experiments demonstrated that Ppy almost completely quenched the fluorescence of nonspecifically adsorbed HRP and HRP-labeled secondary antibodies.

3.1.3 Fluorescence of Ppy modified with the proteins *gp*51 and BSA

The purpose of research presented in this section was to study the fluorescence (Fig. 11) of an immunoanalytical system based on Ppy with entrapped BLV protein *gp*51, to confirm the formation of the antigen/antibody (*gp*51/anti-*gp*51–Ab) and antigen/antibody/secondary (*gp*51/anti-*gp*51–Ab/Ab*) antibody complexes by detection of enzymatic HRP activity. The first part of this research was to investigate the formation of the *gp*51/anti-*gp*51–Ab complex. Therefore the Ppy/*gp*51 layer was incubated in 10 times diluted blood serum of BLV-infected cattle containing anti-gp51–Ab antibodies. It is supposed that antigen entrapped in the polymer interacted with the antibody in the BLV-infected blood serum and formed the *gp*51/anti-*gp*51–Ab complex. Nevertheless, the fluorescence intensity recorded before (Fig. 11, curve 1) and after (Fig. 11, curve 2) incubation in the BLV-infected blood serum was comparable. The fluorescence yield of the formed *gp*51/anti-*gp*51–Ab complex is relatively low. To prove the formation of antigen/antibody complex, the Ppy/*gp*51/anti-*gp*51–Ab layer was incubated in a solution containing HRP-labeled secondary antibodies (Ab*) selectively recognizing anti-*gp*51–Ab. Figure 11 curve 3 shows the increase of fluorescence intensity of the Ppy/*gp*51 layer after incubation in Ab* solution. The integrated fluorescence intensity of the spectrum of the Ppy/*gp*51/anti-*gp*51–Ab/Ab* layer is 2.7 times higher than integrated fluorescence intensity of Ppy/*gp*51 layer. The increase of fluorescence intensity can be attributed to fluorescence of HRP. This effect confirms binding of Ab* to the *gp*51/anti-*gp*51–Ab complex and formation of the *gp*51/anti-gp51–Ab/Ab* complex. The experiment with nonspecific Ab* demonstrated that the fluorescence of nonspecifically adsorbed Ab* was completely quenched by the Ppy substrate (Fig. 11 curves 7 and 8). Also for demonstration of the formation of the *gp*51/anti-*gp*51–Ab/Ab* complex, 3,3',5,5'-tetramethylbenzidine and hydrogen peroxide were added to the Ppy/*gp*51/anti-*gp*51–Ab/Ab* layer for induction of enzymatic reaction, which is catalyzed by HRP.

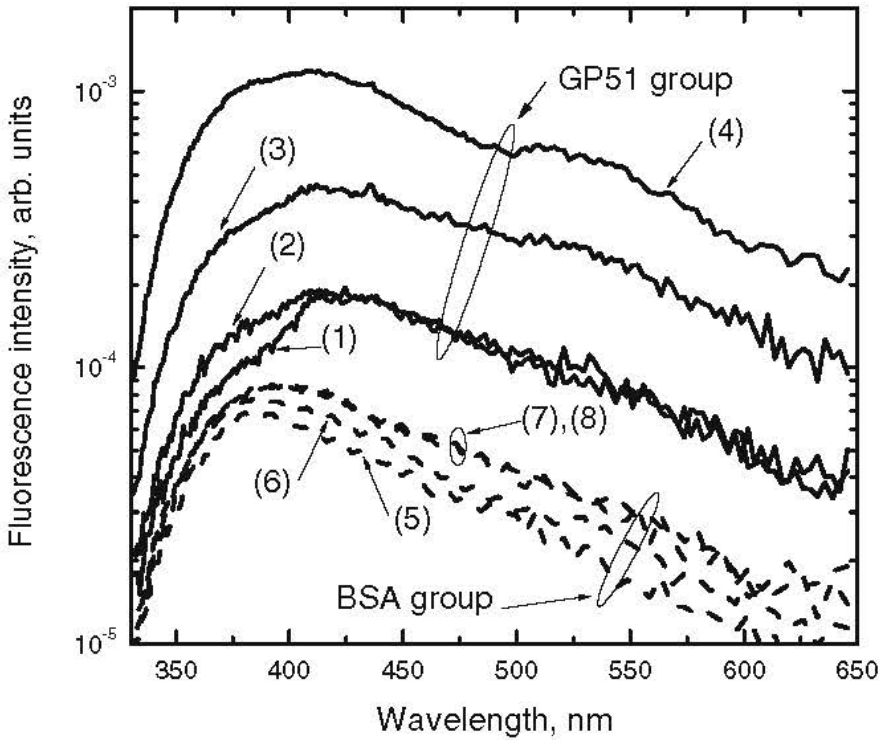

Fig. 11. *The fluorescence spectra of the Ppy layer modified by gp51 (group of solid lines) and BSA (group of dashed lines). The fluorescence spectra of Ppy/gp51 layer: (1) before treatment; (2) after 30 min incubation in blood serum of BLV-infected cattle containing anti-gp51–Ab; (3) after 30 min incubation in HRP-labeled secondary antibody solution; (4) after 1 h treatment with 1.0 mmolL^{-1} 3,3',5,5' - tetramethylbenzidine and 10 mmolL^{-1} H_2O_2. The fluorescence spectra of the BSA/Ppy layer: (5) before treatment; (6) after 30 min incubation in blood serum of BLV-infected cattle; (7) after 30 min incubation in HRP-labeled secondary antibody solution; (8) after 1 h treatment with 3,3',5,5' - tetramethylbenzidine solution.*

The reaction products formed increase integrated fluorescence intensity of the spectrum of the modified Ppy layer with *gp*51/anti-*gp*51–Ab/Ab* complex (Fig. 11, curve 4) 6.1 times compared with the Ppy layer modified solely with *gp*51/anti-*gp*51–Ab complex (Fig. 11, curve 2). Analysis of the fluorescence of all the modification steps of the Ppy layer demonstrated the formation of *gp*51/anti-*gp*51–Ab and *gp*51/anti-*gp*51–Ab/Ab* complexes. Moreover the increase of fluorescence after the HRP-catalyzed reaction also

confirmed the binding of the Ab* to *gp*51/anti-*gp*51–Ab complex. It could be concluded that the limit of detection of the immunosensing system presented here was within the physiological level, because real bovine blood serum was used for all these investigations.

The second stage of the research was analysis of the effect of nonspecific binding on the fluorescence properties of the described system. Experiments analogous to that presented in previously were performed with bovine serum albumin (BSA) solution instead of blood serum; this had no specificity towards anti-*gp*51–Ab. The Ppy layer modified by BSA (Ppy/BSA) was formed electrochemically and its fluorescence intensity was low (Fig. 11 curve 5). Next the fluorescence of the Ppy/BSA layer was recorded after treatment with anti-gp51–Ab under the same conditions. After this treatment the fluorescence intensity of the Ppy/BSA layer had increased slightly (Fig.11, curve 6), because on the Ppy/BSA nonspecifically adsorbed proteins (that are present in the blood serum with BSA) have some fluorescence properties. The integrated fluorescence intensity of spectrum of the Ppy/BSA layer after incubation in Ab* solution increased only 1.3 times (Fig. 11, curve 7) compared with the fluorescence of Ppy/ BSA layer. This increase was a factor of 2 lower than the value of fluorescence increase of a similarly treated Ppy/ gp51 layer (Fig. 11, curve 3). Moreover, subsequent addition of 3,3',5,5'-tetramethylbenzidine and hydrogen peroxide did not increase the fluorescence of Ppy/BSA layer (Fig. 11, curve 8). This means that any HRP enzymatic activity was detected in this case. In case of formed *gp*51/anti-*gp*51–Ab/Ab* complex particularly significant changes in fluorescence were detected after the addition of HRP substrates. Experimental results illustrate that the Ab* did not form any complexes with the Ppy/BSA layer and the interaction between the Ppy/BSA layer and proteins present in the blood serum of BLV-infected cattle was based solely on nonspecific sorption. The absence of the specific interactions with the Ppy/BSA layer resulted in small changes of fluorescence after each treatment step (Fig. 11, curves 6–8) and only slightly increased the fluorescence of the dried Ppy/BSA layer. Similar effects of signal distortion by

nonspecifically adsorbed materials can reduce the sensitivity and selectivity of any fluorescence-based bioanalytical system and should always be taken into account during the construction of analytical systems. In this case, quenching of the fluorescence of nonspecifically adsorbed fluorescent agents that are close enough to the Ppy surface and the low fluorescence background of the Ppy layer itself are advantages suitable for the design of fluorescence sensors. The application of Ppy increases the selectivity of the immunosensor, because the Ppy almost completely quenches the fluorescence of nonspecific fluorescent markers that are adsorbed directly on the Ppy surface.

Differences between integrated fluorescence intensities for different stages of the experiment, as ($I_i - I_1$) difference and the ratio of integrated fluorescence intensities minus 1 ($I_i/I_1 - 1$) were calculated (Fig. 12); here *"i"* is the stage of the experiment, I_i is the integrated fluorescence intensity in stage *"i",* and I_1 is the integrated fluorescence intensity in stage "1". Stage "1" represents the integrated fluorescence intensity of the Ppy layer modified by *gp*51 or BSA before any treatment (Ppy/*gp*51 or Ppy/BSA); Stage "2" represents the integrated fluorescence intensity of the modified Ppy layer after 30 min incubation in blood serum of BLV- infected cattle containing anti-gp51–Ab; Stage "3" represents the integrated fluorescence intensity of the modified Ppy layer after treatment as described in stage "2" and an additional 30 min incubation in HRP-labeled secondary antibody solution; Stage "4" represents the integrated fluorescence intensity of the modified Ppy layer after treatment as described in stage "3" and an additional 1 h treatment with 1 $mmolL^{-1}$ 3,3',5,5'-tetramethylbenzidine and 10 $mmolL^{-1}$ H_2O_2. The output of the proposed sensor could be the difference (Fig. 12A) of integrated fluorescence intensities ($I_i - I_1$) and/or the ratio (Fig. 12B) of the integrated fluorescence intensities minus1 ($I_i/I_1 - 1$). I_1 is characterized by the weak fluorescence intensity of Ppy/*gp*51 or Ppy/ BSA layers and was used as a reference signal for control of variation of the fluorescence signal.

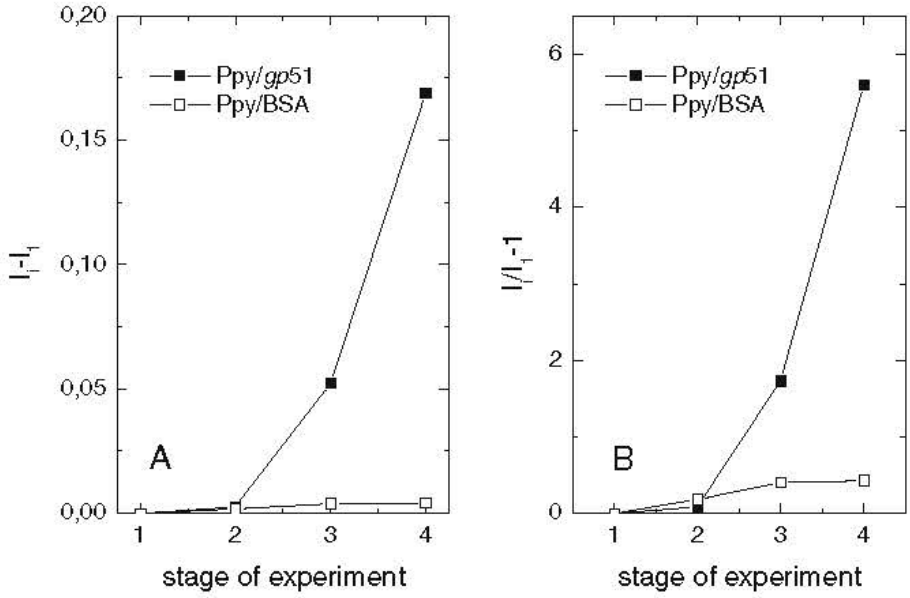

Fig. 12. *Combination of the fluorescence output shown for different stages of the experiment, (A) (I_i–I_1) and (B) (I_i/I_1–1). Results obtained by use of Ppy layer modified with specific antigen gp51 are represented by black squares; results obtained by use of Ppy layer modified with nonspecific BSA are represented by white squares.*

The output signal increases 42 times (Fig. 12A) or 14 times (Fig. 12B), respectively, when the *gp*51/anti-*gp*51–Ab/ Ab* complex is created and after the HRP-catalyzed reaction (stage 4, closed points) comparing with the corresponding nonspecific interactions of the Ppy/BSA layer after its consecutive treatment:

1. with anti-*gp*51–Ab containing blood serum;
2. with Ab*-containing solution;
3. with solution containing both HRP substrates (stage 4, open points).

Comparison of the fluorescence intensity of selectively bound *gp*51/anti-*gp*51–Ab/Ab* complex with the fluorescence intensity of free HRP deposited on Ppy/*gp*51 enables approximate estimation of the reduction of fluorescence quenching by the increase of the distance between HRP and the Ppy layer. Formation of the antigen/antibody/(secondary antibody) complex

results in an increase of the fluorescence by at least a factor of 2.5. Note that the number of fluorescent HRP moieties can be significantly reduced in the sample gp51/anti-gp51–Ab/Ab* by washing nonselectively bound fractions before each fluorescence measurement, as described in the Experimental section. This proposed concept for a fluorescence-based sensor is expected to result in an increase of the selectivity of the immunosensor by application of Ppy.

Section 3.1 conclusions

A fluorescent protein (HRP) and a fluorescence-quenching polymer (Ppy) were used to increase the selectivity and sensitivity of an immunoanalytical system. The Ppy had two major functions in the described immunosensors:

(i) Primarily Ppy was used as a matrix for immobilization of proteins (*gp*51) with biological recognition properties towards specific antibodies (anti-*gp*51–Ab); and

(ii) Ppy was used as fluorescence quencher, which increased the selectivity of biosensing system.

This study showed the possibility of future application of conducting polymer polypyrolle as fluorescence quenchers in the design of novel fluorescence-based biosensing systems.

Detection of analytes still demands development of analytical methods and devices with enhanced sensitivity, specificity, precision, cost-effectiveness, robustness, fast detection time, rapid response, multiplex analysis, reiterated usage.

3.2 Glucose oxidase self-encapsulated within polypyrrole fluorescence measurements

3.2.1 Glucose oxidase's fluorescence

As mentioned in the literature section, it is worth to repeat that the GOx is a homodimer with two non-covalently bound cofactor flavin adenine dinucleotide (FAD) residues. The FAD consists of riboflavin, adenine, two

phosphates and ribose (Fig. 13.). It can exist in two different redox states that are converted by accepting or donating electrons. The oxidized form (FAD) accepts two electrons and two protons and become reduced form ($FADH_2$). The isoalloxazine ring of the riboflavin is responsible for the FAD's fluorescence. Previously, the oxidized form of FAD was believed to be non-fluorescent, but later it was reported that this form is also fluorescent [152]. The reduced form of $FADH_2$ shows higher fluorescence intensity than the oxidized form under the same conditions [152].

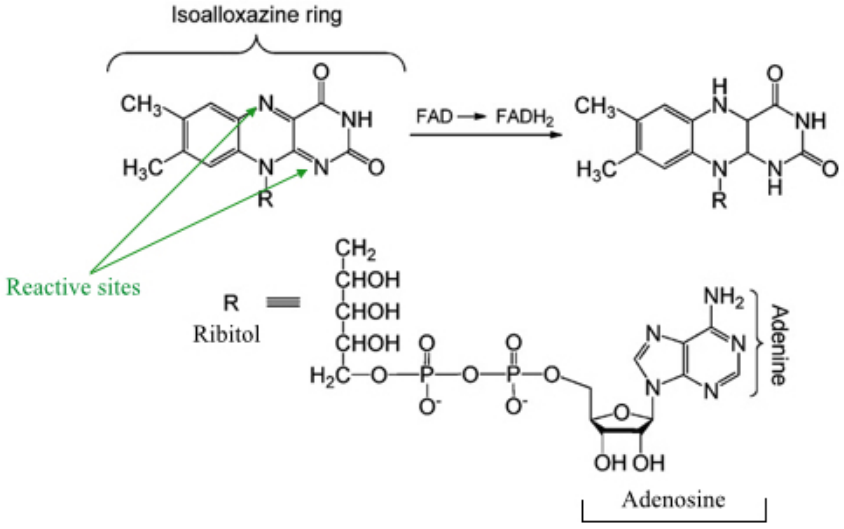

Fig. 13. *Structural formula of oxidized (FAD) and reduced ($FADH_2$) forms of flavin adenine dinucleotide.*

Changes of the FAD fluorescence are observed in the presence of glucose during oxidation–reduction reaction. Oxidation of glucose to gluconolactone is followed by the concomitant reduction of FAD to $FADH_2$. The formed gluconolactone rapidly hydrolyses to gluconic acid. Dissolved oxygen in solution reoxidizes the $FADH_2$ and produces H_2O_2. Both forms of FAD are fluorescent.

3.2.2 Glucose oxidase coated with polypyrrole shell fluorescence response to pH measurements

In the study [153], dependence of the chemical formation of polypyrrole on pH was investigated by measuring optical absorption. Polymerization solutions were composed of four main compounds: pyrrole, as polymerizable monomer; glucose oxidase, as hydrogen peroxide producing enzyme; glucose, as reducing substrate; dissolved oxygen, as oxidizing substrate. In the presence of glucose and dissolved oxygen, GOx started to generate hydrogen peroxide and lactone of gluconic acid (gluconolactone). Close to the GOx active site, locally lowered pH and high concentration of oxidator (H_2O_2) created optimal conditions for the polymerization of pyrrole and self-encapsulation of GOx within a polypyrrole shell (GOx/Ppy-nanoparticles). The appearance of a band at 460 nm in the absorption spectra proved the formation of polypyrrole oligomers [153, 154]. The results showed that the pH for GOx initiated polypyrrole formation was in a broad pH range from pH 3.0 to 9.0. The pH value of the polymerization solution also had an influence on the polymerization rate [153].

In this work we studied the influence of pH on the fluorescence of polymerization solutions (Fig. 14.). An integrated intensity was calculated from the recorded fluorescence spectra, which were measured for each solution. Solutions with pH values in the range from 5.0 to 7.0 showed higher fluorescence intensity; while the maximal value was registered for solutions with pH 5.5 and 6.0. In the literature the enzyme activity depends on the pH, which is optimal at pH 5.8–6.0 [155]. Therefore, a solution with pH 6.0 was chosen for further analysis, because it was the most suitable to study fluorescence intensity.

Whereas in an acidic medium the pyrrole polymerization reaction takes place faster, therefore more Ppy is produced during the same period. A thicker Ppy layer more efficiently decreases the intensity of the fluorescence of FAD,

in agreement with results demonstrating fluorescence quenching induced by Ppy [81].

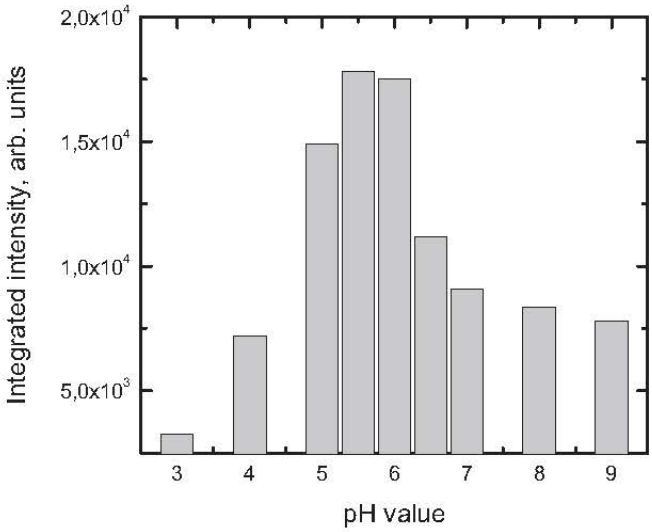

Fig. 14*. Fluorescence spectra integrated intensity dependence on pH value.*

3.2.3 Glucose oxidase coated with polypyrrole fluorescence

Fluorescence sensing based on the variation in the shape and intensity of fluorescence spectra of the GOx during the polymerization reaction was developed for the characterization of GOx covered by Ppy. The maximum of fluorescence excitation was at 325 nm. The GOx absorption spectrum consists of two bands peaking at approximately 380 and 450 nm [156] and corresponding to π–π* transitions along the three cycles of the isoalloxazine ring in FAD (see fig. 15.). These bands are characteristic features of the oxidized form of flavin groups [157]. Therefore, changes in intrinsic fluorescence can be applied to monitor structural changes in a protein.

The aim of the present experiment was to investigate denaturation of GOx within 14 days. Before embedment of GOx enzyme in the polymeric matrix of Ppy, the time-induced unfolding process of GOx was studied by fluorescence measurements. Fluorescence spectra of the GOx solution at different periods after preparation were recorded. Fluorescence spectra of GOx

in a Na-acetate buffer at 325 nm photoexcitation are shown in figure 15.

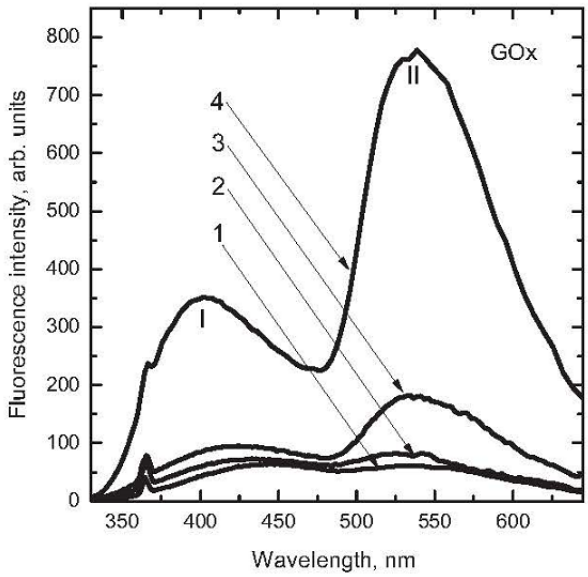

Fig. 15. *Fluorescence spectra of GOx in 0.05 M Na-acetate buffer, pH 6.0, recorded immediately after preparation of solution and then correspondingly after 3, 6 and 14 days. (1) Fluorescence spectra after 1 day, (2) fluorescence spectra after 3 days, (3) fluorescence spectra after 6 days, and (4) fluorescence spectra after 14 days.*

The fluorescence spectra consist of two bands. The maximums of spectrum recorded at the first day of the preparation were registered at 447 and 538 nm. After 14 days the peaks blue-shifted to 401 and 535 nm, respectively. It is known that GOx exhibits autofluorescence in the ultraviolet and visible regions. Due to tyrosine and tryptophan residues it is shifted to 401 nm and due to flavine residues it is shifted to 535 nm. Selected excitation excludes excitation of tyrosine and tryptophan residuals. Recorded emission of GOx can be attributed to the fluorescence of FAD. Each GOx molecule includes two non-covalently bound moieties of FAD. The FAD consists of the tricyclic isoalloxazine ring (see fig. 13.). The fluorescence of FAD corresponds to a π–π^* transition of the isoalloxazine and the emission maximum is at 535 nm for dissolved FAD. The fluorescence maximum at 447 nm appears almost at the same wavelength and it is very similar to that of alloxazine derivatives

dissolved in water [158]. During the denaturation of GOx, the FAD is released. As a consequence of partial protein unfolding and the release of FAD molecules, the fluorescence intensity, which was attributed to released FAD, increases. The autofluorescence of FAD can be used for monitoring of structural changes of the enzyme and determination of FAD molecules dissociated from unfolded/denaturated protein. Fig. 15 shows that after 3 days of the preparation of GOx solution in Na-acetate buffer, the fluorescence spectrum has slight changes. After 6 days, the proportion between fluorescence peaks at 447 and 535 nm has significantly changed and fluorescence at 535 nm becomes dominating.

After 14 days the changes of shape and intensity of the fluorescence spectra become considerable. The total fluorescence intensity significantly increases and the fluorescence intensity at 535 nm increases about 14 times if compared with the fluorescence intensity measured on the first day. The spectra allow one to assume that after 14 days a larger part of the GOx denaturized and the FAD molecules dissociated from the unfolded protein.

To obtain information on stability of GOx after formation of Ppy/GOx-nanoparticles, fluorescence properties of a polymerization solution composed of pyrrole, glucose oxidase, glucose and dissolved oxygen was studied. During biocatalytic reaction of GOx, hydrogen peroxide is produced and it initiates the polymerization of pyrrole. The amount of formed GOx/Ppy-nanoparticles increases with time due to special conditions suitable for the polymerization at the interface between GOx and solution. We studied fluorescence properties of the polymerization solution during a 14-day period. Fig. 16 shows the fluorescence spectra of the polymerization solution at the moment of preparation and 3, 6 and 14 days after preparation.

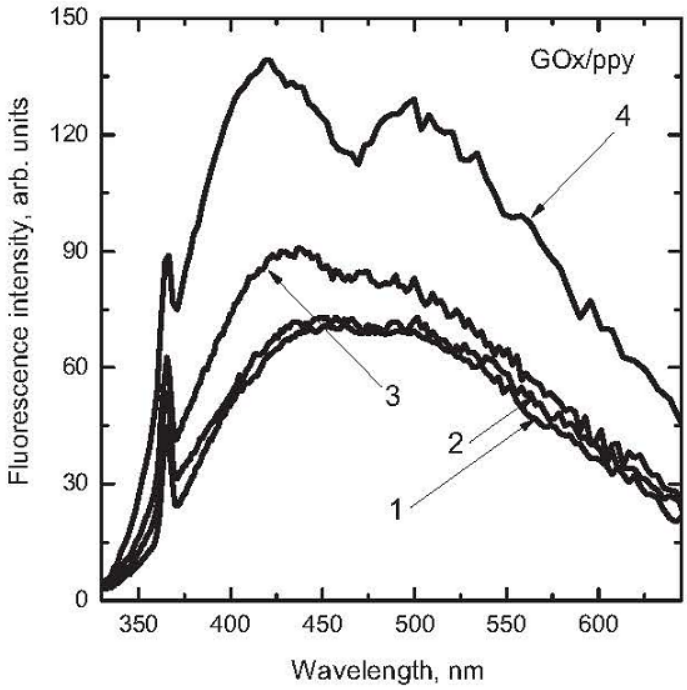

***Fig. 16**. Fluorescence spectra of polymerization solution recorded immediately after preparation of solution and then correspondingly after 3, 6 and 14 days. (1) Fluorescence spectra after 1 day, (2) fluorescence spectra after 3 days, (3) fluorescence spectra after 6 days, and (4) fluorescence spectra after 14 days.*

The fluorescence spectra consist of two bands with peaks at about 445 and 498 nm. After 3 days the intensity of the fluorescence spectrum slightly increases, but the shape of this spectrum is similar to that measured on the first day. After 6 days, the shape and intensity of fluorescence spectrum begins to change. The band at 445 nm becomes more distinct and it is blue-shifted to 432 nm, and the overall intensity of spectrum increases. The most significant changes were registered after 14 days. Two bands dominate in the fluorescence spectrum with peaks at 419 and 500 nm. The fluorescence intensity at 419 nm increases by 1.96 times compared to that for the first day. Correspondingly, the intensity at 500 nm increases by 1.84 times, while after 14 days the fluorescence intensity of a solution containing just GOx at 535 nm increases by 14 times. Also, the total fluorescence intensity of the polymerization solutions increases less than the intensity of GOx solutions over the same time period.

Taking into account that more GOx is covered by Ppy during 14 days, we can assume that coverage by Ppy prevents the GOx from unfolding. A negligible amount of unmodified GOx denatures within 14 days resulting in insignificant changes to the fluorescence spectra.

3.2.4 Fluorescence response at different initial composition of solution

The polymerization solution was composed of pyrrole, GOx, glucose and dissolved oxygen. For better understanding the behaviour of this complex system, we investigated the influence of each component's concentration on the fluorescence emission intensity. Each sample solution was prepared in Na-acetate buffer, pH 6.0, by changing the concentration of a single component. Fluorescence measurements were carried out after 3, 6 and 14 days from the date of solution preparation. Experimental data are shown in Figs. 17–19. The fluorescence spectrum recorded immediately after preparation of solution is not presented in these figures due to only slight differences from the spectrum measured after 3 days from preparation. Fig. 17 presents fluorescence spectra of the polymerization solution with different concentrations of GOx.

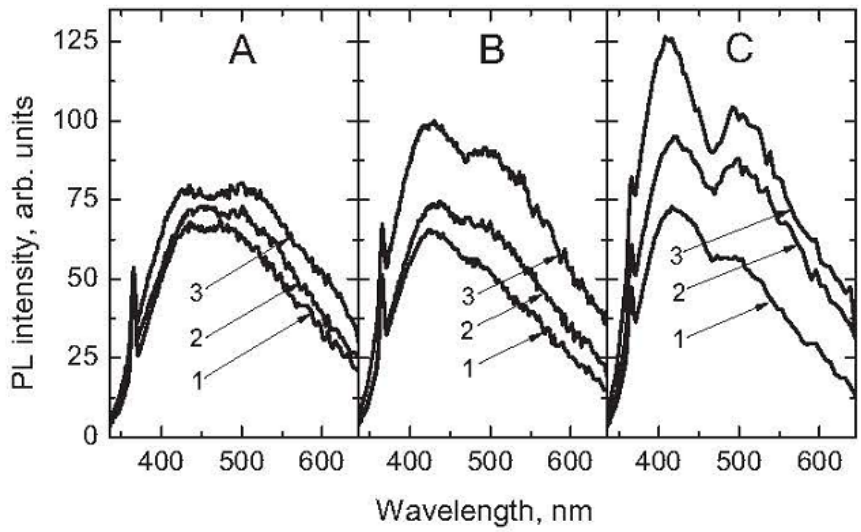

Fig. 17*. Fluorescence intensity dependence on the GOx concentration in the solution: (1) 0.57 mgmL^{-1}, (2) 1.1 mgmL^{-1} and (3) 4.5 mgmL^{-1}. Fluorescence spectra recorded after 3 days (A), 6 days (B) and 14 days (C).*

As can be seen in the figure, the fluorescence intensity increases with increasing GOx concentration in solution. This is consistent with the assumption that fluorescence intensity is proportional to the number of fluorescing molecules, such as cofactor FAD in our system. Moreover these spectra show that higher luminescence intensity is observed in the region of shorter waves. Fig. 18 shows fluorescence spectra of solutions, which were prepared by changing the glucose concentration.

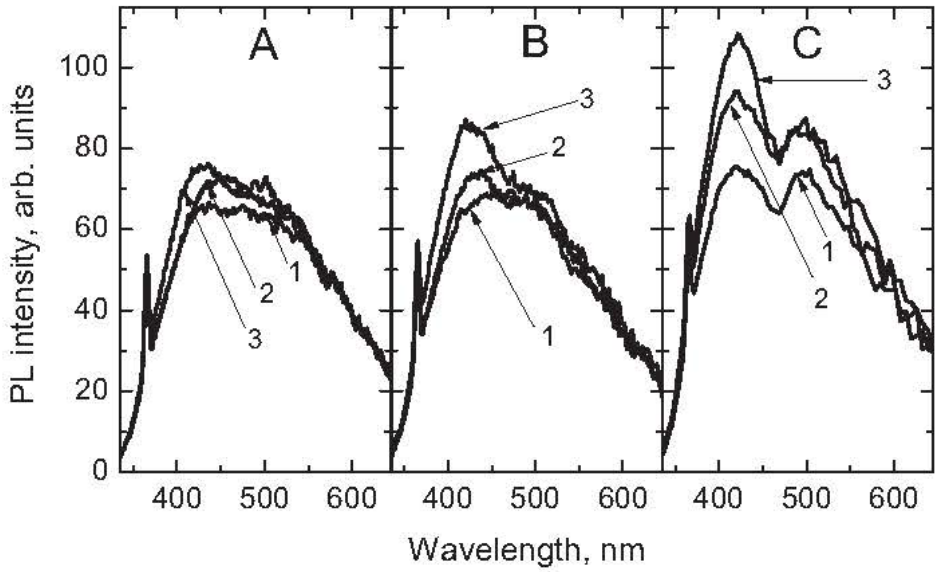

Fig. 18. *Fluorescence intensity dependence on the glucose concentration in the solution: (1) 28.2mM, (2) 16.0mM and (3) 8.9mM. Fluorescence spectra recorded after 3 days (A), 6 days (B) and 14 days (C).*

Fluorescence intensity increases at 425 nm and in the whole investigated spectra with lowering the glucose concentration in solution (Fig. 8A–C). It is known that glucose quenches FAD fluorescence [15]. The shape of spectra of solutions with a lower concentration of glucose differs from the spectra of solutions with a higher concentration of glucose. Intensities of peaks attributed to Raman-scattering of water at 360 nm are almost equal in all three solutions with different glucose concentrations. In other cases the intensity at 425 nm is higher than at 500 nm. We believe that glucose concentration has a more significant influence on FAD emission in the green region of the spectra.

Fig. 19 presents fluorescence spectra when the pyrrole concentrations in the solution are different.

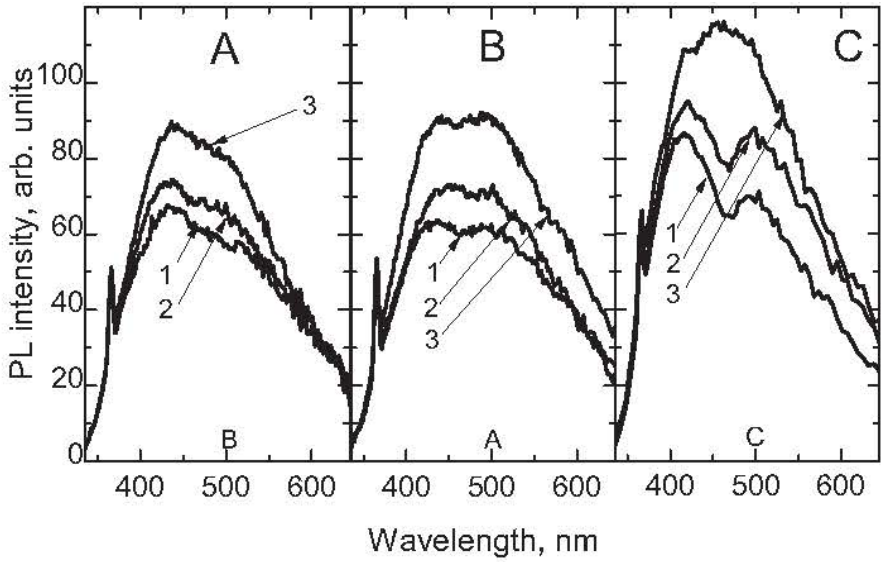

Fig. 19. *Dependence of fluorescence intensity on the pyrrole concentration in the solution: (1) 119mM, (2) 236mM and (3) 464mM. Fluorescence spectra recorded after 3 days (A), 6 days (B) and 14 days (C).*

The intensity of the peak at shorter wavelength is higher than the peak at longer wavelength. The luminescence intensity decreases by lowering the pyrrole concentration. We assume that pyrrole significantly reduces the GOx fluorescence quenching by glucose. The shape of the fluorescence spectra significantly depends on polymerization duration if solution contains the highest concentration of pyrrole. The spectrum registered after 14 days shows that the second peak (at approximately 500 nm) begins to dominate and it shifts to shorter wavelengths.

It should be noted that the polymerization solution composed of GOx, glucose, pyrrole and dissolved oxygen is a complex sys- tem. The coenzyme FAD, during catalytic action of GOx, periodically appears in oxidized and reduced forms. Therefore, a variety of fluorescence quenching and energy transfer possibilities are foreseen in such a complex system. All these processes take place simultaneously and therefore it is difficult to distinguish

their individual influence on the observed fluorescence spectra.

The general effect of GOx self-encapsulation within polypyrrole is evident. Free GOx fluorescence increases almost 14 times after two weeks from solution preparation. This indicates a relatively fast unfolding process of GOx and FAD dissociation from the enzyme. Fluorescence of GOx coated by a Ppy shell increases less than 2 times during the same period of time. Most probably this residual fluorescence increase is attributed to inactive GOx, which remains not coated by Ppy and therefore FAD easily dissociates from the enzyme.

In order to evaluate the influence of Ppy layer on stability of the GOx in GOx/Ppy-nanoparticles a comparison of enzymatic activities of GOx and GOx/Ppy-nanoparticles, which were stored at 20°C, was performed. Significant stabilization of GOx enclosed within Ppy was observed (Table 1).

Table 1. *Comparison of relative catalytic activity and relative fluorescence signals of GOx in GOx solution and GOx/Ppy suspension observed after different periods of incubation at 20°C.*

	1st day	3rd day	6th day	14th day
[a]GOx solution	8 ± 2 %	11 ± 2 %	21 ± 5 %	100 ± 10 %
[a]Gox/Ppy suspension	55 ± 5 %	56 ± 5 %	62 ± 8 %	100 ± 8 %
[b]GOx solution	100 ± 11 %	42 ± 5 %	22 ± 5 %	6 ± 4 %
[b]Gox/Ppy suspension	100 ± 8 %	84 ± 9 %	48 ± 5 %	25 ± 5 %

[a]Results based on photoluminescence intensity at 500 nm measurements;
the max photoluminescence of Gox and GOx/Ppy-nanoparticles at 14th day is normalized to 100%.
[b]Results based on electrochemical measurements;
the max activity of each type of electrode is normalized to 100%.

However the general activity of GOx significantly decreased if it was encapsulated within Ppy, but it should be taken into account that such inactivation effect is usually observed if substrates of enzymes are passing polymeric layers, which decreases the diffusion rate of the substrate towards the active site of the enzyme [94]. A comparison of relative GOx catalytic activity, which was registered amperometrically, and fluorescence signals observed after different periods of incubation at 20°C (Table 1) lead one to

conclude that a high extent of GOx-inactivation is related to the dissociation of FAD from the apo-GOx, which is reflected by an increase of fluorescence attributed to FAD release.

3.2.5 Glucose oxidase coated with polypyrrole fluorescence decays

Imaging of intrinsic fluorescence rather than fluorescence labeling is much more attractive while environmental conditions in biological systems can be maintained without any extra fluorescence probes. Fluorescence decay measurements can enhance the potential of fluorescence microscopy because lifetime measurements are an inherent property of a fluorophore.

The steady – state absorption and fluorescence spectra of GOx are shown in figure 20. As can be seen, GOx exhibits two absorption bands, which are attributed to FAD absorption bands, with peaks at 375 nm and 450 nm, which are assigned to the $S_2 \leftarrow S_0$ and $S_1 \leftarrow S_0$ and transitions, respectively. These transitions are ascribed to the $\pi-\pi^*$ transition along the three cycles of the isoalloxazine ring in FAD. Absorbance and fluorescence spectra are enhanced with increasing measurement days. This can be explained with unfolding the FAD from the enzyme.

GOx fluorescence lifetime have been measured at a fixed 425 nm, 450 nm and 530 nm wavelengths. Unmodified GOx exhibited a fluorescence emission peak at 530 nm upon excitation at 375 nm (fig. 20, (b)).

Glucose oxidase enzyme can exist in several spatial conformations within its active site FAD can have “twisted” (stacked) or “unwound” (planar) structure [159-161]. In a planar configuration, flavins have a long lifetime of nanoseconds, except for the stacked conformation of FAD, where intramolecular electron transfer between the flavin isoalloxazine ring and the adenine moiety takes shorter lifetime periods [161].

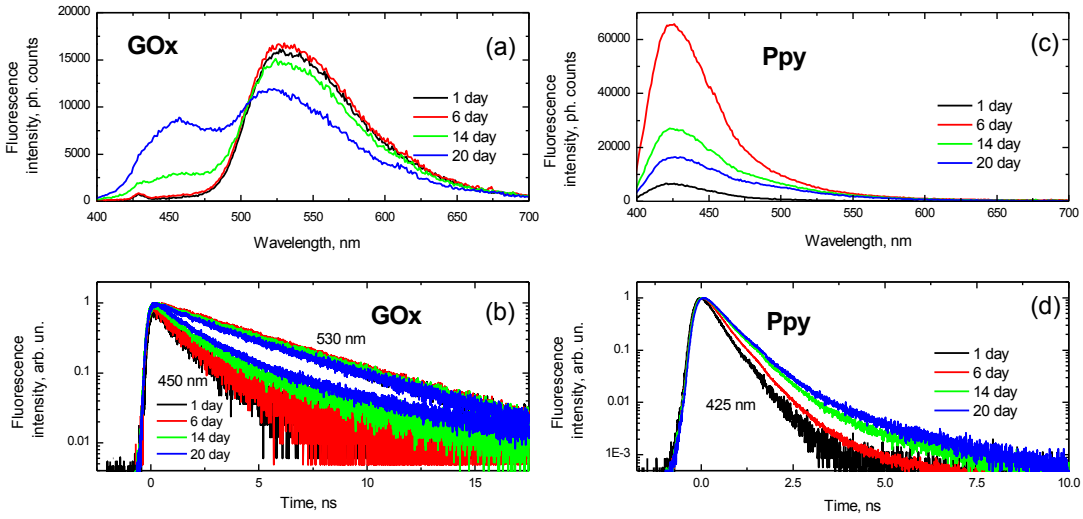

Fig. 20. *Fluorescence spectra (a, c) and fluorescence decay kinetics (b, d) dynamic of glucose oxidase (a, b) and polypyrrole in Na-acetate buffer, pH 6.*

Fluorescence relaxation kinetics upon 530 nm is two-exponential function with 1.3 nm and 4.5 nm components. A few days later in the glucose oxidase solution there were observations of reduced FAD fluorescence band at 460 nm.

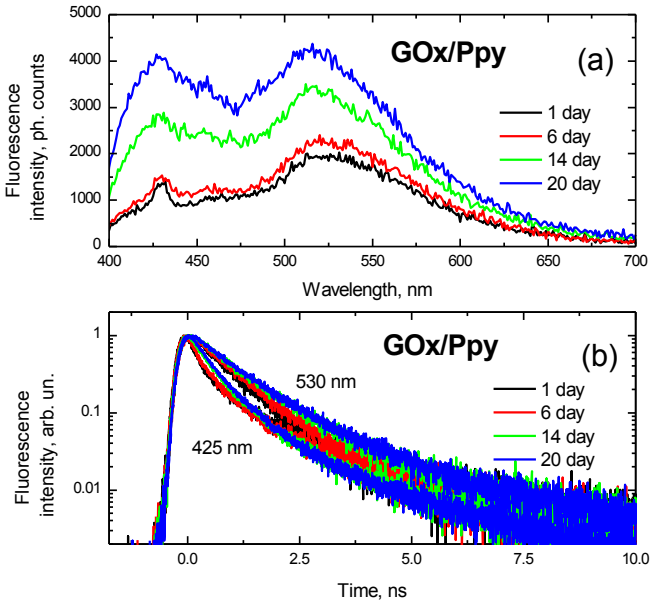

Fig. 21*. Fluorescence spectra (a) and fluorescence decay kinetics (b) dynamic of glucose oxidase and polypyrrole composite in Na-acetate buffer, pH 6.*

Polypyrrole kinetics of fluorescence at 425 nm decays function in one-exponential model with 0.4 ns characteristic relaxation time is shown in fig. 20 (d). After a few days solution with polypyrrole begins to form complexes, which have a very broad fluorescence band at 500 nm with a fluorescence characteristic relaxation time of 2 ns. The influence of the formation of Ppy complexes at 425 nm can also be seen – after a few days fluorescence decay kinetics becomes non - exponential with 0.4 ns and 2 ns relaxation times. Over time, 2 ns component contribution increases. Polypyrrole fluorescence spectrum intensity after 6 days begins to decline - a solution forms larger complexes which strongly quenches the fluorescence of polypyrrole.

When coating glucose oxidase with Ppy, a 5 - 8 times weaker fluorescence is observed. The fluorescence decay kinetics can be well approximated by a two-exponential model with characteristic lifetimes (τ) of 0.7 ns and 2.5 ns. Polypyrrole affects the enzymes active center relaxation processes. Exponential member whose lifetime is approximately 2.5 ns is associated with the FAD cofactor.

It can be seen (fig. 20 and fig 21), that when comparing modified with Ppy and unmodified GOx fluorescence lifetime measurements, Ppy influences the fluorescence intensities decrease and the decrease of average lifetime, at the peak at 530 nm, from 4.4 ns to 1.1 ns. We also see that polypyrrole stabilizes the enzyme, preventing the active center FAD cofactor of rapidly unfolding from glucose oxidase.

Section 3.2 conclusions

It was determined that GOx coated by a polypyrrole shell is more stable than free GOx in solution. Non-encapsulated GOx dissociates to FAD and apo-GOx. Therefore the fluorescence attributed to dissolved FAD significantly increases. The incorporation of enzyme within the Ppy matrix prevents the GOx from unfolding and releasing the FAD. Thus the Ppy layer stabilizes the GOx. Ppy influences the fluorescence intensities measurements decreasing the average lifetime of GOx. Ppy effectively quenches GOx fluorescence.

3.3 Deposition of polyelectrolyte-bounded gold nanoparticles

Introduction. Increasing attention is paid to preparation of gold mono- and multi-layers. A research on colloid gold monolayers [117] described a method suitable for the formation of gold nanoparticle based monolayers on quartz or glass wafers functionalized by alkoxysilanes using nanoparticles of average diameter of 18 nm. The authors obtained maximum 15% surface coverage by nanoparticles, but they do not provide any information on particle transport conditions and the physicochemical parameters of the deposition procedure. The only parameter mentioned was that the adsorption time reached up to 24 hours. Similar results were reported by the same author [162] but the investigations were supplemented by the application of new techniques, which are suitable for the characterization of monolayers, including atomic force microscopy (AFM), field emission scanning electron microscopy (FE-SEM) and near-field scanning optical microscopy (NSOM). Although the gold monolayers did not exhibit high coverage, the efficient application of such films requires a complete and accurate characterization because the enhancement effect in that type of investigations strongly depends on the monolayers' properties.

Brust and coworkers [163] developed an interesting strategy for self-assembly of gold nanoparticles on glass substrate modified by 3-(mercaptopropyl)-trimethoxysilane. The process of gold nanoparticle deposition from suspension was carried out for 3 hours. Repeating deposition of gold nanoparticles and selected thiols the authors obtained gold multilayers, which were applied in optics and electronics. However, no quantitative information on the coverage was reported in this work.

Only very few papers were devoted to kinetic aspects of gold nanoparticle deposition on solid substrates. One of the first reports in this field was the work of Shmitt and co-workers [164] which described the kinetics of 15 nm diameter gold nanoparticle deposition on the poly(allylamine hydrochloride) (PAH)-modified mica. In this work, it was proved that the

kinetics of particle adsorption is reasonably well described as a diffusion-limited process. However the maximum gold nanoparticles coverage obtained using various solid substrates (glass, quartz, mica) and anchoring layers (PAH, PEI, EDA) did not exceeded 15%.

Systematic studies on the deposition of gold nanoparticles on the solid surface were also carried out [118, 165, 166] in some papers. The authors investigated the influence of ionic strength on the deposition kinetics of citrate-stabilized gold nanoparticles, which were of 13 nm diameters. The coverage by particles was determined using AFM and calculated from the reflectometric signal applying 'thin island film theory'. It was proved that with the increasing ionic strength the coverage by nanoparticles increases. Experimentally observed effect is in accordance with the theoretical predictions. On the basis of the Derjaguin, Landau, Verwey and Overbeek (DLVO) theory the average inter-particle distance decreases with increasing ionic strength, leading to an increase of the overall coverage. One can, therefore, conclude that despite a few exemptions [118, 119, 165, 166] no results were reported in the literature concerning adsorption kinetics of gold nanoparticles in well-defined systems interpreted in terms of appropriate theoretical approaches. Considering this deficiency, the goal of this work was to evaluate diffusion-controlled transport based results of gold nanoparticle layer formation from the suspensions with varying electrophoretic mobility and different electrokinetic charge density. PAH modified mica was used as convenient substrate because of its molecular smoothness and homogeneity of charge distribution whose magnitude can be regulated within broad limits by pH, ionic strength and polyelectrolyte adsorption. Bulk pieces of mica can be easily cleaved into thin sheets; it eliminates the necessity of mica surface cleaning prior the experiments. After the assembling of two mica sheets into a channel cell, one can also characterize its electrokinetic charge under wet conditions by using the streaming potential measurements [167].

3.3.1 Colloidal gold particles measurements

UV-Vis spectra were recorded in order to characterize stability of Au-NPs in colloidal solutions (Fig. 22.).

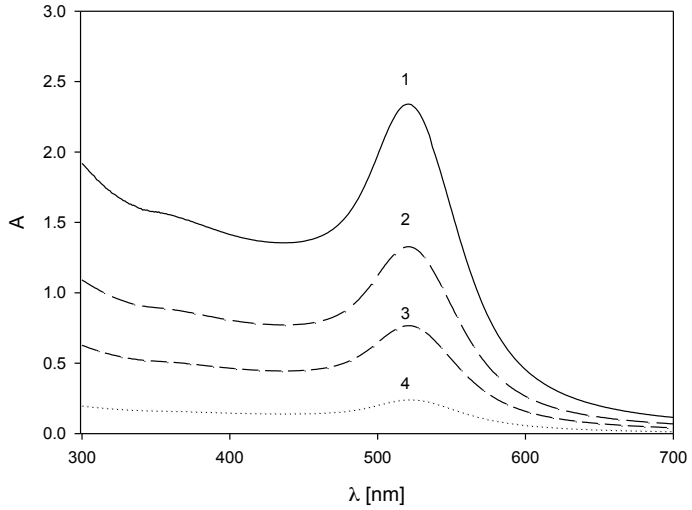

Fig. 22. *The UV-Vis absorption spectra of the suspensions of gold nanoparticles for various bulk concentrations: 1) (_) 63 mgL^{-1}, 2) (- - -) 31 mgL^{-1}, 3) (---) 15 mgL^{-1}, 4) (...) 7 mgL^{-1}.*

Absorption maximum was observed at ca. 521 nm (Fig. 22.), which is related to plasmon resonance of Au-NPs. The absorbance of nanoparticles decreases while decreasing the concentration, but the surface plasmon excitation band position remains fixed at λ_{max}=521 nm and it is rather narrow, which indicates that the sample does not contain agglomerated particles [168] and that the gold nanoparticles are monodisperse.

The size distribution and morphology of gold nanoparticles were determined from AFM, (Fig. 23 A), TEM (Fig. 24 A) and SEM (Fig. 25 A) micrographs. As can be seen, the particles are nearly spherical in shape and monodisperse. The nanoparticle diameter was calculated as the average value from two perpendicular directions. The histogram obtained from the AFM image (Figs. 23 A, B) indicates that the average diameter of particles was 17 nm with a standard deviation of ±5 nm.

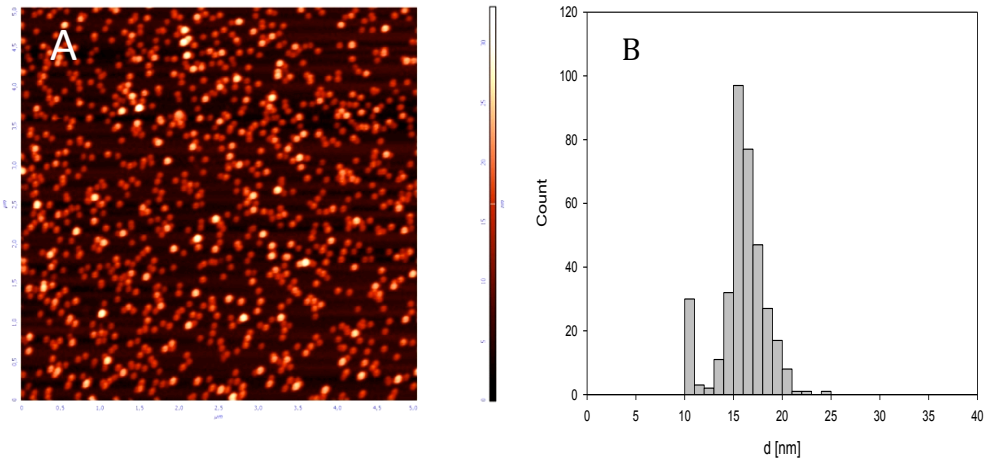

Fig. 23. *(A) The AFM image (scan area of 5 μm × 5 μm) of gold nanoparticles adsorbed on mica modified by the PAH monolayer obtained from colloidal gold suspension of 20 mgL^{-1}, in 10^{-2} M solution of NaCl, pH 6.0, deposition time 9 min; (B) the size distribution of the gold particles.*

Analogously, the average diameter of particles obtained by TEM (see Fig. 24) is 15 ± 3 nm.

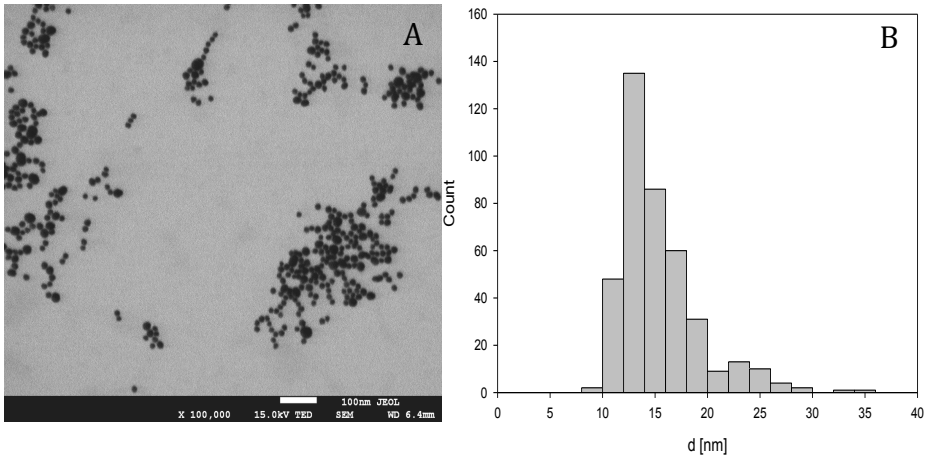

Fig. 24. *(A) TEM micrograph of gold nanoparticles; (B) size distribution of gold nanoparticles.*

A much higher value of 35 ± 5 nm was obtained by SEM (see Fig. 25), which is due to presence of a supporting chromium underlayer.

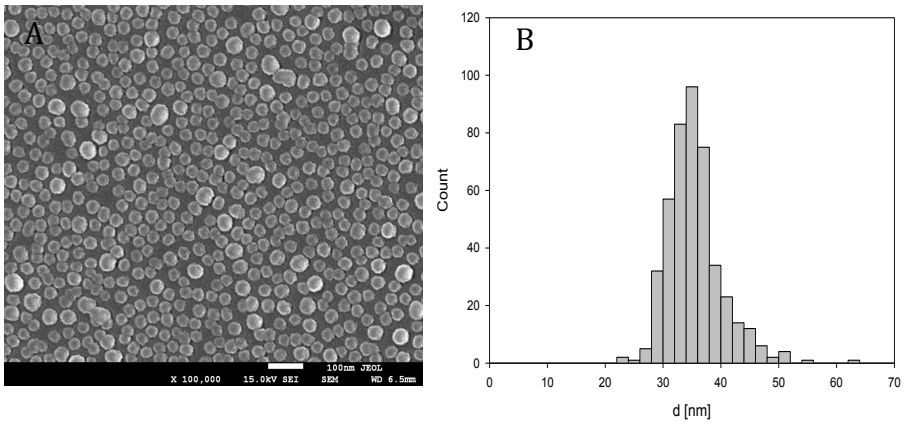

Fig. 25. *(A) SEM micrograph of gold nanoparticles; (B) size distribution of gold nanoparticles.*

3.3.2 The evaluation of electrophoretic mobility and zeta potential parameters

In addition to the particle size, the electrophoretic mobility and zeta potential (ζ) are key parameters for quantitative evaluation of particle stability in suspensions. The electrophoretic mobility was measured using the laser Doppler velocimetry (technique LDV).

The dependence of electrophoretic mobility of gold nanoparticles on pH, for ionic strength $I = 10^{-2}$ M NaCl is shown in Fig 26. As can be seen, the mobility is negative over the entire range of pH, indicating that the particles acquired a net negative charge. Moreover, μ_e decreases with pH, from – 2.46 μm cm (V s)$^{-1}$ for pH 2.0 to – 3.91 μm cm (V s)$^{-1}$ for pH 11. Because the ionic strength is the most important parameter that affects the interactions between nanoparticles, the dependence of electrophoretic mobility on ionic strength for various pH was also determined. As can be noticed (Fig. 27), the electrophoretic mobility of gold nanoparticles increases with ionic strength of solution independently of their pH. Thus, for pH 9 and $I=10^{-4}$ M, μ_e =-4.29 μm cm (V s)$^{-1}$, whereas for pH 9 and I=0.1 M NaCl, μ_e =-3.14 μm cm (V s)$^{-1}$. These highly negative values for electrophoretic mobility suggest that the gold suspension should remain stable for the above range of pH and ionic strength.

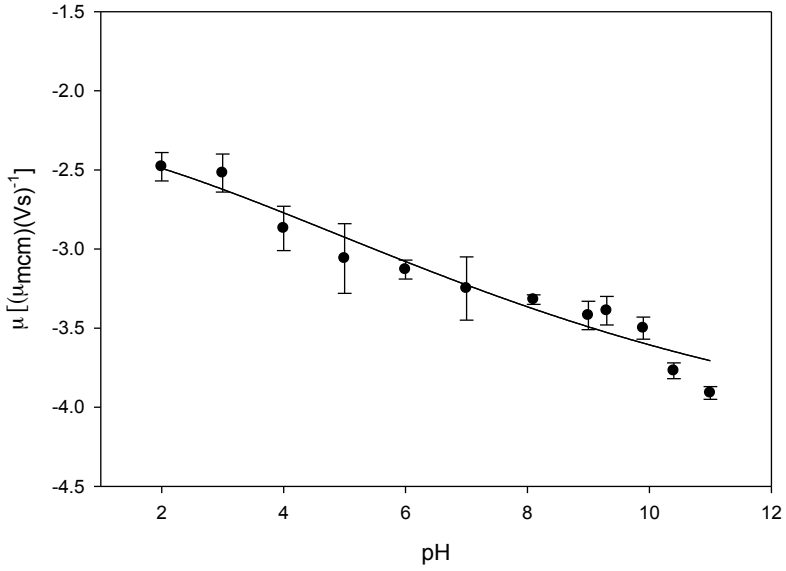

Fig. 26. *The dependence of the electrophoretic mobility of gold nanoparticles on pH for $I=10^{-2}$ M NaCl, T=298 K, the sol concentration was 50 mgL^{-1}. The solid line denotes the non-linear fit of experimental data.*

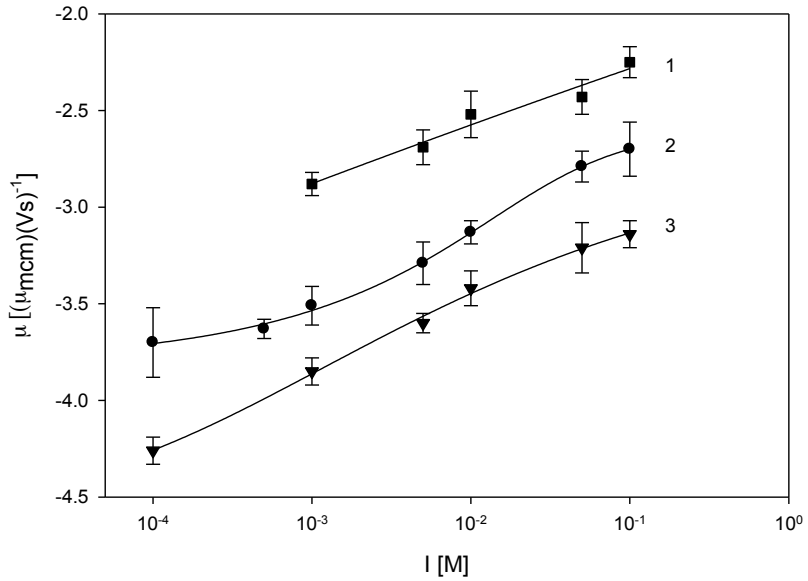

Fig. 27. *The dependence of the electrophoretic mobility of gold particles on ionic strength for: 1) (■) pH 3.0, 2) (●) pH 5.9, 3) (▼) pH 9.0, T=298 K, sol concentration 50 mg L^{-1}. The solids lines denote non-linear fits of experimental data.*

Knowing the electrophoretic mobility of particles for given conditions, one can calculate the zeta potential, a parameter commonly used to characterize nanoparticle suspensions and predict their stability. It was calculated using Henry's equation:

$$\zeta_p = \frac{\eta}{\varepsilon f(\kappa d_p)} \mu_e ,$$

where ζ_p is the 'zeta potential' of particles, ε is the dielectric permittivity of the medium , η is dynamic viscosity of the dispersion medium, $f(\kappa d_p)$ is the correction function of the dimensionless parameter κd_p, where

$$\kappa^{-1} = \left(\frac{\varepsilon k T}{2 e^2 I} \right)^{1/2}$$

is the thickness of the electric double layer [169] and I is the ionic strength of the electrolyte solution,

$$I = \frac{1}{2} \sum_{i=1} c_i z_i^2$$

where c is the ion concentration and z is the valency of ions.

For thin double layers (κd_p > 10), $f(\kappa d_p)$ approaches unity (Smoluchowski's approximation) and for thick double layers (κd_p > 1), $f(\kappa d_p)$ approaches $^2/_3$ (Hückel approximation). The values of the zeta potential of the particles are provided in the table 2.

Knowing the electrophoretic mobility one can estimate the electrokinetic (uncompensated) charge of nanoparticles from the Lorentz – Stokes relationship:

$$N_c = \frac{30 \pi \eta}{1.602} d_H \mu_e$$

where N_c is the number of elementary charges per particle (it should be remembered that $e = 1.602 \cdot 10^{-19}$ C), η is the dynamic viscosity of the solvent (expressed in g(cm s)$^{-1}$, d_H is the hydrodynamic diameter of nanoparticles

expressed in nm and μ_e is the electrophoretic mobility expressed in μm cm (V s)$^{-1}$.

For a more complete characterization of gold nanoparticles, the two-dimensional electrokinetic charge density can also be defined using the equation:

$$\sigma_e = \frac{N_c}{\pi d_p^{\,2}}$$

In order to facilitate further considerations, the values of the electrophoretic mobilities and charge densities for a broad range of ionic strength and pH are provided in Table 2.

Table 2. *Electrophoretic mobility, number of elementary charge and zeta potential of gold nanoparticles for various ionic strength (T = 298 K, sol concentration 50 mgL^{-1}).*

pH	Ionic strength [M]	μ_e [μm cm (Vs)$^{-1}$]	N_c	σ [e nm^{-2}]	ζ_p [mV] Smoluchowski's model	ζ_p [mV] Henry's model
	0.001	− 2.88	− 23	− 0.0319	− 36.7	− 53.6
	0.005	− 2.69	− 21	− 0.0298	− 34.2	− 48.6
3	0.01	− 2.52	− 20	− 0.0279	− 32.1	− 44.7
	0.05	− 2.43	− 19	− 0.0269	− 30.9	− 39.9
	0.1	− 2.25	− 18	− 0.0249	− 28.6	− 35.3
	0.0001	− 3.70	− 29	− 0.0410	− 47.1	− 70.4
	0.001	− 3.51	− 27	− 0.0389	− 44.7	− 65.3
5.9	0.005	− 3.29	− 26	− 0.0364	− 41.9	− 59.4
	0.01	− 3.13	− 24	− 0.0346	− 39.8	− 55.5
	0.05	− 2.80	− 22	− 0.0310	− 35.6	− 45.9
	0.01	− 2.70	− 21	− 0.0299	− 34.3	− 47.8
	0.0001	− 4.26	− 33	− 0.0472	− 54.2	− 80.9
	0.001	− 3.85	− 30	− 0.0426	− 48.9	− 71.6
9	0.005	− 3.60	− 28	− 0.0398	− 45.8	− 64.9
	0.01	− 3.42	− 27	− 0.0379	− 41.2	− 57.4
	0.05	− 3.21	− 25	− 0.0355	− 40.8	− 52.6
	0.01	− 3.14	− 25	− 0.0348	− 39.9	− 49.2

It should be noted that such data have not been reported in scientific literature before. The N_c decrease from the highest value of -18 observed in 0.1 M, NaCl at pH 3 to -33 in 10^{-4} M, NaCl at pH 9 was registered. As can be seen, N_c decreases monotonically with increase of both ionic strength and pH. These data indicate that the gold nanoparticles exhibit a high negative charge for a broad range of pH and ionic strength, which is expected to promote their efficient deposition on positively charged substrates.

3.3.3 Kinetics of gold particle deposition

The kinetics of gold particle deposition on mica was studied according to the above-described procedure. In our experiments, the bulk concentrations of the gold suspensions were 5, 10, 20 and 50 mg L^{-1}. The value of pH was 5.9.

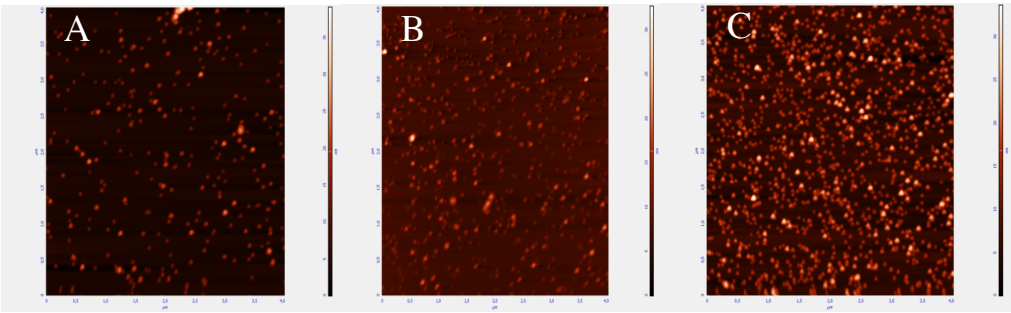

Fig. 28. *AFM images (scan area of 4 µm ×4 µm) of gold nanoparticles adsorbed on mica modified by the PAH monolayer: (A) deposition time 6 min, (B) deposition time 11 min, (C) deposition time 25 min. Deposition conditions: bulk suspension concentration 20 mg L^{-1}, pH 5.9, I = 10^{-2} M NaCl, T = 293 K.*

The surface concentration (coverage) of formed monolayers was determined *ex-situ* by AFM and SEM. The number of particles per unit area of the surface was determined from AFM images using image-analysis software. As can be seen in Fig. 28 the coverage of gold nanoparticles on mica systematically increases with the time of deposition. Quantitatively, the kinetic runs obtained for various bulk suspension concentrations are presented in Fig.

30 as the dependence of the surface concentration of particles on the square root of the adsorption time. This coordinate system is appropriate for the diffusion-controlled kinetics as shown in previous papers dealing with nanoparticle deposition on solid substrates [170, 171].

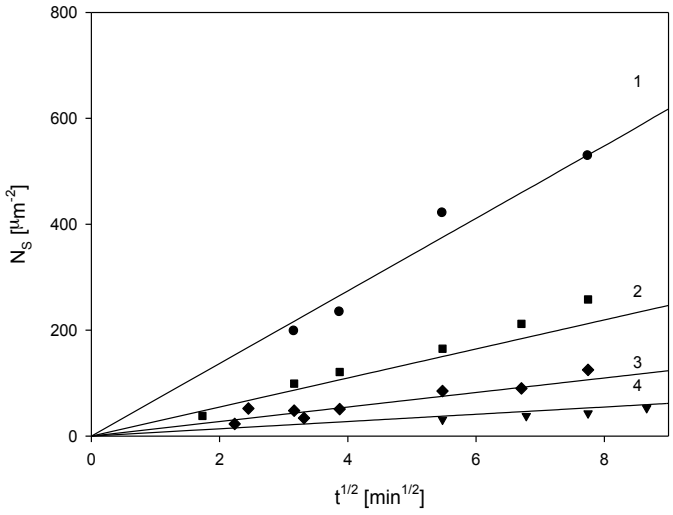

Fig. 29. *The kinetics of gold nanoparticle adsorption on PAH modified mica determined for various bulk suspension concentrations: 1) (●) 50 mg L^{-1}, 2) (■) 20 mg L^{-1}, 3) (♦) 10 mg L^{-1}, 4) (▼) 5 mg L^{-1}, I=10^{-2} M NaCl, pH=5.9, T=293 K. The points denote experimental result obtained using AFM and the solid lines represent the theoretical data calculated from the RSA model.*

As can be seen, particle surface concentration increases linearly with $t^{1/2}$, with the slope proportional to the bulk particle concentration. This agrees with the theoretical predictions (solid lines in Fig. 29) derived for the hybrid model where the bulk diffusion transport equation is numerically solved by the finite-difference method with the boundary condition (blocking function) is derived from the random sequential adsorption (RSA) model [170, 171].

Additionally, the maximum coverage of gold particle monolayers was determined as a function of ionic strength using AFM and SEM imaging. For the 10^{-4} M NaCl concentration the maximum coverage was 10% increasing to 13% for 10^{-3} M NaCl and 15%, for 10^{-2} M NaCl.

There are many published reviews about gold nanoparticles and their possible applications in biosensors [172-174]. The gold monolayers evaluated in this paper can be easily applied for biosensing [175, 176]. The surface plasmon resonance phenomenon and a direct electron transfer across the monolayer provide a wide range of applications in optical and electrochemical biosensors. Therefore AuNPs-based platform optimization with nanoparticle coverage modulation is useful in sensor development while the coverage, composition and surroundings of the nanoparticles affect their optical properties [177].

In order to investigate the influence of direct electron transfer across the polyelectrolyte and gold nanoparticles layer, carbon rod electrodes, modified with PAH, based on adsorbed polypyrrole-coated glucose oxidase with gold nanoparticles were prepared. The influence of the PAH layer over the electrodes of designed biosensing system was investigated.

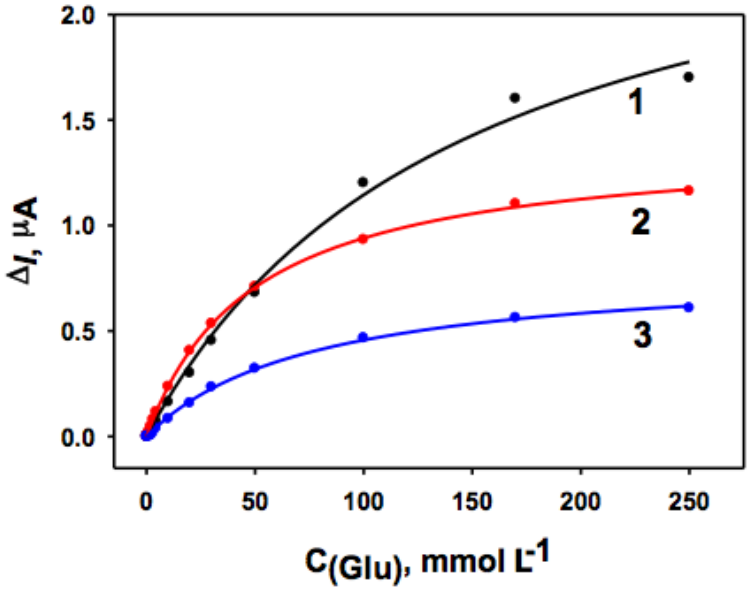

Fig. 30. *Calibration plots of carbon rod electrodes based on adsorbed polypyrrole-coated glucose oxidase with gold nanoparticles. 1 curve represents electrode modified with PAH, GOx, AuNPs and polypyrrole; 2 curve represents electrode without PAH, modified with AuNPs and with GOx and polypyrrole; 3 curve represents control electrode without polypyrrole layer with modification of PAH, GOx and AuNPs. The size of AuNPs – 13 nm.*

Polymerization time – 16 h, measurement in 0.05 M Na–acetate buffer, pH 6 containing 2 mmol L^{-1} PMS, at +0.3V vs. Ag/AgCl/KCl.

Chemical polymerization of pyrrole over GOx/AuNP/PAH/CR electrodes were performed in 0.05 Na-acetate buffer, pH 6, 16 $mmolL^{-1}$ glucose, 1.1 $mgmL^{-1}$ GOx and 236 $mmolL^{-1}$ pyrrole.

All electrochemical measurements were performed using a computerized potentiostat PGSTAT 30/Autolab (EcoChemie, Netherlands) with GPES 4.9 software in amperometry modes (the first conditioning potential +0.3V $Ag/AgCl/KCl_{3M}$). A conventional three-electrodes system comprising a prepared working graphite electrode, 2 cm^2 platinum as an auxiliary electrode and $Ag/AgCl/KCl_{3M}$ Metrhom (Herisau, Switzerland) as a reference was employed for all electrochemical experiments. Between measurements all electrodes were stored at +4°C in a closed vessel hanging over the solution of buffer to maintain constant humidity. The results of all electrochemical measurements are reported as the mean value of three independent experiments.

The kinetic parameters: the maximal speed of an enzymatic reaction and the apparent Michaelis-Menten constant are correspondingly *a* and *b* parameters of hyperbolic function $y = ax/(b+x)$ used for approximation of results.

PAH showed a positive effect on the amperometric signals of GOx/AuNP/CR modified electrodes (fig. 30.). This polyelectrolite layer significantly increased electron transfer rate from GOx to surface of graphite electrode. When attaching AuNPs onto modified electrode with PAH, ΔI is approximately 2 times higher compared to electrode with attached AuNP by physical absorbtion on graphite electrode without PAH.

Ppy increases the amperometric signal (fig. 30, curves 1, 2) of modified with Ppy electrodes compared with the electrode without polypyrrole nanoparticles (fig. 30. curves 3). Ppy nanoparticles effectively interacts with Au nanoparticles [178, 179]. Recent studies have shown that Au-NPs in a

combination with enzymatically formed polypyrrole layer offered some advantages for the design of electrochemical biosensors. Also, smaller Au-NPs based systems exhibited higher amperometric responses at the same concentration of glucose before and after the formation of polypyrrole layer [99].

PAH effectively attaches AuNPs and in such way increases surface area of electrodes. PAH contains amine functionalities which have high affinity for anionic gold nanoparticles [180]. AuNPs, in turn, more efficiently acts as redox mediator in this enzymatic system, while reduces insulating properties of GOx shell and paves the way of a shorter path for electrons exchange from enzyme's active center to the electrode.

Varying surface coverage of gold nanoparticles on modified electrodes with PAH can offer some very attractive advantages in the design of biosensing system.

Section 3.3 conclusions

Monodisperse, spherical, negatively charged gold nanoparticles were synthetized and thoroughly characterized by dynamic light scattering (DLS) and microelectrophoretic measurements. For the first time in the literature the electrokinetic charge of particles was quantitatively evaluated for a broad range of pH and ionic strength. Systematic studies of particle deposition kinetics on PAH modified mica carried out by AFM and SEM methods confirmed that this process was diffusion controlled, with the initial rate proportional to the bulk concentration of particles. On the other hand, for long adsorption times, the saturation coverage was attained, which systematically increased with the ionic strength of the particle suspension. It was shown that the adsorption kinetic runs could be adequately interpreted in terms of the hybrid theoretical model, where the bulk diffusion transport equation is solved with the boundary condition derived from the RSA model. Besides confirming the validity of this theoretical approach, our results proved that it is feasible to

produce uniform gold particle monolayers of a desired coverage controlled by varying the bulk suspension concentration and the ionic strength.

3.4 Fluorescence measurements of glucose oxidase with gold nanoparticles encapsulated in polypyrrole matrix.

Introduction. Gold nanoparticles have been used for enhancing electron-transfer rate between the active redox center of enzyme and electroactive species [181]. Also it was shown that gold nanoparticles affects the efficient enzyme immobilization. Gold nanoparticles provides (i) the immobilization of biomolecules, (ii) the catalysis of electrochemical reactions, (iii) the enhancement of electron transfer, (iv) labeling of biomolecules and even acting as reactant [182].

3.4.1 Evaluation of colloidal composite consisting of glucose oxidase, gold nanoparticles and polypyrrole.

Nanoparticles in general have been reported to either affect or leave unchanged enzyme structure and function. The way how biological environment interacts with nanoparticles is basically through the formation of tightly and/or loosely bound layers around the nanoparticles [128].

Gold nanoparticles, known to have high electrochemically active surface, are often used as redox mediators for efficient electron transfer at the time of the enzymatic reaction. AuNPs allows the enzyme molecules move freely, thus increasing the possibility of the active center of FAD prosthetic groups readily interact with the metal surface of the nanoparticles. In such way the effectiveness of electron transfer increases. Figure 31 illustrates the unfolding process of FAD from GOx with the increase of fluorescence relaxation time from 2.6 ns to 4.3 ns. In the case of added glucose (Glu) in the system, fluorescence relaxation kinetics at 530 nm (fig. 32, (b)) after 7 days did not changed and one – exponentially relaxation with 4.6 ns decay length. It

can be assumed that glucose accelerates unwrapped FAD stabilization. It can also be noted that glucose slows the formation of reduced FAD ($FADH_2$) (Fig. 31 (b)).

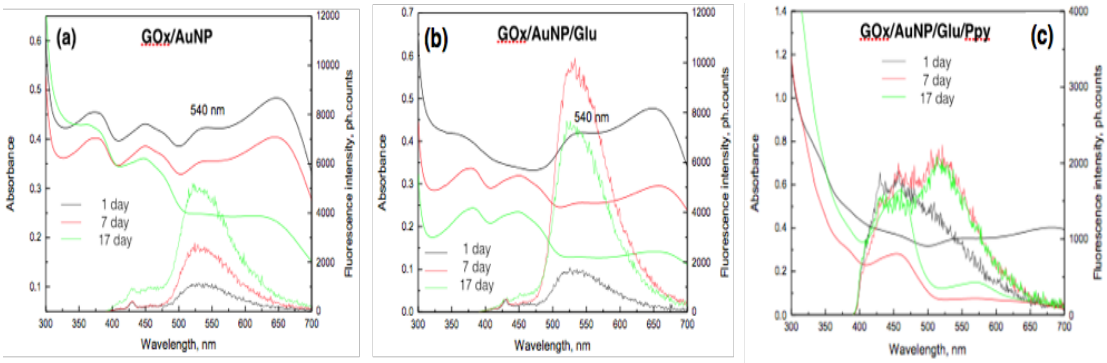

Fig. 31. *Fluorescence spectra of glucose oxidase (a) with gold nanoparticles, (b) with gold nanoparticles and glucose, (c) with gold nanoparticles, glucose and polypyrrole. All in Na – acetate buffer, pH 6, consisting of 16 mmol L^{-1} glucose, 1.1 $mgmL^{-1}$ GOx and 236 $mmolL^{-1}$ pyrrole. Diameter of AuNPs – 13 nm.*

The fluorescence intensity spectrum (Fig. 31.) shows a peak at around 540 nm attributed to FAD isoalloxazine moiety, which remains in all measurements.

Ppy efficiently stabilizes the systems (Fig. 31, (c)) within the immobilization aspect. Furthermore, Ppy reduces the influence of interfering species [183].

Flavin nucleotide strongly binds to apo-enzyme, which leads to spatial barrier to electron transfer, but we assume that gold nanoparticles react with reduced form of FAD of immobilized glucose oxidase and speeds up the unfolding process with the direct electron transfer assistance [183].

3.4.2 Time-resolved fluorescence measurements of colloidal composite.

Figures 31 and 32 demonstrates that the enzyme FAD unfolding from the GOx center is accelerated to 2 times compared to composite without gold

nanoparticles, because the FAD electron interaction with gold nanoparticles act as efficient “puller” from the enzymes active center.

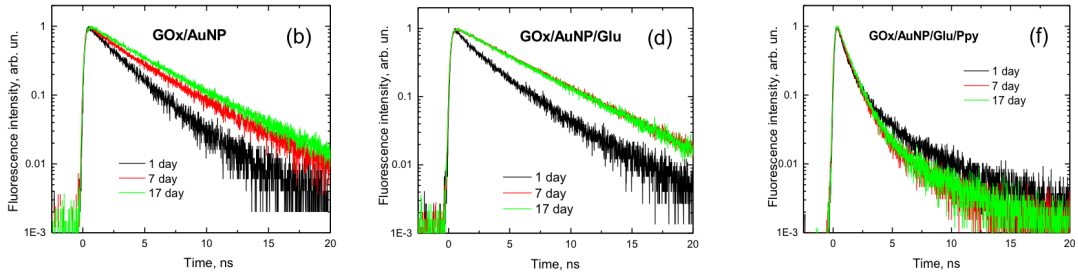

Fig. 32. *Fluorescence decay kinetics of (a) glucose oxidase with gold nanoparticles, (b) glucose oxidase with gold nanoparticles and glucose, (c) glucose oxidase with gold nanoparticles incapsulated in polypyrrole, and glucose. Na – acetate buffer, pH 6, consisting of 16 mmolL^{-1} glucose, 1.1 mgmL^{-1} GOx and 236 mmolL^{-1} pyrrole. Diameter of AuNPs – 13 nm.*

Polypyrrole strongly quenches FAD fluorescence (Fig. 32 (c)). Fluorescence intensity at 530 nm is reduced by more than 2 times. Over time, the gold nanoparticles strongly pronounced FAD fluorescence at 530 nm (Fig. 31 (c), Fig. 32 (c)). It means, that FAD dissociation from the center of the enzyme is accelerated by ~ 2 times because the interaction of delocalized FAD electrons with the gold nanoparticles.

Conclusions for section 3.4.

Gold nanoparticles have been used as electron-transfer mediators of the active center of an enzyme without unfolding its structure. It was shown that AuNPs increase the efficiency of enzyme immobilization and enhances the electron transfer rate.

General Conclusions

- It was determined that cofactor – flavin adenine dinucleotide – is diffusing out from glucose oxidase much slower if the enzyme is encapsulated within polypyrrole matrix by ‘enzymatic‘ polymerisation.
- Polypyrrole substrate increases the sensitivity of fluorescent sensors, due to quenching of fluorescence of non-specifically absorbed florescent materials.
- Kinetics of monodispersed, spherical, negatively charged gold nanoparticle deposition on a solid surface is controlled by diffusion, with the initial rate proportional to the bulk concentration of nanoparticles. For long adsorption times, the saturation coverage systematically increased with the ionic strength of the nanoparticle suspension.
- Gold nanoparticles increase the efficiency of enzyme immobilization and acts as electron – transfer mediators enhancing the electron –transfer rate.

Validation of the results:

List of publications by the author of the dissertation:

U. Bubniene, M. Ocwieja, B. Bugelyte, Z. Adamczyk, M. Nattich-Rak, J. Voronovic, A. Ramanaviciene, A. Ramanavicius (2013), Deposition of gold nanoparticles on mica modified by poly(allylamine hydrochloride) monolayers, pp. 204-210, *Colloids and Surfaces A Physicochemical and Engineering Aspects*.

A. Ramanavicius, N. Ryskevic, A. Kausaite-Minkstimiene, **U. Bubniene**, I. Baleviciute, Y. Oztekin, Almira Ramanaviciene (2012), Fluorescence study of glucose oxidase self-encapsulated within polypyrrole, pp. 753-759, *Sensors and Actuators B: Chemical*.

A. Ramanavicius, N. Ryskevic, Y. Oztekin, A. Kausaite-Minkstimiene, S. Jursenas, J. Baniukevic, J. Kirlyte, **U. Bubniene**, A. Ramanaviciene (2010), Immunosensor based on fluorescence quenching matrix of the conducting polymer polypyrrole, pp. 3105-3113, *Analytical and Bioanalytical Chemistry*.

List of manuscripts (in preparation) by the author of the dissertation:

U. Bubniene, B. Bugelyte ,P. Genys, A. Ramanavicius, Gold nanoparticle multilayers formation by Layer-by-Layer technique.

U. Bubniene, R. Karpicz, V. Gulbinas, A. Ramanavicius, Time-resolved fluorescence measurements of glucose oxidase self-encapsulated with conducting polymer polypyrrole.

List of conferences, where the results of the dissertation were presented:

N. Ryskevic, **U. Bubniene**, S. Jursenas, J. Baniukevic, J. Kirlyte, A. Ramanaviciene, A. Ramanavicius, Conducting polymer based fluorescence quenching matrix for immunosensor design, 9th International Electrochemistry Meeting in Turkey, 25-29 September, 2011, Izmir, Turkey.

A. Ramanavicius, N. Ryskevic, A. Kausaite – Minkstimiene, **U. Bubniene**, A. Ramanaviciene, Glucose oxidase self-encapsulated within polypyrrole research in fluorescence spectroscopy, 2nd International Conference on Competitive Materials and Technology Processes, 8 - 12 October, 2012, Miskolc-Lillafüred, Hungary.

U. Bubniene, M. Ocwieja, B. Bugelyte, Z. Adamczyk, M. Nattich, A. Ramanavicius, J. Voronovic, Metal Nanoparticle Adsorption Study, Bio-Tribocorrosion Training Courses - Conference, 11 -15 February, 2013, Ecole Centrale Paris, France.

U. Bubniene, B. Bugelyte, M. Ocwieja, Z. Adamczyk, M. Nattich, J. Voronovic, A. Ramanavicius, Metal nanoparticle Characteristic Study for Fluorescence Applications, The International Conference of Young Chemists "Nanotechnology and Nanomaterials", 7 -9 December, 2012, Palanga, Lithuania.

B. Bugelyte, **U. Bubniene,** M. Ocwieja, Z. Adamczyk, M. Nattich, J. Voronovic, A. Ramanavicius, Gold Nanoparticles Study of absorption kinetics, The International Conference of Young Chemists "Nanotechnology and Nanomaterials", 7 -9 December, 2012, Palanga, Lithuania

U. Bubniene, Z. Balevicius, A. Ramanaviciene, B. Bugelyte, A. Ramanavicius, Adsorption of gold nanoparticle multilayers, 2nd International conference on Nanotechnologies and Biomedical Engineering, 18 – 20 April, 2013, Chisinau, Moldova.

U. Bubniene, B. Bugelyte, A. Ramanavicius, Gold nanoparticle multilayers formation by Layer-by-Layer deposition technique, 18th International Scientific Conference "EcoBalt 2013", 25 – 27 October, 2013, Vilnius, Lithuania.

U. Bubniene, R. Karpicz, V. Gulbinas, A. Ramanavicius, Time-Resolved Fluorescence Spectroscopy of Polypyrrole Polymer Immobilized Glucose Oxidase, Functional Materials and Nanotechnologies Conference (FM&NT-2015), 5 - 8 October, 2015, Vilnius, Lithuania. (Abstract submitted and accepted)

List of workshops, where the results of the dissertation were presented:

U. Bubniene, A. Ramanavicius, E.-J. Podlaha-Murphy, Synthesis of gold nanoparticles and deposition onto solid surfaces, IRSES FP7 workshop, Aleksandras Stulginskis University, 13th of November, 2013, Kaunas, Lithuania.

Author's contribution:

Author personally performed fluorescence measurements on glucose oxidase self-encapsulated within polypyrrole, Ppy fluorescence quenching, and deposition of gold nanoparticles on monolayers.

Author prepared and performed synthesis of gold nanoparticles, polypyrrole particles. Performed AFM, SEM (with assistance), spectrophotometric measurements, estimated RSA model analysis (with assistance), performed laser Doppler velocimetry (technique LDV) technique, densitometer measurements.

Before measurements author prepared all the necessary samples for investigation.

Author also significantly contributed in the analysis of the results, the writing of scientific publications and the preparation of conference material.

References

1. A.J. Ozinskas, *Principles of Fluorescence Immunoassay*, in *Topics in Fluorescence Spectroscopy. Probe Design and Chemical Sensing*, J.R. Lakowicz, Editor. 1994, Plenum Press: New York. p. 449-490.
2. S.E. Braslavsky, *Glossary of terms used in photochemistry, 3rd edition.* Pure Appl. Chem., 2009. **79**(3): p. 293-465.
3. P.F. Smet, I. Moreels, Z. Hens, D. Poelman, *Luminescence in Sulfides: A Rich History and a Bright Future.* Materials, 2010. **3**: p. 2834-2883.
4. D. Costenaro, F. Carniato, G. Gatti, L. Marchese, C. Bisio, *Preparation of luminescent ZnO nanoparticles modified with aminopropyltriethoxy silane for optoelectronic applications.* New J. Chem., 2013. **37**(7): p. 2103-2109.
5. V.K.A. Sreenivasan, A.V. Zvyagin, E.M. Goldys, *Luminescent nanoparticles and their applications in the life sciences.* J. Phys.: Cond. Matt., 2013. **25**(19): p. 194101-194124.
6. E. Peik, *Long-lasting photoluminescence in polymers.* J. Phys. D: Appl. Phys., 2007. **40**(11): p. 3330.
7. W. J. Feast, F. Cacialli, A.T.H. Koch, R. Daik, C. Lartigau, R.H. Friend, D. Beljonned, J.-L. Brédase, *Control of luminescence in conjugated polymers through control of chain microstructure.* J. Mater. Chem., 2007. **17**(9): p. 907-912.
8. J. Heine, K. Müller-Buschbaum, *Engineering metal-based luminescence in coordination polymers and metal–organic frameworks.* Chem. Soc. Rev.,, 2013. **42**(24): p. 9232-9242.
9. W. Cho, H.J. Lee, S. Choi, Y. Kim, M. Oh, *Highly effective heterogeneous chemosensors of luminescent silica@coordination polymer core-shell micro-structures for metal ion sensing.* Sci. Rep., 2014. **4**.
10. C.M. Augustin, B. Oswald, O.S. Wolfbeis, *Time-Resolved Luminescence Energy Transfer Immunobinding Study Using a*

Ruthenium–Ligand Complex as a Donor Label. Anal. Biochem., 2002. **305**(2): p. 166–172.

11. T.S. Wehrman, G. von Degenfeld, P.O. Krutzik, G.P. Nolan, H.M. Blau, *Luminescent imaging of β-galactosidase activity in living subjects using sequential reporter-enzyme luminescence.* Nat. Meth., 2006. **3**(4): p. 295 - 301.
12. S.M. Gautier, L.J.B., P.R. Coulet, *Fibre-optic biosensor based on luminescence and immobilized enzymes: microdetermination of sorbitol, ethanol and oxaloacetate.* J. Biolumin. Chemilumin., 1990. **5**(1): p. 57-63.
13. M.G. Acker, D.S.A., *Considerations for the design and reporting of enzyme assays in high-throughput screening applications.* Persp. Sci., 2014. **1**(1-6): p. 56–73.
14. G.G. Stokes, *On the Change of Refrangibility of Light. No. I.* Phil. Trans. R. Soc. Lond., 1852. **142**: p. 463-562.
15. J.R. Lakowicz, *Principles of Fluorescence Spectroscopy*. 3 ed. 2006, New York: Springer US. 954.
16. R.C. Groza, A.C., A.G. Ryder, *A fluorescence anisotropy method for measuring protein concentration in complex cell culture media.* Anal. Chim. Acta, 2014. **821**: p. 54-61.
17. S. Bi, L.Y., B. Pang, Y. Wang, *Investigation of three flavonoids binding to bovine serum albumin using molecular fluorescence technique.* J. Lumin., 2012. **132**(1): p. 132-140.
18. J. Widengren , V.K., M. Antonik, S. Berger, M. Gerken, C.A. Seidel, *Single-Molecule Detection and Identification of Multiple Species by Multiparameter Fluorescence Detection.* Anal. Chem., 2006. **78**(6): p. 2039–2050.
19. J.R. Lakowicz, M.H.C., K. Ray, J. Zhang, Y. Fu, R. Badugu, C.R. Sabanayagam, K. Nowaczyk, H. Szmacinski, K. Aslan, C.D. Geddes *Plasmon-controlled fluorescence: A new detection technology* Proc SPIE Int Soc Opt Eng. , 2006. **6099**.

20. K. Schmitz, *Introduction to Bioorganic Chemistry and Chemical Biology*. 1st ed, ed. V.D.V.V.u.G.A. Weiss. Vol. 125. 2013: Garland Science.
21. X. Song, W.H., J. Shi, J.W. Park, B.I. Swanson, *Conjugated polymers as efficient fluorescence quenchers and their applications for bioassays* Chem. Mater. 2002. **14**(5): p. 2342–2347.
22. A. Ramanaviciene, A. R.amanavicius, *Application of polypyrrole for the creation of immunosensors.* Crit. Rev. Anal. Chem., 2002. **32**(3): p. 245–252.
23. Z. Zhang, R.R., F.J. Dugre, D. Tessier, L.H. Dao *In vitro biocompatibility study of electrically conductive polypyrrole-coated polyester fabrics.* J. Biomed. Mate.r Res., 2001. **57**(1): p. 63–71.
24. B. Liu, G.C. Bazan, *Optimization of the molecular orbital energies of conjugated polymers for optical amplification of fluorescent sensors.* J. Am. Chem. Soc., 2006. **128**(4): p. 1188–1196.
25. A. Ramanaviciene, A. Finkelsteinas, A. Ramanavicius, *Basic electrochemistry meets nanotechnology: electrochemical preparation of artificial receptors based on a nanostructured conducting polymer, polypyrrole.* J. Chem. Educ., 2006. **83**(8): p. 1212–1214.
26. A. Kausaite-Minkstimiene, A. Ramanaviciene, J. Kirlyte, A. Ramanavicius *Comparative study of random and oriented antibody immobilization techniques on the binding capacity of immunosensor.* Anal. Chem., 2010. **82**(15): p. 6401–6408.
27. A. Ramanaviciene, A.Ramanavicius, *Molecularly imprinted polypyrrole-based synthetic receptor for direct detection of bovine leukemia virus glycoproteins.* Biosens. Bioelectron., 2004. **20**(6): p. 1076–1082.
28. Y.L. Pan, *Detection and characterization of biological and other organic-carbon aerosol particles in atmosphere using fluorescence.* J. Quant. Spectrosc. Radiat. Transfer, 2015. **150**: p. 12-35.

29. M.V. Pástor, *Direct immunofluorescent labeling of cells*, in *Immunocytochemical Methods and Protocols*, C. Oliver and M.C. Jamur, Editor. 2010, Humana Press: New York. p. 135-142.
30. T.G.M. Schalkhammer, *Analytical Biotechnology. Methods and Tools in Biosciences and Medicine*. 2012, Berlin: Birkhäuser.
31. M. Sauer, J.H., J. Enderlein, *Handbook of Fluorescence Spectroscopy and Imaging: From Ensemble to Single Molecules*. Vol. 1. 2011, Weinheim, Germany: WILEY-VCH 290.
32. R. Esposito, D.I., M. Lepore, *Time-resolved flavin adenine dinucleotide fluorescence study of the interaction between immobilized glucose oxidase and glucose.* J Fluoresc., 2013. **23**(5): p. 947-955.
33. M.N. Jones, P.M., A. Wilkinson, *The dissociation of glucose oxidase by sodium n-dodecyl sulphate.* Biochem J. , 1982. **203**(1): p. 285-291.
34. K Kusai, I. Sekuzu, B. Hagihara, K. Okunuki, S. Yamauchi, M. Nakai, *Crystallization of glucose oxidase from Penicillium amagaskiense.* Biochim. Biophys. Acta 1960. **40**: p. 555-557.
35. D. Zhong, A.H.Z., *Femtosecond dynamics of flavoproteins: charge separation and recombination in riboflavine (vitamin B2)-binding protein and in glucose oxidase enzyme.* Proc Natl Acad Sci USA, 2001. **98**(21): p. 11867-11872.
36. T. Nakamura, Y.O., *Kinetic studies on the action of glucose oxidase.* J Biochem. Tokyo, 1962. **52**(3): p. 214-220.
37. R. Wilson, *Glucose oxidase: an ideal enzyme.* Biosen. Bioelectron., 1991. **7**(3): p. 165-185.
38. H. Maeda, S. Matsu-ura, T. Senba, S. Yamasaki, H. Takai, Y. Yamauchi, H. Ohmori, *Resorufin as an electron acceptor in glucose oxidase-catalyzed oxidation of glucose.* Chem. Pharm. Bull. (Tokyo). 2000. **48**(7): p. 897-902.
39. V. Leskovaca, S.T., G. Wohlfahrt, J. Kandrac, D. Pericin, *Glucose oxidase from Aspergillus niger: the mechanism of action with molecular*

oxygen, quinones, and one-electron acceptors. The International Journal of Biochemistry & Cell Biology 2005. **37**: p. 731-750.

40. A. Ramanavicius, N. Ryskevic, A. Kausaite-Minkstimiene, U. Bubniene, I. Baleviciute, Y. Oztekin, A. Ramanaviciene, *Fluorescence study of glucose oxidase self-encapsulated within polypyrrole.* Sens. Actuators B, 2012. **171-172**: p. 753-759.
41. W.W. Cleland, *The kinetics of enzyme-catalyzed reactions with two or more substrates or products: I. Nomenclature and rate equations.* Biochim. Biophys. Acta, 1963. **67**: p. 104-137.
42. Q.H. Gibson, B.E.S., V. Massey, *Kinetics and mechanism of action of glucose oxidase.* J. Biol. Chem. , 1964. **239**: p. 3927–3934.
43. D'Auria S, H.P., Rossi M, Lakowicz JR., *The fluorescence emission of the apo-glucose oxidase from Aspergillus niger as probe to estimate glucose concentrations.* Biochem Biophys Res Commun., 1999. **263**(2): p. 550-553.
44. D. Muller, *Oxidation von Glukose mit Extrakten aus Aspegillus niger.* Biochemische Zeitschrift, 1928: p. 199.
45. R. Bentley, *Glucose oxidase*, in *The Enzymes*, P. D. Boyer, H. Lardy, K. Myrback, Editors. 1963, Academic Press: London. p. 567-586.
46. R.F. Anderson, *Energetics of the one-electron reduction steps of riboflavin, FMN and FAD to their fully reduced forms.* Biochim. Biophys. Acta (BBA) - Bioenergetics, 1983. **722**(1): p. 158-162.
47. S. Ghisla, V.Massey, *Mechanisms of flavoprotein-catalyzed reactions.* Eur. J. Biochem., 1989. **181**(1): p. 1-17.
48. T. Nakabayashi, M.S.I., N. Ohta, *Fluorescence decay dynamics of flavin adenine dinucleotide in a mixture of alcohol and water in the femtosecond and nanosecond time range.* J Phys Chem B, 2010. **114**(46): p. 15254-15260.
49. J.M. Miller, L.D.M., C. Olson, K.G. Gillette, *Virus-like particles in phytohemagglutinin-stimulated lymphocyte cultures with reference to bovine lymphosarcoma.* J Natl Cancer Inst., 1969. **43**(6): p. 1297-1305.

50. A. Burny, Y.C., R. Kettmann, M. Mammerickx, G. MarbaixD. , Portetelle, A. van den Broeke, L. Willems, R. Thomas, *Bovine leukaemia: Facts and hypotheses derived from the study of an infectious cancer.* Vet Microbiol, 1988. **17**(3): p. 197–218.
51. C.A. Rosen, J.G.S., R. Kettman, A. Burny, W.A. Haseltine., *Trans activation of the bovine leukemia virus long terminal repeat in BLV-infected cells.* Science, 1985. **227**(4684): p. 320-322.
52. A. Araujo, N.S., H. Takahashi, W.W. Hall., *Concomitant Infections with Human Immunodeficiency Virus Type 1 and Human T-Lymphotropic Virus Types 1 and 2*, in *Polymicrobial Diseases*, G.J. Brogden KA, Editor. 2002, ASM Press: Washington (DC).
53. W. Uckert, M.G., G. Beaudreau, *Translational order of bovine leukemia virus gag and env gene-coded proteins.* Virology, 1984. **135**(1): p. 288-292.
54. S. M. Rodríguez, A.F., N. Gillet, A. de Brogniez, M. T. Sánchez-Alcaraz, M. Boxus, F. Boulanger, G. Gutiérrez, K. Trono, I. Alvarez, L. Vagnoni, and L. Willems., *Preventive and Therapeutic Strategies for Bovine Leukemia Virus: Lessons for HTLV.* Viruses, 2011. **3**(7): p. 1210–1248.
55. S.I. Lim, W.J., D.S. Tark, D.K. Yang, C.H. Kweon, *Agar gel immunodiffusion analysis using baculovirus-expressed recombinant bovine leukemia virus envelope glycoprotein (gp51/gp30T-).* J. Vet. Sci., 2009. **10**(4): p. 331-336.
56. F.W. Eaves, M.J., C.K. Dimmock, L.E. Eaves, *A field evaluation of the polymerase chain reaction procedure for the detection of bovine leukemia virus proviral DNA in cattle.* Vet. Microbiol., 1994. **39**(3-4): p. 313-321.
57. M. Reichert, S.J., *Simultaneous use of two primer pairs increases the efficiency of polymerase chain reaction assay in the diagnosis of bovine leukemia virus infection.* J. Vet. Diagn. Investig., 1999. **11**: p. 543-547.

58. E.J. Kelly, J.M., G. Marsolais, J.D. Morrey, R.J. Callan, *Early detection of bovine leukemia virus in cattle by use of the polymerase chain reaction.* Am. J. Vet. Res., 1993. **54**(2): p. 205-209.

59. N. Sagata, T.Y., J. Tsuzuku-Kawamura, K. Ohishi, Y. Ogawa, Y. Ikawa, *Complete nucleotide sequence of the genome of bovine leukemia virus: its evolutionary relationship to other retroviruses.* Proc Natl Acad Sci USA, 1985. **82**(3): p. 677-681.

60. J.C. Kuckleburg, C.C.C., E.A. Nelson, S.A.E. Marras, M.A. Dammen, J. Christopher-Hennings, *Detection of bovine leukemia virus in blood and milk by nested and real-time polymerase chain reactions.* J. Vet. Diagn. Invest. 2003. **15**(1): p. 72-76.

61. B. J. Beaty, J.C., K. L. Brown, C. B. Gundersen, D. Nelson, J. T. McPherson, W.H. Thompson, *Indirect Fluorescent-Antibody Techniquefor Serological Diagnosis of La Crosse (California) Virus Infections.* J. clin. microb., 1982. **15**(3): p. 429-434.

62. S. Boonpucknavig, O. Vuttivirojana, J. Siripont, P. Futra-kul, S. Nimmannitay, *Indirect fluorescent anti- body technique for demonstration of serum antibody in dengue hemorrhagic fever cases.* Am. J. Clin. Pathol., 1975. **64**: p. 365-371.

63. E. Kaczmarczyk, B.B.-N., O. Cybulska, *Comparative analysis of an elisa and fluorescent antibody test for the diagnosis of bovine leukaemia virus infection in cattle.* Bull. Vet. Inst. Pulawy. 2008. **52**: p. 19-22.

64. A. Ramanaviciene, G.S., A. Ramanavicius, *Piezoelectric affinity biosensor for diagnosing bovine leukemia.* Biologija, 2004. **1**: p. 33-35.

65. A. Ramanavicius, A. Finkelsteinas, H. Cesiulis, A. Ramanaviciene, *Electrochemical impedance spectroscopy of polypyrrole based electrochemical immunosensor.* Biochem., 2010. **79**(1): p. 11-16.

66. J. Baniukevic, J. Kirlyte., A. Ramanavicius, A.Ramanaviciene, *Comparison of oriented and random antibody immobilization techniques on the efficiency of immunosensor.* Procedia Engineering, 2012. **47**: p. 837-840.

67. L.V. Pyrohova , M.F.S., V.P. Artiukh , L.I. Nahaieva , H.I. Dobrosol, *Express diagnostics of bovine leucosis by immune sensor based on surface plasmon resonance.* Ukr Biokhim Zh 2002. **74**(3): p. 88-92.
68. N. C. Veitch, *Horseradish peroxidase: a modern view of a classic enzyme.* Phytochem., 2004. **65**(3): p. 249-259.
69. L. Hassani, *Chemical modification of Horseradish peroxidase with carboxylic anhydrides: Effect of negative charge and hydrophilicity of the modifiers on thermal stability.* J. Molec. Catal. B, 2012. **80**: p. 15-19.
70. L. Hassani, *The Effect of Chemical Modification with Pyromellitic Anhydride on Structure, Function, and Thermal Stability of Horseradish Peroxidase.* Appl. Biochem. Biotechnol., 2012. **167**(3): p. 489-497.
71. D. Garcia, J.L. Marty, *Chemical modification of horseradish peroxidase with several methoxypolyethylene glycols.* Appl. Biochem. Biotechnol., 1998. **73**(2-3): p. 173-184.
72. Abuknesha RA, L.C., Griffith HH, Maragkou A, Iakovaki D., *Efficient labelling of antibodies with horseradish peroxidase using cyanuric chloride.* J Immunol Methods, 2005. **306**(1-2): p. 211-217.
73. S. Chairam, P. Buddhalee, M. Amatatongchai, *A Novel Hydrogen Peroxide Biosensor Based on Horseradish Peroxidase Immobilized on Poly(aniline-co-o-aminobenzoic acid) Modified Glassy Carbon Electrode Coated with Chitosan Film.* Int. J. Electrochem. Sci., 2013. **8**: p. 10250 - 10264.
74. R. Yang, C.Ruan, J. Deng, *A H2O2 biosensor based on immobilization of horseradish peroxidase in electropolymerized methylene green film on GCE.* J. Appl. Electrochem., 1998. **28**(11): p. 1269 - 1275.
75. M. Tertis, A. Florea, R. Sandulescu, C. Cristea, *Carbon Based Electrodes Modified with Horseradish Peroxidase Immobilized in Conducting Polymers for Acetaminophen Analysis.* Sens. (Basel), 2013. **13**(4): p. 4841 - 4854.

76. R. Balint, N.J. Cassidy, S.H. Cartmell, *Conductive polymers: Towards a smart biomaterial for tissue engineering.* Acta Biomat., 2014. **10**(6): p. 2341-2353.

77. D.D. Ateh, H.A. Navsaria, P. Vadgama, *Polypyrrole-based conducting polymers and interactions with biological tissues.* J. R. Soc. Interf., 2006. **3**(11): p. 741-752.

78. S. Zhang, K. Zhu, G. Lv, G. Wang, D. Yu, J. Shao, *UV-Catalytic Preparation of Polypyrrole Nanoparticles Induced by H2O2.* J. Phys. Chem. C, 2015. **119**(32): p. 18707-18718.

79. K. Leonavicius, A. Ramanaviciene, A. Ramanavicius, *Polymerization Model for Hydrogen Peroxide Initiated Synthesis of Polypyrrole Nanoparticles.* Langmuir, 2011. **27**(17): p. 10970 - 10976.

80. X. Cui, J. Wiler, M. Dzaman, R.A. Altschuler, D.C. Martin, *In vivo studies of polypyrrole/peptide coated neural probes.* Biomaterials, 2003. **24**(5): p. 777-787.

81. A. Ramanavicius, N. Ryskevic, Y.Oztekin, A. Kausaite-Minkstimiene, S.Jursenas, J. Baniukevic, J. Kirlyte, U. Bubniene, A. Ramanaviciene, *Immunosensor based on fluorescence quenching matrix of the conducting polymer polypyrrole.* Anal. Bioanal. Chem., 2010. **398**(7-8): p. 3105–3113.

82. Malinauskas, A., *Electrocatalysis at conducting polymers.* Synth. Met., 1999. **107**(2): p. 75-83.

83. A. Ramanaviciene, A. Kausaite, S. Tautkus, A. Ramanavicius, *Biocompatibility of polypyrrole particles: an in vivo study in mice.* J. Pharm. Pharmacol., 2007. **59**(2): p. 311–315.

84. D.-H. Han, H.J. Lee, S.-M. Park, *Electrochemistry of conductive polymers XXXV: Electrical and morphological characteristics of polypyrrole films prepared in aqueous media studied by current sensing atomic force microscopy.* Electrochim. Acta, 2005. **50**(15): p. 3085-3092.

85. A. Ramanaviciene, A. Ramanavicius, *UV Solid-State Light Emitters and Detectors*. Series II: Mathematics, Physics and Chemistry ed. M.S.S.a.Z. A. Vol. 144. 2004, Netherlands: Kluwer Academic Publishers.

86. C.C. Moser, J.L.R. Anderson., P.L. Dutton, *Guidelines for tunneling in enzymes.* Biochim. Biophys. Acta 2010. **1797**(9): p. 1573-1586.

87. D. Bélanger, J. Nadreau, G. Fortier, *Rotating ring-disk electrode studies of polypyrrole-glucose oxidase biosensors.* Electroanal., 1992. **4**(10): p. 933-940.

88. N.F. Almeida, E.J. Beckman, M.M. Ataai, *Immobilization of glucose oxidase in thin polypyrrole films: influence of polymerization conditions and film thickness on the activity and stability of the immobilized enzyme.* Biotechnol. Bioeng., 1993. **42**(9): p. 1037-1045.

89. T. Ahuja, I.A. Mir, D. Kumar, Rajesh, *Biomolecular immobilization on conducting polymers for biosensing applications.* Biomat., 2007. **28**(5): p. 791-805.

90. A. Ramanaviciusa, Y. Oztekin, Z. Balevicius, A. Kausaite-Mikstimiene, V. Krikstolaityte, I. Baleviciute, V. Ratautaite, A. Ramanaviciene, *Conducting and Electrochemically Generated Polymers in Sensor Design.* Procedia Engineering, 2012. **47**: p. 825-828.

91. D. T. Hoa , T.N.S. Kumar, N.S. Punekar , R.S. Srinivasa, R. Lal, A.Q. Contractor, *A biosensor based on conducting polymers.* Anal. Chem., 1992. **64**(21): p. 2645-2646.

92. Md.M. Rahman, X.-B. Li, N.S. Lopa, S.J. Ahn, J.-J. Lee, *Electrochemical DNA Hybridization Sensors Based on Conducting Polymers.* Sensors, 2015. **15**: p. 3801-3829.

93. J. Wang, N.V. Myung, M. Yun, H.G. Monbouquette, *Glucose oxidase entrapped in polypyrrole on high-surface-area Pt electrodes: a model platform for sensitive electroenzymatic biosensors.* J. Electroanal. Chem., 2005. **575**: p. 139-146.

94. A. Ramanavicius, A. Kausaite, A. Ramanaviciene, *Self-encapsulation of oxidases as a basic approach to tune upper detection limit of amperometric biosensors.* The Analyst 2008. **133**(8): p. 1083–1089.
95. A. Ramanavicius, A. Kausaite, A. Ramanaviciene, *Polypyrrole-coated glucose oxidase nanoparticles for biosensor design.* Sens. Actuators, B, 2005. **111-112**: p. 532-539.
96. M. Trojanowicz, W.M., M. Podsiadła, *Enzyme entrapped polypyrrole modified electrode for flow-injection determination of glucose.* Biosens Bioelectron. , 1990. **5**(2): p. 149-156.
97. A. Ramanavicius, A. Malinauskas, A. Ramanaviciene, *Catalytic biosensors based on conducting polymers*, in *Advanced Biomaterials for Medical Applications*, D.W. Thomas, Editor. 2004, Springer Netherlands. p. 93-109.
98. A. Ramanaviciene, G. Nastajute, V. Snitka, A. Kausaite, N. German, D. Barauskas-Memenas, A. Ramanavicius, *Spectrophotometric evaluation of gold nanoparticles as red-ox mediator for glucose oxidase.* Sens. Actuators, B, 2009. **137**(2): p. 483-489.
99. N. German, A. Ramanavicius, J. Voronovic, A. Ramanaviciene, *Glucose biosensor based on glucose oxidase and gold nanoparticles of different sizes covered by polypyrrole layer,* Colloids Surf., A, 2012. **413**: p. 224-230.
100. H. G. Boyen, G. Kastle, F. Weigl, B. Koslowski, C. Dietrich, P. Ziemann, J.P. Spatz, S. Riethmüller, C. Hartmann, M. Möller, G. Schmid, M.G. Garnier, P. Oelhafen, *Oxidation-Resistant Gold-55 Clusters.* Science, 2002. **297**: p. 1533-1536.
101. J. Baniukevic, I.H. Boyaci, A.G. Bozkurt, U. Tamer, A. Ramanavicius, A. Ramanaviciene, *Magnetic gold nanoparticles in SERS-based sandwich immunoassay for antigen detection by well oriented antibodies.* Biosens. Bioelectron., 2013. **43**: p. 281-288.

102. D. M. Schaadt, B. Feng, E.T. Yu, *Enhanced semiconductor optical absorption via surface plasmon excitation in metal nanoparticles.* Appl. Phys. Lett., 2005. **86**(6).
103. N. Lopez, T.V.W. Janssens, B.S. Clausen, Y. Xu, M. Mavrikakis, T. Bligaard, J.K. Nørskov, *On the origin of the catalytic activity of gold nanoparticles for low- temperature CO oxidation.* J. Catal., 2004. **223**(1): p. 232–235.
104. J. Kneipp, H. Kneipp, W.L. Rice, K. Kneipp, *Optical probes for biological applications based on surface-enhanced Raman scattering from indocyanine green on gold nanoparticles.* Anal. Chem., 2005. **77**(8): p. 2381–2385.
105. L. Polavarapu, Q.H.X., *Water-soluble conjugated polymer-induced self-assembly of gold nanoparticles and its application to SERS.* Langmuir, 2008. **24**(19): p. 10608-10611.
106. X.-M. Qian, S.M. Nie, *Single-molecule and single-nanoparticle SERS: from fun- damental mechanisms to biomedical applications.* Chem. Soc. Rev., 2008. **37**: p. 912–920.
107. J. Jia, B. Wang, A. Wu, G. Cheng, Z. Li, S. Dong, *A method to construct a third-generation horseradish peroxidase biosensor: self-assembling gold nanoparticles to three-dimensional sol–gel network.* Anal. Chem., 2002. **74**(9): p. 2217–2223.
108. K.L. Wustholz, A.I. Henry, J.M. McMahon, R.G. Freeman, N. Valley, M.E. Piotti, M.J. Natan, G.C. Schatz, R.P. Van Duyne, *Structure–activity relationships in gold nanoparticle dimers and trimers for surface-enhanced Raman spectroscopy.* J. Am. Chem. Soc., 2010. **132**(31): p. 10903–10910.
109. Y. Golan, L.Margulis, I. Rubinstein, *Vacuum-deposited gold films. I. Factors affecting the film morphology.* Surf. Sci., 1992. **264**(3): p. 312–326.
110. N.G. Semaltianos, E.G.Wilson, *Investigation of the surface morphology of thermally evaporated thin gold films on mica, glass, silicon and*

calcium fluoride substrates by scanning tunneling microscopy. Thin Solid Films, 2000. **366**(1-2): p. 111-116.

111. M. Okumura, S. Nakamura, S. Tsubota, T. Nakamura, M. Azuma, M. Haruta, *Chemical vapor deposition of gold on Al2 O3 , SiO2 , TiO2 for the oxidation of CO and H2,* Catal. Lett., 1998. **51**(1-2): p. 53-58.
112. M.J. Hostetler, R.W. Murray, *Colloids and self-assembled monolayers.* Curr. Opin. Colloid Interface Sci., 1997. **2**(1): p. 42-50.
113. K. Aslan, J.R. Lakowicz, C.D. Geddes, *Rapid deposition of triangular silver nanoplates on planar surfaces: application to metal-enhanced fluorescence.* J. Phys. Chem., B 2005. **109**(13): p. 6247–6251.
114. K. Kim, H. Ryoo, Y.M. Lee, K.S. Shin, *Adsorption characteristics of Au nanoparticles onto poly(4-vinylpyridine) surface revealed by QCM, AFM, UV/vis, and Raman scattering spectroscopy.* J. Colloid. Interf. Sci., 2010. **342**(2): p. 479–484.
115. E.S. Kooij, E.A.M. Brouwer, H. Wormeester, B. Poelsema, *Ionic strength medi- ated self organization of gold nanocrystals: an AFM study.* Langmuir, 2002. **18**(20): p. 7677-7682.
116. S. Meltzer, R. Resch, B.E. Koel, M.E. Thompson, A. Madhukar, A.A.G. Requicha, P. Will, *Fabrication of nanostructures by hydroxylamine seeding of gold nanoparticle templates.* Langmuir, 2001. **17**(5): p. 1713–1718.
117. K.C. Grabar, R.G.Freeman, M.B. Hommer, M.J. Natan, *Preparation and characterization of Au colloid monolayers.* Anal. Chem., 1995. **67**(4): p. 735-743.
118. E.A.M. Brouwer, E.S. Kooij, M. Hakbijl, H. Wormeester, B. Poelsema, *Deposition kinetics of nanocolloidal gold particles.* Colloids Surf., A 2005. **267**(1-3): p. 133–138.
119. J. Schmitt, P. Machtle, D. Eck, H. Möhwald, C.A. Helm, *Preparation and optical properties of colloidal gold monolayers.* Langmuir, 1999. **15**(9): p. 3256–3266.

120. G. Bar, S. Rubin, R.W. Cutts, T.N. Taylor, T.A. Zawodzinski, *Dendrimer-modified silicon oxide surfaces as platforms for the deposition of gold and silver colloid monolayers: preparation method, characterization, and correlation between microstructure and optical properties.* Langmuir, 1996. **12**(5): p. 1172–1179.

121. K. Saha , S.S. Agasti, C. Kim, X. Li, V.M. Rotello, *Gold Nanoparticles in Chemical and Biological Sensing.* Chem. Rev., 2012. **112**(5): p. 2739-2779.

122. G.E.N. Pauli, A. de la Escosura-Muniz, C. Parolo, I. H. Bechtold, A. Merkoçi, *Lab-in-a-syringe using gold nanoparticles for rapid immunosensing of protein biomarkers.* Lab Chip, 2015. **15**(2): p. 399-405.

123. J. Bailes, S. Gazi, R. Ivanova, M. Soloviev, *Effect of gold nanoparticle conjugation on the activity and stability of functional proteins.*, in *Nanoparticles in Biology and Medicine*, M. Soloviev, Editor. 2012, Humana Press: New York. p. 89-99.

124. J. Deka, A. Paul, A. Chattopadhyay, *Modulating enzymatic activity in the presence of gold nanoparticles.* RSC Adv., 2012. **2**(11): p. 4736-4745.

125. M. Mahmoudi, I. Lynch, M.R. Ejtehadi, M.P. Monopoli, F.B. Bombelli, S. Laurent, *Protein-nanoparticle interactions: opportunities and challenges.* Chem Rev, 2011. **111**(9): p. 5610-5637.

126. S.R. Saptarshi, A. Duschl, A.L. Lopata, *Interaction of nanoparticles with proteins: relation to bio-reactivity of the nanoparticle.* J. Nanobiotechnol., 2013. **11**(26): p. 1-12.

127. A. Verma, F. Stellacci, *Effect of surface properties on nanoparticle-cell interactions.* Small, 2010. **6**(1): p. 12-21.

128. G. Brancolini, A. Corazza, M. Vuano, F. Fogolari, M.C. Mimmi, V. Bellotti, M. Stoppini, S. Corni, G. Esposito, *Probing the Influence of Citrate-Capped Gold Nanoparticles on an Amyloidogenic Protein.* ACS Nano, 2015. **9**(3): p. 2600-2613.

129. J.E. Gagner, M.D. Lopez, J.S. Dordick, R.W. Siegel, *Effect of gold nanoparticle morphology on adsorbed protein structure and function.* Biomater., 2011. **32**(29): p. 7241-7252.
130. A. Ramanavicius, A. Kausaite, A. Ramanaviciene, *Polypyrrole-coated glucose oxidase nanoparticles for biosensor design.* Sens. Actuators B, 2005. **111-112**: p. 532–539.
131. A. Ramanavicius, *Amperometric biosensor for the determination of creatine.* Anal. Bioanal.Chem. 2007. **387**(5): p. 1899-1906.
132. G. Frens, *Controlled Nucleation for the Regulation of the Particle Size in Monodisperse Gold Suspensions.* Nat. Phys. Sci., 1973. **241**: p. 20-22.
133. J. Kimling, M. Maier, B. Okenve, V. Kotaidis, H. Ballot, A. Plech, *Turkevich method for gold nanoparticle synthesis revisited.* J. Phys. Chem. B, 2006. **110**(32): p. 15700-15707.
134. E.S Kooij, E.A.M. Brouwer, H. Wormeester, B. Poelsema, *Formation and optical characterisation of colloidal gold monolayers.* Colloids Surf. A., **222**(1-3): p. 103-111.
135. A. Tabrizi, F. Ayhan, H. Ayhan, *Gold Nanoparticle Synthesis and Characterisation.* Hacettepe J. Biol. & Chem., 2009. **37**(3): p. 217-226.
136. M. Oćwieja, Z. Adamczyk, K. Kubiak, *Tuning properties of silver particle monolayers via controlled adsorption-desorption processes.* J. Colloid. Interf. Sci., 2012. **376**(1): p. 1-11.
137. Z. Adamczyk, M. Zembala, A. Michna, *Polyelectrolyte adsorption layers studied by streaming potential and particle deposition.* J. Colloid Interface Sci., 2006. **303**(2): p. 353-364.
138. M. Morga, Z. Adamczyk, *Monolayers of cationic polyelectrolytes on mica--electrokinetic studies.* J. Colloid Interface Sci., 2013. **407**: p. 197-204.
139. Z. Adamczyk, B. Jachimska, Marta Kolasińska, *Structure of colloid silica determined by viscosity measurements.* J. Colloid Interface Sci., 2004. **273**(2): p. 668-674.

140. K. Habermuller, W. Schuhmann, *A low volume electro- chemical cell for the deposition of conducting polymers and entrapment of enzymes.* Electroanal. 1998. **10**: p. 1281-1284.
141. S. Bender, O.A. Sadik, *Direct Electrochemical Immunosensor for Polychlorinated Biphenyls.* Environ. Sci. Technol.,, 1998. **32**(6): p. 788-797.
142. A. Ramanaviciene, V. Snitka, R. Mieliauskiene, R. Kazlauskas, A. Ramanavicius, *AFM study of complement system assembly initiated by antigen–antibody complex.* Cent. Europ. J. Chem., 2006. **4**(1): p. 194-206.
143. A. Ramanaviciene, D. Virzonis, G. Vanagas, A. Ramanavicius, *Capacitive micromachined ultrasound transducer (cMUT) for immunosensor design.* Analyst, 2010. **135**(7): p. 1531-1534.
144. A. Ramanaviciene, J. Acaite, A. Ramanavicius, *Circulating immune complexes as indicators of environmental contamination.* Environ. Toxicol. 2004. **19**(5): p. 505-509.
145. B. Kurtinaitiene, D. Ambrozaite, V. Laurinavicius, A. Ramanaviciene, A. Ramanavicius, *Amperometric immunosensor for diagnosis of BLV infection.* Biosens Bioelectron, 2008. **23**(10): p. 1547–1554.
146. W. Schuhmann, C. Kranz, H. Wohlschlager, J. Strohmeier, *Pulse technique for the electrochemical deposition of polymer-films on electrode surfaces.* Biosens. Bioelectron. 1997. **12**(12): p. 1157–1167.
147. A. Ramanavicius, N. Kurilcik, S. Jursenas, A. Finkelsteinas, A. Ramanaviciene, *Conducting polymer based fluorescence quenching as a new approach to increase the selectivity of immunosensors.* Biosens. Bioelectron., 2007. **23**: p. 499–505.
148. R.F. Kubin, A.N. Fletcher, *Fluorescence quantum yields of some rhodamine dyes.* J. Luminescence 1983. **27**(4): p. 455–462.
149. M. Fikry, M.M. Omar, L.Z. Ismail, *Effect of host medium on the fluorescence emission intensity of Rhodamine B in liquid and solid phase.* J Fluoresc., 2009. **19**(4): p. 741-746.

150. D.G. Pina, A.V. Shnyrova, F. Gavilanes, A. Rodriguez, F. Leal, M.G. Roig, G.G.Z. I.Y. Sakharov, E. Villar, V.L. Shnyrov, *Thermally induced conformational changes in horseradish peroxidase.* Eur. J. Biochem. 2001. **268**(1): p. 120-126.

151. M. Hengsakul, A.E. Cass, *Protein patterning with a photoactivable derivative of biotin.* Bioconjug. Chem., 1996. **7**(2): p. 249-254.

152. A.M. Hartnett, C.M. Ingersoll, G.A. Baker, F.V. Bright, *Kinetics and thermodynamics of free flavins and the flavin-based redox active site within glucose oxidase dissolved in solution or sequestered within a sol–gel-derived glass.* Anal. Chem., 1999. **71**(6): p. 1215–1224.

153. A. Ramanavicius, A. Kauskaite, A. Ramanaviciene, J. Acaite, A. Malinauskas, *Redox enzyme – glucose oxidase – initiated synthesis of polypyrrole.* Synth. Met. 2006. **156**(5-6): p. 409–413.

154. M.C. Henry, C.C. Hsueh, B.P. Timko, M.S. Freunda, *Reaction of pyrrole and chloroauric acid. A new route to composite colloids.* J. Electrochem. Soc., 2001. **148** p. 155–162.

155. A. Kozhukharova, N. Kirova, Y. Popova, K. Batsalova, *Poperties of glucose oxi- dase immobilized in gel of poluvinylalcohol.* Biotechnol. Bioeng., 1988. **32**(2): p. 245–248.

156. J. Rinuy, P.F. Brevet, H.H. Girault, *Second harmonic generation of glucose oxidase at the air/water interface.* Biophys. J., 1999. **77**(6): p. 3350–3355.

157. P.N. Bartlett, S.Booth, D.J. Caruana, J.D. Kilburn, C. Santamaria, *Modification of glucose oxidase by the covalent attachment of a tetrathiafulvalene derivative.* Anal. Chem., 1997. **69**(4): p. 734–742.

158. M. Sikorski, E. Sikorska, A. Koziolowa, R.G. Moreno, J.L. Bourdelande, R.P. Steer, F. Wilkinson, *Photophysical properties of lumichromes in water.* J. Photochem. Photobiol. B., 2001. **60**(2-3): p. 114–119.

159. R. Esposito, B.D. Ventura, S. De Nicola, C. Altucci, R. Velotta, Damiano Gustavo Mita and Maria Lepore, *Glucose Sensing by Time-*

Resolved Fluorescence of Sol-Gel Immobilized Glucose Oxidase. Sensors, 2011. **11**(4): p. 3483-3497.

160. P.A.W. van den Berg, K.A. Feenstra, A.E. Mark , H.J.C. Berendsen, A. J.W.G. Visser, *Dynamic Conformations of Flavin Adenine Dinucleotide: Simulated Molecular Dynamics of the Flavin Cofactor Related to the Time-Resolved Fluorescence Characteristics.* J. Phys. Chem. B, 2002. **106**(34): p. 8858 - 8869.
161. Y.-T. Kao, C. Saxena, T.-F. He, L. Guo, L. Wang, A. Sancar, D. Zhong, *Ultrafast Dynamics of Flavins in Five Redox States.* J. Am. Chem. Soc., 2008. **130**(39): p. 13132–13139.
162. K.C. Grabar, K.R. Brown, Ch.D. Keating, S.J. Stranick, S.L. Tang, M.J. Natan, *Nanoscale characterization of gold colloid monolayers: a comparison of four techniques.* Anal. Chem., 1997. **69**(3): p. 471–477.
163. M. Brust, D. Bethell, C.J. Kiely, D.J. Schiffrin, *Self-assembled gold nanoparticle thin films with nonmetallic optical and electronic properties,* Langmuir, 1998. **14**(19): p. 5425–5429.
164. J. Schmitt, P. Machtle, D. Eck, H. Möhwald, C.A. Helm, *Preparation and optical properties of colloidal gold monolayers,* Langmuir, 1999. **15**(9): p. 3256–3266.
165. E.S. Kooij, E.A.M. Brouwer, H. Wormeester, B. Poelsema, *Ionic strength mediated self-organization of gold nanocrystals: an AFM study.* Langmuir, 2002. **18**(20): p. 7677–7682.
166. E.S. Kooij, E.A.M. Brouwer, H. Wormeester, B. Poelsema, *Formation and optical characterisation of colloidal gold monolayers.* Colloids Surf., A, 2003. **222**(1-3): p. 103–111.
167. Z. Adamczyk, M. Zaucha, M. Zembala, *Zeta potential of mica covered by colloid particles: a streaming potential study.* Langmuir, 2010. **26**(12): p. 9368–9377.
168. J.M. Zook, V. Rastogi, R.I. MacCuspie, A.M. Keene, J. Fagan, *Measuring agglomerate size distribution and dependence of localized surface plasmon resonance absorbance on gold nanoparticle*

agglomerate size using analytical ultracentrifugation. ACS Nano, 2011. **5**(10): p. 8070–8079.

169. J.D. Clogston, A.K. Patri, *Characterization of Nanoparticles Intended for Drug Delivery*. Methods in Molecular Biology. 2011, New York: Humana Press.
170. M. Ocwieja, Z. Adamczyk, K. Kubiak, *Tuning properties of silver particle monolayers via controlled adsorption–desorption processes.* J. Colloid. Interface Sci., 2012. **376**(1): p. 1–11.
171. M. Ocwieja, Z. Adamczyk, M. Morga, A. Michna, *High density silver nanoparticle monolayers produced by colloid self-assembly on polyelectrolyte supporting layers.* J. Colloid. Interface Sci., 2011. **364**(1): p. 39–48.
172. Y.Li, H.J. Schluesener, S. Xu, *Gold nanoparticle-based biosensors.* Gold Bulletin, 2010. **43**(1): p. 29-41.
173. M. Mascini, S. Tombelli, *Biosensors for biomarkers in medical diagnostics.* Biomarkers, 2008. **13**(7-8): p. 637–657.
174. L.A. Dykman, N.G. Khlebtsov, *Gold nanoparticles in biology and medicine: recent advances and prospects.* Acta naturae, 2011. **3**(2): p. 34–55.
175. P.E. Chow, *Gold nanoparticles: properties, characterization and fabrication*. Nanotechnology Science and Technology. 2011, New York: Nova Science Publishers Inc.,. 343.
176. L.K. Chau, H.T.Chang, *From Bioimaging to Biosensors: Noble Metal Nanoparticles in Biodetection*. 2013, Singapore: Pan Stanford Publishing 322.
177. Y. Yin, Y.L., B. Gates, Y. Xia, *Template-assisted self-assembly: a practical route to complex aggregates of monodispersed colloids with well-defined sizes, shapes, and structures.* J. Am. Chem. Soc., 2001. **123**(36): p. 8718–8729.

178. I. Tiwari, M.G., C. M. Pandey, V. Mishra, *Gold nanoparticle decorated graphene sheet-polypyrrole based nanocomposite: its synthesis, characterization and genosensing application.* Dalton Trans, 2015.
179. E. Shamaeli, N.A., *Functionalized gold nanoparticle-polypyrrole nanobiocomposite with high effective surface area for electrochemical/pH dual stimuli-responsive smart release of insulin.* Colloids Surf B Biointerfaces, 2015. **126**: p. 502-509.
180. Katherine C. Grabar , P.C.S., Michael D. Musick , Jennifer A. Davis , Daniel G. Walter , Michael A. Jackson , Andrea P. Guthrie , and Michael J. Natan, *Kinetic Control of Interparticle Spacing in Au Colloid-Based Surfaces: Rational Nanometer-Scale Architecture.* J Am Chem Soc, 1996. **118**(5): p. 1148 - 1153.
181. W. Putzbach, N.J. Ronkainen, *Immobilization Techniques in the Fabrication of Nanomaterial-Based Electrochemical Biosensors: A Review.* Sensors (Basel), 2013. **13**(4): p. 4811 - 4840.
182. X. Luo, A. Morrin, A.J. Killard, M.R. Smyth, *Application of Nanoparticles in Electrochemical Sensors and Biosensors.* Electroanal., 2006. **18**(4): p. 319 - 326.
183. N. German, A. Kausaite-Minkstimiene, A. Ramanavicius, T. Semashko, R. Mikhailova, A.Ramanaviciene, *The use of different glucose oxidases for the development of an amperometric reagentless glucose biosensor based on gold nanoparticles covered by polypyrrole.* Electrochimica Acta, 2015. **169**: p. 326-333.